

Functional Analysis of the T-Box Genes *Tbx2* and *Tbx3*
in Murine Liver and Lung Development

Von der Naturwissenschaftlichen Fakultät
der Gottfried Wilhelm Leibniz Universität Hannover
zur Erlangung des Grades
Doktor der Naturwissenschaften
Dr. rer. nat.
genehmigte Dissertation
von
Diplom-Biologe Timo Hans-Werner Lüdtké
geboren am 10.04.1978 in Kiel
2011

Referent: Prof. Dr. Andreas Kispert

Koreferent: Prof. Dr. Hans-Jörg Jacobsen

Tag der Promotion: 30.06.2011



Angefertigt am
Institut für Molekularbiologie
der Medizinischen Hochschule Hannover
unter der Betreuung von
Prof. Dr. Andreas Kispert

Wie Blechmann, Vogelscheuche und furchtsamer Löwe stolpern wir durch unser Leben
– abgestumpft, gedankenleer und ohne Mut –
Bis ein kleines Mädchen alles verändert.

Für Freyja Sophie

Table of Contents

	Page
I Summary	5
II Zusammenfassung	7
III Keywords	8
IV Introduction	9
V Aim of this thesis	13
1 Part 1 “Tbx3 promotes liver bud expansion during mouse development by suppression of cholangiocyte differentiation”, Running title: Tbx3 in liver development	15
2 Part 2 “Tbx3 is regulated by canonical Wnt signaling and represses NOTCH mediated biliary differentiation”, Running title: Regulation of Tbx3	30
3 Part 3 “Tbx2 maintains the mesenchymal signaling center of the developing lung”, Running title: Tbx2 in lung mesenchyme	47
VI Concluding remarks	77
VII References	79
VIII Acknowledgements	85
IX List of publications	86
X Curriculum Vitae	87
XI Declaration	88

Summary

T-Box genes encode a family of evolutionary conserved transcription factors named by their key feature – the T-box DNA binding domain. *Tbx2* and *Tbx3*, two closely related members of the *Tbx2* subfamily encode for transcriptional repressors that take over key functions in the organogenesis of the heart and limbs. A functional relevance in the formation of endodermal organs had not been shown so far. Expression analyses of T-box factors and phenotypical characterization of loss-of-function mutants in the mouse suggested the necessity of *Tbx3* in the development of the liver and a function of *Tbx2* in the lung mesenchyme. *Tbx3* mutant mice showed hepatic hypoplasia, *Tbx2* mutant mice formed smaller lungs. Expression analyses showed a strong but transient expression of *Tbx3* in the early liver diverticulum peaking around the 25 somite stage. Early changes of differentiation markers as seen by the loss of the hepatocyte marker genes alpha fetoprotein (*Afp*) and albumin (*Alb*) and premature expression of the cholangiocyte (biliary cell) marker cytokeratin 18 (*Ck18*) revealed a crucial necessity of *Tbx3* in hepatic lineage decision. Misexpression experiments in cell culture and in vivo strengthen these findings as *Tbx3* overexpression in primary hepatoblasts elevates the expression of *Hnf4a*, a key transcription factor for hepatocyte differentiation. Mice overexpressing *Tbx2* lack the formation of bile ducts. Notch signaling had been shown to induce biliary development recently and ectopic bile ducts form in N1ICD (Notch1 intracellular domain) overexpressing mutants. Intriguingly, simultaneous expression of N1ICD and *Tbx2* led to reduced bile duct formation. This strongly suggested that downregulation of *Tbx3* is a prerequisite of bile duct formation and cholangiocyte differentiation. However, *Tbx3* not only regulates hepatic differentiation but also drives proliferation of hepatoblasts and allows the generation of a cell emergent liver bud via maintenance of *Prox1*, a known transcription factor relevant for delamination and migration of hepatocytes. In the lung mesenchyme *Tbx3* is expressed from E10.5 until E14.5. In contrast to the transient expression of *Tbx3* in liver and lung, *Tbx2* is expressed in the mesenchyme of the lung throughout whole embryonal lung development. However, co-expression of *Tbx3* until E14.5 and morphological changes in the *Tbx2* mutant at E16.5 argue for an early functional redundancy of *Tbx3* and a late unique function of *Tbx2*. Analysis of the *Tbx2* loss-of-function mutant showed a loss of proliferation accompanied by upregulation of the cell cycle inhibitors cyclin dependent kinase inhibitor (*Cdkn1a* (*p21*) and *Cdkn1b* (*p27*)). Chromatin immunoprecipitation (ChIP) experiments confirmed a direct repression by *Tbx2*. However, rescue experiments with *p21* and *p27* mutant mice could not restore lung growth. An additionally reduced branching morphogenesis of the bronchial tree, which is known to be regulated by canonical Wnt signaling rose the intriguing possibility of a direct interference of *Tbx2* with this pathway. Indeed *Axin2* was downregulated in the *Tbx2* mu-

tant lung mesenchyme and further chemical and genetical rescue experiments in an organ culture system approved a functional connection. Taken together, this work elucidates the functional requirement of T-Box factors in the formation of endodermal organs and adds new insights in molecular mechanisms of *Tbx2* and *Tbx3* to our store of knowledge.

Zusammenfassung

T-Box Gene kodieren für eine Familie evolutionär konservierter Transkriptionsfaktoren, die benannt wurden nach ihrem Schlüsselmerkmal – der T-Box DNA Bindedomäne. *Tbx2* und *Tbx3*, zwei engverwandte Mitglieder der *Tbx2* Unterfamilie kodieren für transkriptionelle Repressoren, die Schlüsselfunktionen in der Organogenese mesodermaler Organe wie des Herzens und der Gliedmaßen einnehmen. Eine funktionelle Relevanz in der Bildung endodermal abgeleiteter Organe wurde bisher nicht gezeigt. Expressionsanalysen von T-Box Faktoren und phänotypische Charakterisierung von Verlustmutanten der Maus deuten auf eine Notwendigkeit von *Tbx3* in der Leberentwicklung und eine Funktion von *Tbx2* im Lungenmesenchym hin. *Tbx3* mutante Mäuse zeigten eine Hypoplasie der Leber, *Tbx2* Mutanten wiederum bildeten kleine Lungen. Genaue Expressionsanalysen zeigten eine starke aber transiente Expression von *Tbx3*, die in der frühen Leberknospe um das 25 Somiten Stadium gipfelte. Frühe Veränderungen von Differenzierungsmarkern wie dem Verlust der Hepatozyten Markergene alpha Fetoprotein (*Afp*) und Albumin (*Alb*) sowie vorzeitige Expression des Cholangiozyten- (Gallen-) Markergens *Ck18* enthüllten eine kritische Notwendigkeit von *Tbx3* in der Festlegung hepatischer Zellschicksalsentscheidungen. Missexpressionsexperimente in Zellkultur und *in vivo* bestärkten diesen Befund. Überexpression von *Tbx3* in primären Hepatoblasten (Lebervorläuferzellen) erhöht die Expression des hepatischen nukleären Faktors 4 alpha (*Hnf4a*), einem Schlüssel-Transkriptionsfaktor für die Hepatozytenfdifferenzierung. Mäuse, die das mit *Tbx3* verwandte und redundante *Tbx2* überexprimieren, bilden keine Gallengänge. Der Notch Signalweg wurde als Auslöser der Gallenentwicklung beschrieben. Zusätzliche, ektopische Gallengänge formieren sich, wenn die Notch1 intrazelluläre Domäne (NICD), die die Ablesung von Notch-Zielgenen im Nukleus auslöst, in der Leber überexprimiert wird. Interessanterweise führte die zeitgleiche Überexpression von NICD und *TBX2* zu verringerter Gallengangausbildung. Diese Ergebnisse sprechen stark dafür, dass die Herunterregulierung von *Tbx3* während der normalen Gallengangentwicklung Voraussetzung ist für die Cholangiozytendifferenzierung. Allerdings reguliert *Tbx3* nicht nur die Differenzierung sondern fördert auch die Vermehrung der Lebervorläuferzellen und erlaubt die Auswanderung dieser aus dem Vorderdarm- Endoderm.

Im Mesenchym der Lunge wiederum ist *Tbx3* von Embryonalstadium (E) 10,5 bis E14,5 exprimiert. Im gegensatz zu der transienten Expression von *Tbx3* in der Leber ist *Tbx2* in der Embryonalentwicklung durchgehend in der Lunge exprimiert. Koexpression von *Tbx3* bis E14,5 und das Auftreten morphologischer Veränderungen in der *Tbx2* Verlustmutante erst nach diesem Zeitpunkt legten eine frühe funktionelle Redundanz beider Gene sowie eine alleinige späte Funktion von *Tbx2* im Lungenmesenchym nahe. Die Analyse der *Tbx2* Mutante ergab einen

Verlust der Zellvermehrung begleitet von einer Hochregulation zweier Zellzyklusinhibitoren, der zyklinabhängigen Kinasehemmer (Cdkn) 1a und *Cdkn1b*. Chromatin- Immunpräzipitationsexperimente (ChIP) bestätigten eine direkte Repression durch Tbx2. Rettungsexperimente mit genetischen *Cdkn1a* und *1b* verlustmutanten Mäusen konnten jedoch das Lungenwachstum nicht wiederherstellen. Eine zusätzlich verringerte Verzweigung des respiratorischen Baumes, die bekanntermaßen unter anderem durch kanonische Wnt- Signale reguliert wird, eröffnete die äußerst interessante Möglichkeit einer direkten Interaktion von Tbx2 mit diesem Signalweg. In der Tat war ein Zielgen dieses Signalpfades, *Axin2*, im Lungenmesenchym der *Tbx2* Mutante verringert und weitere genetische und chemische Rettungsexperimente befürworteten eine funktionelle Verknüpfung.

Die vorliegende Arbeit beleuchtet die funktionelle Notwendigkeit von T-Box Transkriptionsfaktoren in der Bildung und Entwicklung endodermal abgeleiteter Organe und leistet einen wichtigen Beitrag zu der Erweiterung unserer Erkenntnisse über die molekularen Wirkungsmechanismen von *Tbx2* und *Tbx3*.

Keywords: Tbx2, Tbx3, mouse development

Schlagworte: Tbx2, Tbx3, Mausentwicklung

Introduction

One of the most mesmerizing processes during embryonal development is organogenesis, the development of complex organs from a simple precursor. One of these progenitor structures is the endodermal gut tube - apparently primitive but provided with an immense plasticity and ability to give rise to several diverse organs. During gastrulation the gut tube is formed from the endoderm by morphogenic processes(1). Signaling molecules secreted by the surrounding mesoderm further pattern the gut endoderm along the anterior-posterior (A-P) axis. High levels of Nodal, a member of the TGF β superfamily, commit the formerly naïve endoderm to an anterior fate, whereas posterior endodermal fate requires lower nodal signaling levels(2, 3).

Induced by several signaling cascades a couple of organs arise from the gut endoderm. The dorsal endoderm gives rise to the intestines, while thyroid glands, lung and liver develop from the ventral endoderm(4) (5). The pancreas initially forms at two different positions that later fuse, one in the ventral foregut and the other in the dorsal endoderm(6). Furthermore the endoderm is a multipotent source of not only the gastrointestinal and respiratory epithelium but also glandular and ductal cells of the pancreas and the hepatoblasts, precursor cells for hepatocytes and intrahepatic bile duct cells (cholangiocytes) in the liver(5)(7, 8).

To constrict regional identity of the endoderm and to ensure the local initiation or repression of the different endoderm derived organs, gradients of Fgfs, Wnts, Bmps and retinoic acid are secreted from the adjacent cardiac mesoderm, septum transversum mesenchyme and the mesoderm surrounding the gut tube(5, 9, 10). Overlapping signals define the evolving foregut, midgut and hindgut domains which are characterized by the expression of the transcription factors Hhex in the foregut, Pdx1 in the midgut and Cdx in the posterior endoderm, respectively in a dose dependent manner(9, 11). This model is supported by tissue recombination experiments that showed that the foregut endoderm still can give rise to the intestines when recombined with posterior mesoderm(12-16).

Recent studies in chick and *Xenopus* support the assumption that foregut fate is actively repressed by Fgf4 and Wnts secreted from the posterior mesoderm, while Wnt signaling must be inhibited in the anterior endoderm to establish foregut identity, most likely by the expression of small soluble Wnt inhibitors(16-18) . Consistently, experiments in *Xenopus* showed activated Hhex expression and ectopic liver primordia when β -catenin mediated transcription of the activated canonical Wnt signaling pathway was blocked in the posterior endoderm(18).

In contrast, mouse explant studies suggest that a concentration gradient of FGF is crucial for the establishment of the distinct ventral foregut derived organs. Without addition of FGF to the cultures pancreatic development was observed, the default fate of the ventral foregut endoderm.

High levels of Fgf signaling promoted lung growth and medium levels initiated hepatic development(12, 19-23). Regional restriction of organ emergence requires mediators that assure the activation or repression of gene expression programs to allow the local initiation and specification of the diverse organs. Intriguingly, expression of T-box transcription factors has been reported in the context of endodermal organ development but their functional relevance in endodermal organogenesis has not yet been analyzed.

T-box (*Tbx*) genes encode a family of transcription factors that share a highly conserved eponymous DNA binding motif, the T-box. The T-box is a region of 180 amino acid residues that specifically binds to the T-box binding element (TBE), a conserved DNA-motif with the consensus sequence 5'-AGGTGTGA-3'. This motif was originally identified for Brachyury (T), the founding member of this gene family(24). To date 17 family members divided in five major subfamilies based on sequence conservation of the T-box were described in mammals.

T-box genes hold key functions in multiple developmental processes for example in patterning the mesoderm and in organogenesis. Remarkably, mutations in a number of T-box factors could be allocated to human congenital disorders demonstrating their impact in development and disease.

This study focused on the functional analysis of *Tbx2* and *Tbx3*, members of the *Tbx2* subfamily in vertebrates during endodermal organ development. While *Tbx2* and *Tbx3* were described as transcriptional repressors(25-27), the two other family members *Tbx4* and *Tbx5* are known activators(28). Interestingly *Tbx2* and *Tbx3* are closely related showing ~90% identity of the amino acid sequence in the T-box. Additionally *Tbx2* and *Tbx3* are often co-expressed and functional redundant(29-32). However, while *Tbx4* is likewise related to *Tbx5*, *Tbx2* is linked to *Tbx4* on the chromosome as well as *Tbx3* is linked to *Tbx5*(29, 33). Apparently the *Tbx2* subfamily emerged by an initial tandem duplication of a predecessor. Subsequently the duplications of the evolved gene pairs dispersed onto two different chromosomes(29, 34, 35). While function of *Tbx2* and *Tbx3* in the development of organs of mesodermal origin as the appendages, eyes, and the heart have been extensively analyzed in the last decade, functional relevance of T-box transcription factors in the development of endodermal derived organs is only insufficiently understood.

A prominent organ of endodermal origin is the liver(36). Being the largest endodermal organ it exhibits central metabolic functions for the body. The liver provides essential exocrine functions including production of bile, which is secreted via intrahepatic bile ductules. Important endocrine functions include the release of albumin, clotting factors and glycogen into the blood. The liver is the main storage organ for glycogen and performs the metabolism of nutrients and not least ac-

accomplishes detoxification. Its ability to regenerate from loss of two thirds of its cell mass fascinated physicians and scientists for many years and still captivates laboratories all over the world. The principal and metabolic cell type accounting for ~70-80% of the mass of the adult organ and responsible for the functional diversity of the liver are the hepatocytes(37, 38). Hepatocytes, along with biliary epithelial cells (BECs; also known as cholangiocytes) that form the bile ducts originate from a bipotential endodermal derived precursor cell population, the hepatoblasts(39). Additionally, stromal cells, stellate cells, kuppfer cells and blood vessels all of mesodermal origin contribute to the complex composition of the liver(40).

Detailed studies using mouse embryo foregut explants attended to liver initiation. While unspecified cultured foregut explants express *Alb* in the presence of cardiac mesoderm, in the absence of cardiac mesoderm or after blocking of FGF or BMP, induction of the liver does not take place(12, 23, 41). Moreover, addition of exogenous FGF1 or FGF2 restore *Alb* expression in foregut endoderm explants(22) thus showing that hepatic initiation is indeed dependent on Fgf-signaling.

After hepatic specification the forming mammalian liver undergoes a series of morphological processes from the appearance of an epithelial protuberance to a cell-emergent liver bud(42-44). In the mouse, cellular differentiation of hepatoblasts into hepatocytes or BECs starts approximately at E13.5. Key transcription factors for the differentiation of hepatocytes are *Hnf4a*, *Hnf1a*, while differentiation into BECs is regulated by *Onecut1* and *Hnf1b*(45-47). Hepatoblasts in contact with the portal vein form layer of cuboidal biliary precursors (the ductal plate) that increases expression of *Onecut1* and the biliary differentiation marker *cytokeratin-19* (*CK-19*) but down-regulate hepatic genes suggesting an endothelial signaling source inducing biliary differentiation(48, 49).

In the ectoderm and mesoderm derived mammary glands, *Tbx3* owns an FGF dependent central function in the initiation of the organ(50, 51). However, although the transcriptional repressor *Tbx3* had been reported to facilitate growth of the liver by repression of the cell cycle inhibitor *p19arf* in a late stage of liver expansion(52), relevance for *Tbx3* in early hepatic initiation, specification or differentiation of the respective cell types of the liver is yet unclear.

Expression of T-box transcription factors *Tbx1-5* had been reported in another endodermal organ namely the lung previously(30).

Lung development was a necessary consequence of oxygen penury for fish in continental waters. Unlike the oceans, where variations in temperature are only modest, high temperatures in small lakes caused a lower solubility and availability of oxygen so that oxygen intake by the gills was at

least occasionally insufficient. Since the skin of fresh water fish had to be an efficient barrier for the osmotic pressure arising in these habitats, only the mucous membrane of the mouth and the gut could alternatively serve for the uptake of oxygen. While the first inland water fish swallowed air to satisfy their need for oxygen, land-living vertebrates developed lungs as inversions from the gut tube(53, 54). By establishment of a fine branched epithelial respiratory tree together with formation of highly specialized cell types lining small epithelial cavities called alveoli the respiratory surface area exceeds the body surface by a multiple. In mice the average alveolar surface area (ASA) is $0,068\text{m}^2$ with a lung volume of 0,7ml (man: ASA 82m^2 with 7000ml lung volume)(55). Exhaustive capillarization of the lung provides the base for efficient gas exchange which makes it the key respiratory organ in mammals.

The lung emerges as a diverticulum of the ventral foregut endoderm. Like in the liver the lung is specified by dose dependent Fgf-signaling and other signaling cascades(56). Once specified, a localized expression domain of the homeobox transcription factor Nkx2-1(33), which activates expression of lung-specific surfactant protein genes, is established in the ventral wall of the anterior foregut. The two primary lung buds appear within this domain at E9.5 in the mouse(33). Induced by epithelial-mesenchymal interactions the lung bud undergoes a process of stereotyped branching morphogenesis(57, 58).

Once the primary lung buds have formed, they extend into the surrounding mesenchyme and begin the process of branching morphogenesis. Expression of Fgf10 in the mesoderm and Fgfr2 in the endoderm guides the strictly regulated branching morphogenesis of the respiratory tree(59). Tbx4 and Tbx5 had recently been shown to locally induce Fgf10 expression(60). No bud extension occurs in mutants lacking Fgf10 and branching of the epithelium is reduced in Tbx4/5 antisense oligonucleotide treated cultures which is accompanied by a reduction of mesenchymal Fgf10(60-62). Since Tbx2 and Tbx3 are repressors, these transcription factors might antagonize Tbx4 and Tbx5 function, thereby fine tuning the Fgf-signal intensity or regionally restrict the Fgf source to allow dichotomous branching events. Moreover, mesenchymal Wnt/Ctnnb1 signaling in embryonic lung development controls mesenchymal cell proliferation(63). Furthermore, when *Ctnnb1* is conditionally depleted from the lung mesenchyme, branching morphogenesis is severely impeded(63).

While branching morphogenesis does not continue postnatal, the lungs increase in size for a significant time after birth(64). Intriguingly, Tbx2/3 are known to positively regulate proliferation by repression of cell cycle inhibitors in different cancers, facilitating a presumptive function in organ growth(65-67).

Aim of this thesis

Loss-of-function analyses of *Tbx2* and *Tbx3* in mice has revealed the importance of this closely related pair of transcriptional repressors in a number of organs that originated from the mesoderm like the heart, limbs and mammary glands(68-70)). In contrast, our knowledge of functional relevance of T-box transcription factors in the development of the endoderm and its derivatives is insufficient. However, loss-of-function analyses for *Tbx3* and *Tbx2* in mice revealed hypoplastic livers and dramatically reduced lungs, respectively, suggesting a primary function of these T-box factors in the development of the corresponding organ.

It was unclear at what stage and in which compartment *Tbx3* might regulate liver organogenesis. For that reason in a first subproject, I performed a detailed temporal and spatial expression analysis of *Tbx3* in wildtype mice during all phases of hepatic development. The aim was to find out in combination with morphological and histological examination of the *Tbx3* loss-of-function mutant whether *Tbx3* might have a primary function in hepatogenesis. Early markers for hepatic initiation, specification and differentiation were analyzed to answer the question, which molecular processes were regulated by *Tbx3* during liver formation. Furthermore, ectopic misexpression experiments *in vitro* and *in vivo* complemented the results in order to clarify interactions of *Tbx3* with essential signaling pathways for hepatic development. For that purpose, bipotential mouse embryonic liver cell lines reflecting hepatoblasts and murine hepatoma cells which are similar to differentiated hepatocytes were used. Transfection of biliary epithelial cell (BEC) specific transcription factors in these cells as well as overexpression plasmids of *Tbx3* and a dominant negative form of *Tbx3* or combinations of each, together with RT-PCR analysis were performed to get insight in *Tbx3* function in the cellular differentiation and identity. Additionally, to elucidate how *Tbx3* itself is regulated during liver formation, conditional deactivation and ectopic or prolonged activation of signaling pathways particularly the Notch- and Wnt/*Ctnnb1* pathway were performed.

In a second independent project I analyzed a possible function of *Tbx2* in the mesenchyme of the lung. To determine possible redundancies or antagonistic functions to other T-box factors, again a temporal and spatial expression analysis was performed in addition with extensive morphological and histological examinations of the *Tbx2* loss-of-function mutant. In cell culture experiments, *TBX2* binds to the human promoter of *Cyclin dependent kinase 1 A (CDKN1A)*, a negative cell cycle regulator. One aim of this thesis was to verify an akin function of *Tbx2* in cell cycle regulation *in vivo* in the mouse. Therefore with an *in silico* analysis I scanned the genomic sequences of *Cdkn1a* and *Cdkn1b* for possible transcription factor binding elements (TBE, also

T-site). To ratify candidate sequences, ChIP experiments were used to display binding of Tbx2. Analyses of the different signaling pathways orchestrating the strict morphogenic processes that govern the formation of the bronchial tree furthermore provide important insights on functional significance of *Tbx2*. Hence the examination of regulation of the responsible pathways was completed by additional gain-of-function experiments.

This study was aimed to get insights into the genetic control of early and late organogenic processes of the endoderm, the interaction of *Tbx2* and *Tbx3* with signaling pathways and to add further information to the function of the T-box factors.

Tbx3 promotes liver bud expansion during mouse development by suppression of cholangiocyte differentiation†

Timo H.-W. Lüdtk¹, Vincent M. Christoffels², Marianne Petry¹, Andreas Kispert^{1,‡}

¹From the Institut für Molekularbiologie, Medizinische Hochschule Hannover, Hannover, Germany;

²From the Department of Anatomy & Embryology, Academic Medical Center, University of Amsterdam, Amsterdam, The Netherlands.

Received May 13, 2008; accepted October 12, 2008.

‡Corresponding Author: Andreas Kispert, Medizinische Hochschule Hannover, Institute for Molecular Biology, OE5250, Carl-Neuberg-Str. 1, D-30625 Hannover, Germany. Tel. +49 511 532 4017; Fax: +49 511 5324283; E-mail: kispert.andreas@mh-hannover.de

Published in Hepatology, Volume 49, Issue 3, pages 969–978, March 2009

Reprinted with permission

**JOHN WILEY AND SONS LICENSE
TERMS AND CONDITIONS**

Mar 12, 2011

This is a License Agreement between Timo H. ("You") and John Wiley and Sons ("John Wiley and Sons") provided by Copyright Clearance Center ("CCC"). The license consists of your order details, the terms and conditions provided by John Wiley and Sons, and the payment terms and conditions.

All payments must be made in full to CCC. For payment instructions, please see information listed at the bottom of this form.

License Number	2626650590734
License date	Mar 12, 2011
Licensed content publisher	John Wiley and Sons
Licensed content publication	Hepatology
Licensed content title	Tbx3 promotes liver bud expansion during mouse development by suppression of cholangiocyte differentiation
Licensed content author	Timo H. -W. Lüdtkke,Vincent M. Christoffels,Marianne Petry,Andreas Kispert
Licensed content date	Mar 1, 2009
Start page	969
End page	978
Type of use	Dissertation/Thesis
Requestor type	Author of this Wiley article
Format	Print and electronic
Portion	Full article
Will you be translating?	No
Order reference number	
Total	0.00 USD
Terms and Conditions	

TERMS AND CONDITIONS

This copyrighted material is owned by or exclusively licensed to John Wiley & Sons, Inc. or one of its group companies (each a "Wiley Company") or a society for whom a Wiley Company has exclusive publishing rights in relation to a particular journal (collectively "WILEY"). By clicking "accept" in connection with completing this licensing transaction, you agree that the following terms and conditions apply to this transaction (along with the billing and payment terms and conditions established by the Copyright Clearance Center Inc., ("CCC's Billing and Payment terms and conditions"), at the time that you opened your Rightslink account (these are available at any time at <http://myaccount.copyright.com>)

Terms and Conditions

1. The materials you have requested permission to reproduce (the "Materials") are protected by copyright.
2. You are hereby granted a personal, non-exclusive, non-sublicensable, non-transferable, worldwide, limited license to reproduce the Materials for the purpose specified in the licensing process. This license is for a one-time use only with a maximum distribution equal to the number

<https://s100.copyright.com/App/PrintableLicenseFrame.jsp?publisherID=140&license...> 12.03.2011

Tbx3 Promotes Liver Bud Expansion During Mouse Development by Suppression of Cholangiocyte Differentiation

Timo H.-W. Lüdtke,¹ Vincent M. Christoffels,² Marianne Petry,¹ and Andreas Kispert¹

After specification of the hepatic endoderm, mammalian liver organogenesis progresses through a series of morphological stages that culminate in the migration of hepatocytes into the underlying mesenchyme to populate the hepatic lobes. Here, we show that in the mouse the transcriptional repressor Tbx3, a member of the T-box protein family, is required for the transition from a hepatic diverticulum with a pseudo-stratified epithelium to a cell-emergent liver bud. In *Tbx3*-deficient embryos, proliferation in the hepatic epithelium is severely reduced, hepatoblasts fail to delaminate, and cholangiocyte rather than hepatocyte differentiation occurs. Molecular analyses suggest that the primary function of Tbx3 is to maintain expression of hepatocyte transcription factors, including hepatic nuclear factor 4a (Hnf4a) and CCAAT/enhancer binding protein (C/EBP), alpha (Cebpa), and to repress expression of cholangiocyte transcription factors such as Onecut1 (Hnf6) and Hnf1b. **Conclusion:** *Tbx3* controls liver bud expansion by suppressing cholangiocyte and favoring hepatocyte differentiation in the liver bud. (HEPATOLOGY 2009;49:969-978.)

Hepatocytes and cholangiocytes constitute the liver parenchyme and the bile-transporting cells of the intrahepatic and extrahepatic bile ducts, respectively. Both cell types derive from a bipotential precursor cell, the hepatoblast, whose specification, expansion, and differentiation is intimately linked with morphogenesis of the liver.¹ Liver development in the mouse begins at embryonic day (E) 8.25 after the formation of the definitive endoderm. Signals from the precardiogenic mesoderm and the underlying septum transversum region act in combination to induce and de-

lineate the hepatic from the neighboring pancreatic and intestinal endoderm. Hepatoblasts activate an early liver gene program and form a thickened columnar epithelium that becomes pseudo-stratified at E9.0. Starting from E9.5, the basal lamina degrades, and finger-like protrusions arise from which individual cells migrate into the underlying mesenchyme and populate the hepatic lobes. Although most hepatoblasts differentiate into hepatocytes, a subset of these cells maintain their precursor character and differentiate into cholangiocytes that form the lining of the bile ducts, starting from E13.5. Thus, differentiation of hepatoblasts into hepatocytes or bile duct cells is temporally and spatially separated, suggesting the existence of localized inducers or repressing mechanisms that direct either fate.^{2,3}

Phenotypical analysis of mutant mice has provided substantial insight into a molecular network of transcriptional regulators that control distinct subprograms of liver organogenesis.^{2,3} *Tbx3*, a member of the T-box gene family, has recently emerged as an additional player in the genetic circuit underlying the hepatic lineage decision. Heterozygosity of *TBX3* causes Ulnar-mammary syndrome in humans, an autosomal-dominant disorder characterized by upper limb skeletal malformations, severe hypoplasia of the breast, and hair and genital defects.⁴ *Tbx3*-homozygous mice present ulnar-mammary syndrome-related features, including severe defects in limb and mammary gland development. *Tbx3*-mutant mice bred

Abbreviations: BrdU, bromodeoxyuridine; Cebpa, CCAAT/enhancer binding protein (C/EBP), alpha; Hnf, hepatic nuclear factor; mRNA, messenger RNA; PCR, polymerase chain reaction; Prox, prospero-related homeobox; qRT-PCR, quantitative reverse transcription polymerase chain reaction.

From the ¹Institut für Molekularbiologie, Medizinische Hochschule Hannover, Hannover, Germany; and the ²Department of Anatomy & Embryology, Academic Medical Center, University of Amsterdam, Amsterdam, The Netherlands.

Received May 13, 2008; accepted October 12, 2008.

Supported by funding from the Deutsche Forschungsgemeinschaft (DFG, German Research Foundation) for the Cluster of Excellence REBIRTH (From Regenerative Biology to Reconstructive Therapy).

Address reprint requests to: Andreas Kispert, Institut für Molekularbiologie, OE5250, Medizinische Hochschule Hannover, Carl-Neuberg-Str. 1, 30625 Hannover, Germany. E-mail: kispert.andreas@mh-hannover.de; fax: (49)-511-532-4283.

Copyright © 2008 by the American Association for the Study of Liver Diseases.

Published online in Wiley InterScience (www.interscience.wiley.com).

DOI 10.1002/hep.22700

Potential conflict of interest: Nothing to report.

Additional Supporting Information may be found in the online version of this article.

on a C57Bl6/129 mixed genetic background additionally exhibit a hypoplastic liver that was hypothesized to be secondary to impaired vascularization or hematopoiesis.⁵ However, a recent study has provided strong evidence for a primary requirement of *Tbx3* in hepatogenesis.^{6,7} The authors showed that *Tbx3* expression in multipotent hepatoblasts supports proliferation and hepatic differentiation of these progenitor cells by repression of the tumor suppressor gene *p19^{Arf}* (*Cdkn2a*).

Here, we extend the analysis of hepatic *Tbx3* function and provide novel insight into the temporal and spatial requirement of the gene in orchestrating multiple aspects of early liver organogenesis. We correlate the hepatic expression of *Tbx3* with onset of liver defects in *Tbx3*-deficient embryos and show that *Tbx3* controls morphogenesis of the liver bud by coordinately regulating proliferation, migration, and differentiation of hepatoblasts. Based on molecular phenotyping and overexpression experiments *in vitro*, we propose that de-repression of *p19^{Arf}* and proliferation defects, and impairment of hepatoblast migration is a consequence rather than a cause of aberrant cholangiocyte differentiation.

Materials and Methods

Mice and Genotyping. Mice carrying a null allele of *Tbx3* (*Tbx3^{tm1.1(cre)Vmc}*, synonym: *Tbx3^{cre}*)⁷ were maintained on an outbred NMRI (National Marine Research Institute) background. For timed pregnancies, vaginal plugs were checked in the morning after mating; noon was taken as embryonic day (E) 0.5. Embryos were harvested in phosphate-buffered saline, fixed in 4% paraformaldehyde overnight, and stored in 100% methanol at -20°C before further use. Genomic DNA prepared from yolk sacs or tail biopsy specimens was used for genotyping by polymerase chain reaction (PCR).⁷ All mice received humane care, and their use was approved by the Institutional Animal Care Committee of Hannover Medical School.

Histological Analysis and Immunofluorescence. Embryos were embedded in paraffin wax and sectioned to 5 μm . For histological analyses, sections were stained with hematoxylin-eosin. For the detection of antigens, the following primary antibodies were used: rabbit anti-mouse E-cadherin (gift from Rolf Kemler), laminin (Sigma), and cytokeratin 18 (Acris Antibodies).

In Situ Hybridization Analysis. In situ hybridization analysis on 10- μm transverse sections of embryos was performed following a standard procedure with digoxigenin-labeled antisense riboprobes.⁸

Proliferation and Apoptosis Assays. Cell proliferation in tissues of E9.0 and E9.5 embryos was investigated

by detection of incorporated bromodeoxyuridine (BrdU) similar to published protocols.⁹ A total of nine sections from three individual embryos per genotype and time point were used for quantification. Statistical analysis was performed using the two-tailed Student *t* test. Data were expressed as mean \pm standard deviation. Differences were considered significant when the *P*-value was below 0.05.

For detection of apoptotic cells in 5- μm paraffin sections of E9.5 embryos, the terminal deoxynucleotidyl transferase-mediated nick-end labeling assay was performed as recommended by the manufacturer (Serologicals Corp.) of the ApopTag kit used.

Cell Culture and Transfection. Bipotential mouse embryonic liver cell line 9A1, a kind gift from M.C. Weiss, has been described previously.¹⁰ Murine hepatoma Hepa1-6 cells were obtained from the American Type Cell Culture. Cells were seeded in six-well plates and (co-) transfected after 24 hours with 10 μL lipofectamine 2000 (Invitrogen) and 1250 ng of the expression vectors pcDNA3.GL.Onecut1.Myc, pcDNA3.GL.Tbx3.Myc, pcDNA3.GL.Hnf1b.Myc or pVP16.Tbx2-DB, and 1.5 μg pMACS4.1 (Miltenyi Biotech) for enrichment of transfected cells.¹¹ The total amount of plasmid DNA was adjusted to 4 μg by adding pcDNA3.

Semiquantitative Reverse Transcription PCR. Total RNA was extracted from dissected E9.5 liver buds or cells with RNAPure reagent (Peqlab). RNA (500 ng) was reverse transcribed with RevertAid M-MuLV Reverse Transcriptase (Fermentas). For semiquantitative PCR, the number of cycles was adjusted to the mid-logarithmic phase. Quantification was performed with Quantity One software (Bio-Rad). Assays were performed at least twice in duplicate, and statistical analysis was done as described previously. Primers and PCR conditions are available on request.

Documentation. Documentation of whole-mount specimens and sections was done as described previously.⁹

Results

Liver Hypoplasia in *Tbx3*-Mutant Mice. To study the hepatic requirement of *Tbx3*, we maintained a new *Tbx3* null allele (*Tbx3^{cre}*)⁷ on an NMRI outbred background that supported viability of homozygous mutant embryos until E14.5. At this stage, *Tbx3^{-/-}* embryos showed an overall size reduction and a disproportionately small liver that was filled with blood cells (Fig. 1A, B). *Tbx3*-deficient livers were characterized by a dramatic reduction of the hepatoblast marker gene *alpha fetoprotein* (*Afp*) and the hepatocyte marker gene *albumin* (Fig. 1C), whereas expression of Ck18, an antigen confined to cholangiocytes, was increased and detected

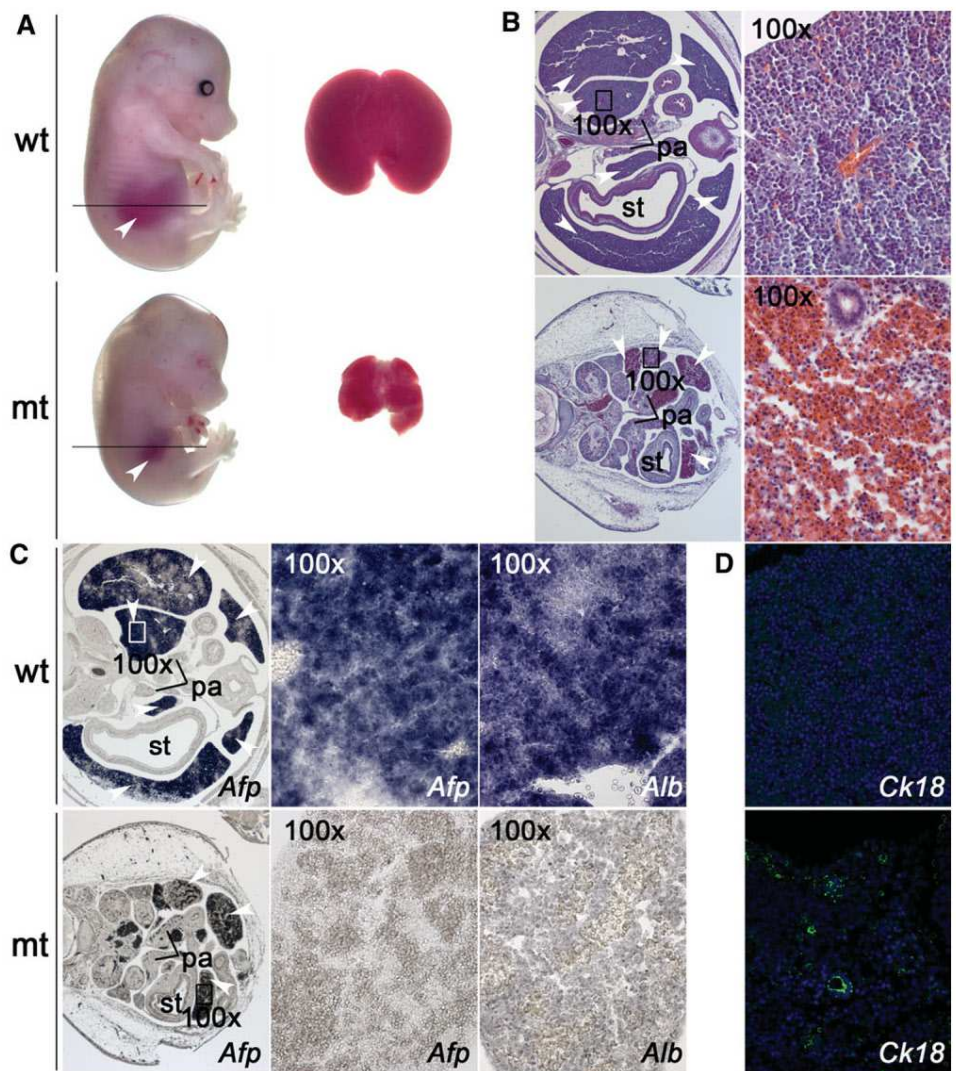


Fig. 1. *Tbx3*-deficient mice exhibit severe liver hypoplasia at E14.5. Morphology of whole embryos and livers (A); and hematoxylin-eosin stainings (B), *in situ* hybridization analysis of *Afp* and *albumin* (*Alb*) (C) expression, and immunofluorescent detection of Ck18 protein (D) on transverse sections of wild-type (wt) and *Tbx3*-deficient (mt) embryos. Section planes and magnified regions are as indicated by lines and boxes, respectively. Mutant livers are still encapsulated and of normal shape but dramatically reduced in size. Blood cells and Ck18⁺-cholangiocytes have replaced *Alb*-expressing hepatocytes. Genotypes and probes are as indicated. White arrowheads point to liver. Abbreviations: pa, pancreas; st, stomach.

in 10% to 20% of cells in the mutant liver (Fig. 1D). This suggests that expansion and differentiation of hepatic progenitors is severely disturbed in *Tbx3*-deficient hepatic tissue.

Early Disruption of Liver Development in *Tbx3*^{-/-} Embryos. To determine at which stage liver organogenesis becomes impaired in *Tbx3*-deficient embryos, we analyzed *Afp* expression on sections to evaluate specification of hepatic tissue and morphogenesis of the organ (Fig. 2). In *Tbx3*^{-/-} embryos of E9.0 (16-somite stage), the ventral foregut endoderm expressed *Afp* indistinguishably from the wild-type, indicating that a hepatic diverticulum with a pseudo-stratified organization was formed. At E9.5, the mutant hepatic epithelium appeared thickened but lacked the characteristic wild-type protrusions and delaminations. At E10.5 the mesenchyme adjacent to the liver bud was densely populated with hepatoblasts in the wild-type, whereas few *Afp*-positive cells were found in the underlying mesenchyme of the mutant. Dramatic re-

duction of *Afp*-positive cells at E12.5 confirmed the complete failure to expand this hepatic cell population in the mutant. In summary, hepatic specification occurred normally in *Tbx3*^{-/-} embryos. However, the hepatic primordium failed to expand and to delaminate hepatoblasts into the underlying mesenchyme.

***Tbx3* Is Strongly Expressed in the Liver Bud.** We performed section *in situ* hybridization analysis to correlate the spatio-temporal profile of *Tbx3* expression with the phenotypical changes in the mutant (Fig. 3). *Tbx3* messenger RNA (mRNA) was first detected at low levels in the hepatic endoderm at the 18-somite stage (E9.0). *Tbx3* expression was strongly up-regulated at the 23-somite stage (E9.5) and completely overlapped expression of *Afp* in the liver bud. At E10.5, *Tbx3* was markedly down-regulated and confined to hepatoblasts populating the hepatic lobes. From E12.5, *Tbx3* expression was barely detectable in the liver by *in situ* hybridization analysis. Hence, the profile of *Tbx3* expression is compatible with

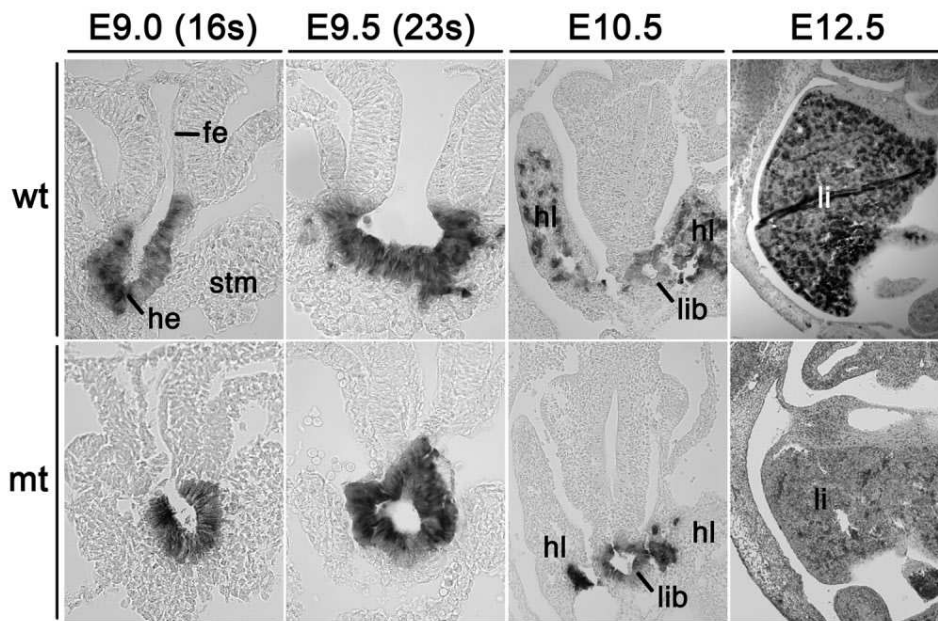


Fig. 2. Hepatic development is disrupted at the emergent liver bud stage in *Tbx3*^{-/-} mice. *In situ* hybridization analysis of *Afp*-expression on transverse sections at the foregut level of wild-type (wt) and *Tbx3*^{-/-} (mt) embryos during liver development. Stages are as indicated in the figure, dorsal is oriented up. *Afp*-expression shows that hepatic fate is specified in the *Tbx3*-deficient foregut endoderm, but delamination of hepatoblasts does not occur. Abbreviations: fe, foregut endoderm; he, hepatic endoderm; hl, hepatic lobe; lib, liver bud; li, liver; stm, septum transversum mesenchyme.

a primary role of *Tbx3* in hepatoblast expansion, migration, or differentiation during liver bud development.

Proliferation Defects in the *Tbx3*^{-/-} Liver Bud.

To evaluate whether changes of cellular proliferation rates may underlie the morphological defects in liver bud expansion in *Tbx3*^{-/-} embryos, we performed a BrdU incorporation assay that detects cells in S-phase of the cell cycle

(Fig. 4A). At the 18-somite stage (E9.0), when *Tbx3* is only weakly expressed, labeling indices of epithelial cells of wild-type and mutant hepatic endoderm were similar. Proliferation in the lateral and dorsal foregut endoderm was higher than that in the hepatic endoderm at this stage but, as expected, was not significantly altered between the two genotypes. At the 23-somite stage, the BrdU labeling

Fig. 3. *Tbx3* is strongly expressed in the liver bud. Analysis of *Tbx3* expression during early liver development by RNA *in situ* hybridization on transverse sections of wild-type embryos at the foregut level. Dorsal is oriented up. Developmental stages are as indicated in the figure. *Tbx3* expression is low in the pseudo-stratified epithelium of the hepatic endoderm (E9.0) but is strongly up-regulated in the hepatic endoderm during expansion of the liver bud and delamination of hepatoblasts into the stroma (E9.25-E9.5). Expression in hepatoblasts is strongly reduced at E10.5, and barely detected at later stages. Abbreviations are as in Fig. 2.

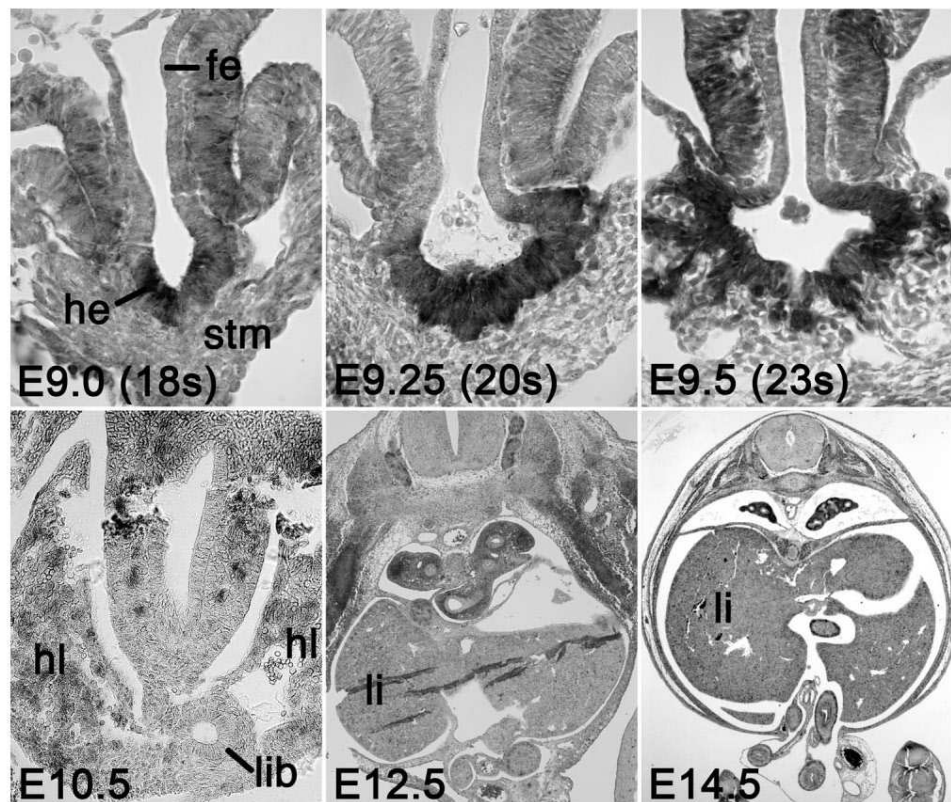
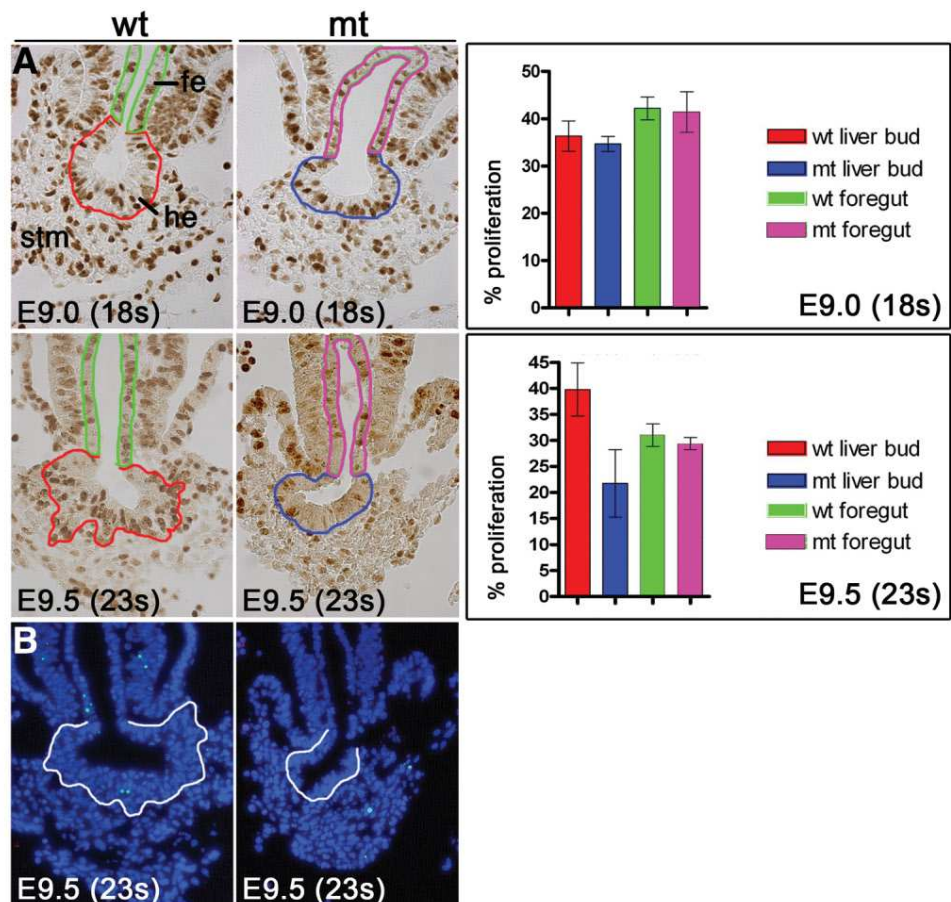


Fig. 4. Proliferation of hepatic endoderm is severely reduced in *Tbx3*^{-/-} embryos. (A) Analysis of cell proliferation in hepatic and lateral foregut endoderm performed on transverse sections of wild-type (wt) and *Tbx3*-mutant embryos (mt) at E9.0 (18-somite stage, 18s) and E9.5 (23s) by immunohistochemistry for BrdU. Quantified regions, the epithelium of the lateral foregut, and the hepatic epithelium of the liver primordium, respectively, are marked by colors. Statistical analysis of proliferation rates (% proliferation, as defined by the ratio of BrdU-positive cells to total cell number in the analyzed area) at E9.0 and E9.5 of regions and genotypes as color-coded. Proliferation rates between wild-type and mutant differ significantly in the hepatic endoderm but remain similar in the foregut endoderm that is devoid of *Tbx3* expression at E9.5. (B) Terminal deoxynucleotidyl transferase-mediated nick-end labeling staining for apoptosis (white outline) in the hepatic endoderm (white outline) at E9.5 (23s) does not reveal differences between wild-type and *Tbx3*-mutant embryos. Abbreviations are as in Fig. 2.



index remained high in the wild-type liver bud, exceeding the value of the lateral foregut endoderm considerably. The proliferation rate in the mutant hepatic endoderm reached only half of the wild-type level and was severely decreased in comparison with the adjacent foregut endoderm. Terminal deoxynucleotidyl transferase-mediated nick-end labeling staining showed that apoptosis was unaffected in mutant liver at this stage (Fig. 4B). Hence, severe reduction of cell proliferation in the hepatic epithelium at E9.5 is likely to cause the failure of hepatoblast liver bud expansion in *Tbx3*^{-/-} mice.

Expression of Cell-Cycle Regulators Is Unchanged in *Tbx3*-Deficient Liver Buds. Several studies have implicated *Tbx3* in the control of the cell cycle by direct repression of genes encoding inhibitors of cell-cycle-dependent kinases. To uncover the primary molecular changes that may underlie the proliferation defect of the *Tbx3*^{-/-} hepatic endoderm, we analyzed expression of a number of genes encoding cell-cycle regulators by in situ hybridization analysis in the liver bud at E9.5 when morphological differences were manifested (Supporting Fig. 1A). Expression of *p15^{INK4b}*, *p16^{INK4a}*, *p18^{INK4c}*, *p19^{INK4d}*, *p19^{Arf}*, and *p27^{Kip1}* was detected in the hepatic endoderm of neither wild-type

nor mutant embryos, although extrahepatic expression domains confirmed the quality of probes and experimental conditions. Expression of *p21^{Cip1}* was found throughout the hepatic and foregut endoderm in either genotype. *p57^{Kip2}* was expressed in the hepatic endoderm and in the underlying mesenchyme in wild-type and indistinguishably in mutant embryos.

Targeted mutations have demonstrated the requirement for the genes encoding hepatocyte growth factor (*Hgf*) and its receptor *c-Met* for proliferation or survival of hepatocytes.¹² Expression of *c-Met* in the hepatic endoderm, and of *Hgf* in the underlying mesenchyme was unaltered in the mutant. Expression of the proto-oncogene *c-Myc*, and of the genes encoding the cell cycle regulator cyclin D1 (*Ccnd1*) and the forkhead transcription factor *Foxm1* were similarly unaffected (Supporting Fig. 1B).

Quantitative PCR on reverse-transcribed mRNA isolated from E9.5 liver buds (qRT-PCR) independently confirmed that expression levels of the cell cycle regulators *p19^{Arf}*, *p21^{Cip1}*, *p27^{Kip1}*, *Cdk1*, and *CyclinD1* are unchanged in *Tbx3*^{-/-} liver buds (Supporting Fig. 1C). Therefore, it is unlikely that phenotypical defects in *Tbx3*^{-/-} liver buds are an immediate consequence of

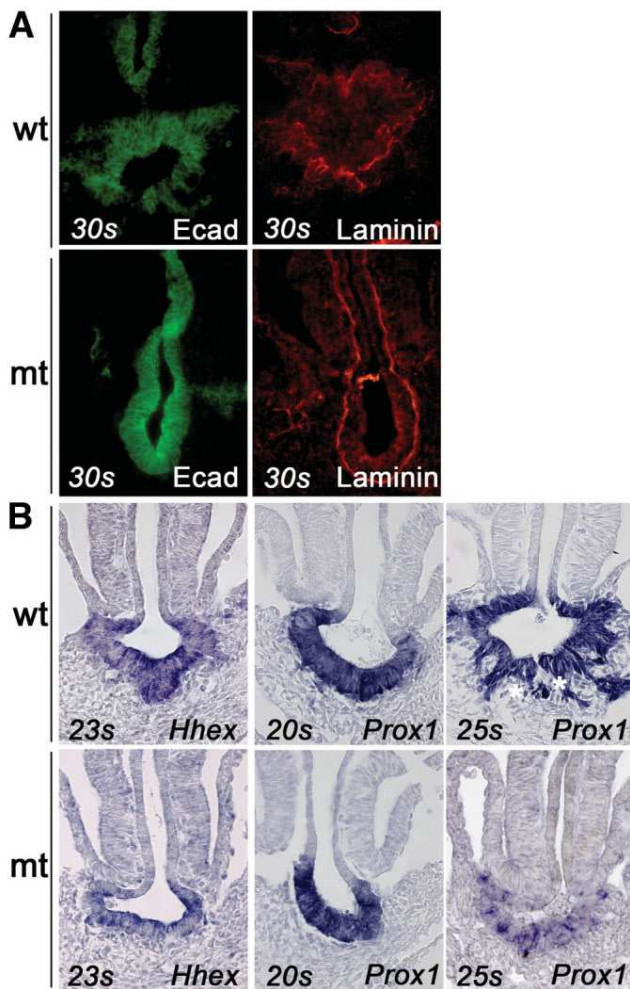


Fig. 5. *Tbx3* controls hepatoblast migration. (A) Immunofluorescent detection of E-cadherin and laminin expression on transverse sections through the foregut region of wild-type (wt) and *Tbx3*^{-/-} embryos (mt) at the 30-somite stage. Expression of both antigens remains high in the mutant liver bud. (B) *In situ* hybridization analysis for hematopoietically expressed homeobox 1 and *Prox1* expression in the hepatic epithelium at the indicated stages. *Prox1* expression is severely down-regulated at the 25-somite stage.

transcriptional deregulation of these cell-cycle regulators, particularly p19^{Arf}.

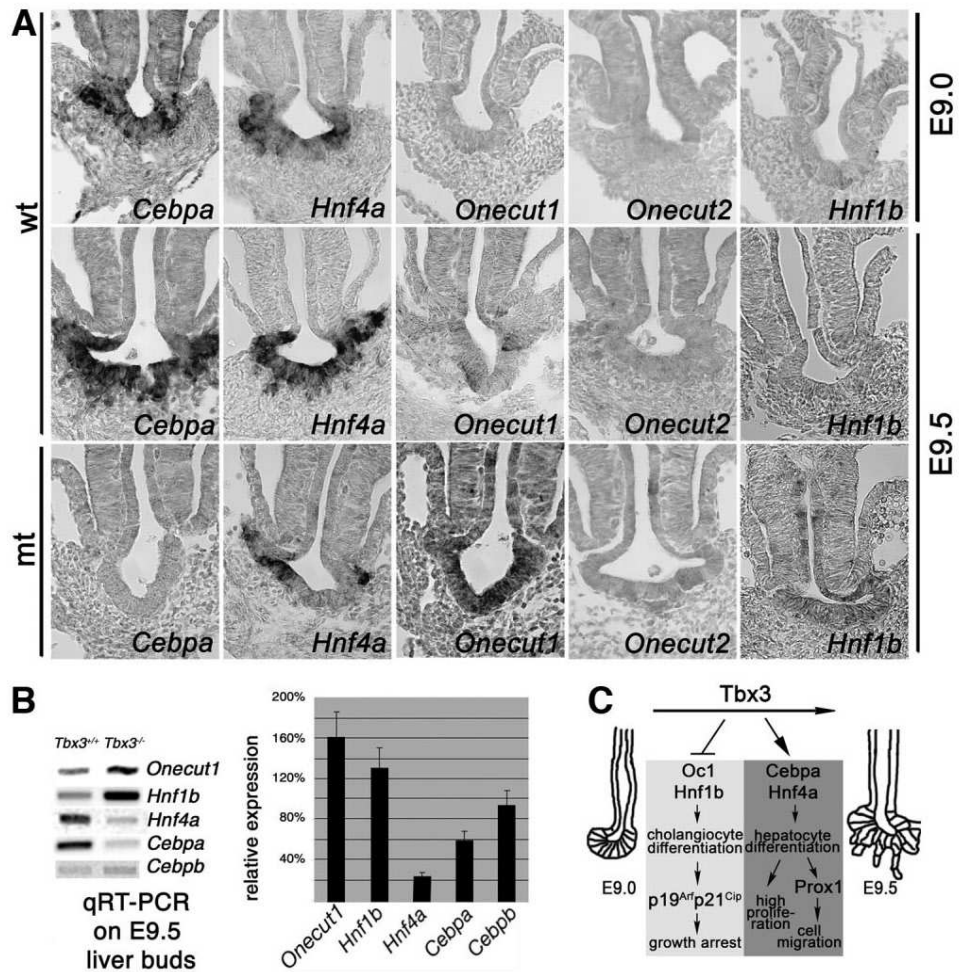
Hepatoblast Migration Requires *Tbx3*. After establishment of the pseudo-stratified hepatic epithelium at E9.0, tissue protrusions arise from which hepatoblasts delaminate. This process is accompanied by down-regulation of the cell adhesion molecule E-cadherin and disintegration of the basal lamina (Fig. 5A). In *Tbx3*-mutant embryos, hepatic cords did not protrude from the liver bud, and hepatoblasts failed to invade the underlying septum transversum mesenchyme. E-cadherin remained high in the hepatic epithelium at the 30s-stage, and the basal lamina that surrounded it stayed intact (Fig. 5A). To score for molecular changes

instrumental in this phenotype, we analyzed expression of genes regulating migration of hepatoblasts. Expression of *hematopoietically expressed homeobox* that regulates the transition from a columnar to a pseudo-stratified epithelium¹³ was unchanged in the *Tbx3*-deficient liver bud at E9.5 (Fig. 5B). Similarly, expression of the genes encoding the H2.0-like homeodomain protein (Hlx) and the Zn-finger transcription factors GATA-binding proteins 4 and 6 (*Gata4* and *Gata6*)^{14,15} was unaltered in the mesenchyme of the septum transversum region (Supporting Fig. 2). In *Prospero-related homeobox 1* (*Prox1*) mutant mice, proliferation of hepatoblasts is decreased and delamination from the hepatic diverticulum is disturbed.¹⁶ Expression of *Prox1* in the *Tbx3*^{-/-} hepatic epithelium was unchanged at E9.0 but severely down-regulated at E9.5 (Fig. 5B). Thus, failure of migration of hepatoblasts into the surrounding mesenchyme may be caused by the inability to maintain *Prox1* expression.

Hepatic Differentiation Defects in *Tbx3*^{-/-} Embryos. Absence of *albumin*-expressing hepatocytes but presence of Ck18-positive cholangiocytes at E14.5 (Fig. 1C,D) indicated that the hepatoblast lineage decision was affected in *Tbx3*-deficient livers. To determine the temporal onset of differentiation defects and their possibly causal relation with the observed cellular defects in proliferation and migration of hepatoblasts, we analyzed expression of a panel of genes central to hepatocyte and cholangiocyte lineage decision, respectively, at E9.0 and at E9.5, that is, before and at the onset of phenotypic changes in the *Tbx3*^{-/-} liver bud (Fig. 6A).

CCAAT/enhancer binding protein (C/EBP), alpha (*Cebpa*) and hepatic nuclear factor 4a (*Hnf4a*) encode transcription factors that are involved in the early stages of hepatocyte differentiation,¹⁷⁻¹⁹ whereas the transcriptional regulators *Onecut1* (*Hnf6*), *Onecut2*, and *Hnf1b* control cholangiocyte differentiation.²⁰⁻²² At E9.0, *Cebpa* and *Hnf4a* were expressed in the hepatic endoderm, whereas expression of *Onecut1*, *Onecut2*, and *Hnf1b* was hardly detected. In the hepatic epithelium of E9.5 wild-type embryos, hepatocyte genes *Hnf4a* and *Cebpa* were strongly expressed, whereas expression of *Onecut1*, *Onecut2*, and *Hnf1b* was not detected, arguing that hepatoblasts started to differentiate into hepatocytes. Down-regulation of *Cebpa* and *Hnf4a* and up-regulation of *Hnf1b* and *Onecut1* expression in the *Tbx3*^{-/-} hepatic epithelium suggest that hepatoblast differentiation became redirected to cholangiocytes. QRT-PCR analysis on mRNA obtained from E9.5 liver buds independently confirmed the observed changes of expression (Fig. 6B). Expression of *Pdx1*, a marker for pancreatic fate,²³ was unchanged in the *Tbx3*^{-/-} embryo (Supporting Fig. 2),

Fig. 6. Hepatobiliary differentiation is affected in the hepatic endoderm of *Tbx3*^{-/-} mice. (A) *In situ* hybridization analysis of expression of genes controlling hepatic differentiation on transverse sections through the foregut region of wild-type (wt) and *Tbx3*^{-/-} (mt) embryos at E9.0 and E9.5. Dorsal is oriented up. Genotypes, probes, and stages are as indicated in the figure. (B) QRT-PCR analysis of marker genes on mRNA from E9.5 liver buds. Expression levels are relative to wild-type (100%). Expression of *Cebpa* and *Hnf4a* is down-regulated, *Onecut1* and *Hnf1b* expression is up-regulated in the E9.5 *Tbx3*^{-/-} liver bud, indicating that the hepatocyte fate is lost at the expense of the cholangiocyte fate. (C) Scheme for the role of Tbx3 in liver development. Tbx3 promotes the progression from the pseudo-stratified epithelium (E9.0) to a cell-emergent liver bud (E9.5). Cholangiocyte differentiation is prevented by repression of *Onecut1* (and its target *Hnf1b*), whereas *Cebpa* and *Hnf4a* expression is maintained, leading to differentiation of hepatocytes with their high proliferation and migration potential.



arguing against an expansion of pancreatic fates into the liver region. Expression of the gene encoding the signaling molecule Sonic hedgehog (*Shh*) remained excluded from the hepatic endoderm in the *Tbx3*-mutant embryo (Supporting Fig. 2), indicating that deregulation of *Sonic hedgehog* does not underlie this hepatic phenotype as proposed for *hematopoietically expressed homeobox*-mutant mice.¹³

Together these findings suggest that *Tbx3* controls hepatic development by suppressing cholangiocyte and favoring hepatocyte differentiation in the liver bud at E9.5 (Fig. 6C).

***Tbx3* and *Onecut1* Antagonistically Regulate Hepatobiliary Fate Decision.** To further decipher the molecular pathways regulated by *Tbx3* in hepatoblast differentiation, we employed overexpression approaches in cellular systems (Fig. 7). For loss-of-function experiments, we used a *Tbx2-VP16* expression construct encoding the *Tbx2* DNA-binding domain in fusion with the viral transcriptional activation domain VP16. *Tbx2-VP16* competes with *Tbx3* for the same conserved DNA binding sites and activates transcription, thus acting as a dominant negative version of the transcriptional repressor

Tbx3. We performed overexpression experiments with *Tbx3* and *Onecut1* to analyze the role of either factor in cholangiocyte differentiation in both the hepatoblast cell line 9A1¹⁰ and the hepatoma cell line Hepa1-6.²⁴ Semi-quantitative RT-PCR was used to judge the changes in expression of hepatocyte (*albumin*) and cholangiocyte (*Ck7*)²⁵ differentiation markers, of transcriptional regulators for the hepatocyte (*Hnf4a*, *Cebpa*) and cholangiocyte lineage (*Onecut1*), and for the cell cycle inhibitor *p19^{Arf}*. Overexpression of *Tbx3* in 9A1 hepatoblasts led to increased levels of *Hnf4a* and *Cebpa* whereas expression of *Tbx2-VP16* resulted in downregulation of *Hnf4a*, *Cebpa* and *albumin* (Fig. 7A). This supports the *in vivo* analysis and suggests that *Tbx3* is required to maintain and enhance hepatocyte differentiation. Because *Tbx2-VP16* represents a constitutive transcriptional activator, downregulation of *Hnf4a* and *Cebpa* is compatible with the notion that *Tbx3* functions indirectly by repressing a transcriptional repressor of these genes. Transfection of a *Onecut1* expression construct similarly resulted in downregulation of *Hnf4a* and *Cebpa* (Fig. 7A). Inhibition of *Tbx3* function by *Tbx2-VP16* in the hepatocyte cell line

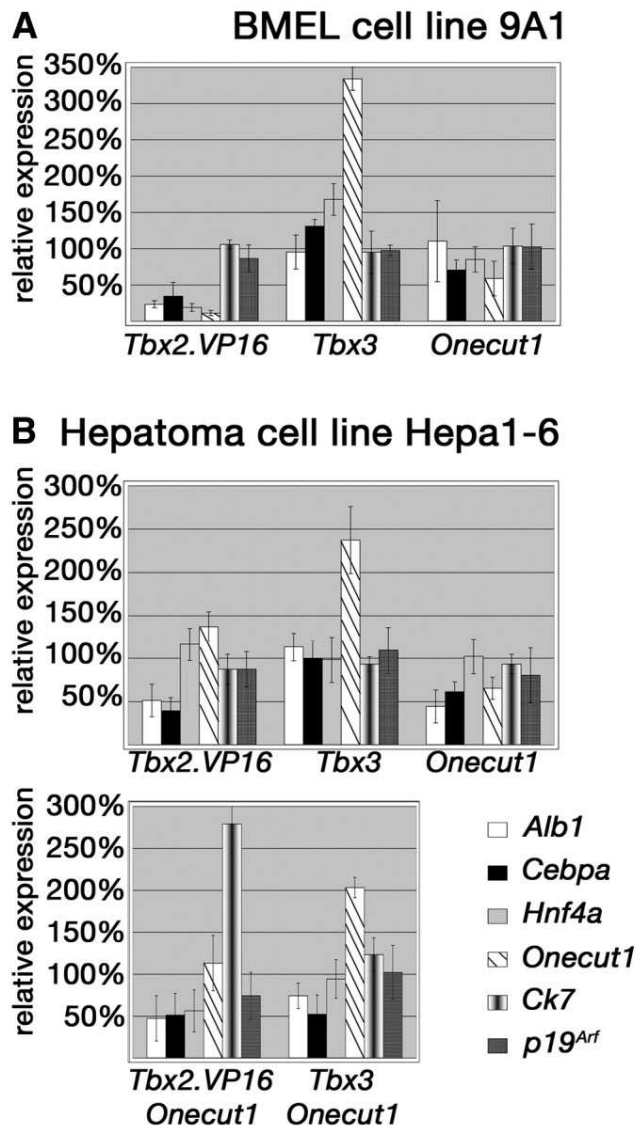


Fig. 7. Tbx3 and Onecut1 antagonistically regulate hepatobiliary fate decision in cellular systems. Analysis of marker gene expression by qRT-PCR in the hepatoblast cell line 9A1 (A) and the hepatoma cell line Hepa1-6 (B) 48 hours posttransfection with expression constructs for Tbx3, Tbx2-VP16 (a dominant-negative version of Tbx3), Onecut1, and their combinations. Messenger RNA expression of indicated markers is shown relative to the empty vector control. Tbx3 enhances and maintains hepatocyte marker expression, whereas Onecut1 down-regulates hepatocyte markers and up-regulates in combination with Tbx2-VP16 the cholangiocyte marker gene *Ck7*.

Hepa1-6 also resulted in the repression of hepatocyte marker genes, arguing that continued albeit low-level expression of Tbx3 is required to maintain the phenotype of hepatocytes (Fig. 7B). Cotransfection of Onecut1 in these cells further repressed *Hnf4a* expression and activated the cholangiocyte differentiation marker *Ck7*, robustly suggesting that inhibition of *Tbx3* and activation of *Onecut1* synergize in (trans-) differentiation into cholangiocytes (Fig. 7B). However, it is unlikely that endogenous Onecut1 mediates Tbx3 function

on hepatocyte marker genes in these cellular systems, because *Onecut1* expression was surprisingly activated by Tbx3 in all cell lines tested (Fig. 7). Levels of *p19^{Arf}* were unaffected by changes of Tbx3 and Onecut1 expression, providing additional evidence that *p19^{Arf}* is not involved in the hepatobiliary lineage decision.

In summary, our *in vitro* experiments further support the role of Tbx3 in the maintenance of hepatocyte differentiation by controlling an early transcription factor network. They indicate an important role of Onecut1 as an inducer of cholangiocyte differentiation.

Discussion

Differentiation of hepatoblasts in hepatocytes and bile duct cells is temporally and spatially separated during liver development. Although the bulk of hepatoblasts in the liver bud differentiates into hepatocytes, cholangiocytes derive from a group of hepatoblasts located in proximity to the portal vein.^{26,27} In the latter case, the existence of inducing signals from the mesenchyme surrounding the portal vein has been suggested,²⁸ whereas it was less clear how hepatocyte differentiation is favored in early liver development. Here, we have identified Tbx3 as a transcriptional regulator of hepatobiliary lineage decision in the liver bud. We propose that Tbx3 maintains the hepatocyte and suppresses the cholangiocyte lineage by antagonistically regulating expression of transcription factor genes required for either differentiation pathway. Proliferation and migration defects in the *Tbx3*-deficient liver bud are a consequence rather than a cause of aberrant cell differentiation.

A Primary Function of Tbx3 in Hepatobiliary Cell Fate Decision. We found changes in the gene expression pattern of the epithelium of the *Tbx3*-deficient liver bud, including down-regulation of *Hnf4a*, *Cebpa*, and the hepatocyte marker *albumin*, and up-regulation of *Onecut1*, *Hnf1b*, and the biliary marker CK18 at later stages that are fully compatible with the notion that Tbx3 controls hepatobiliary fate decision by antagonistically regulating expression of key transcriptional mediators of the hepatocyte and cholangiocyte pathways. On the molecular level, gene expression and cell fate changes can be rationalized by two opposing models. First, *Tbx3* is primarily required to maintain expression of *Cebpa* and *Hnf4a*; thus, the hepatocyte gene program in the hepatic epithelium.^{2,19,27} Down-regulation of *Cebpa* in *Tbx3* mutants may cause premature biliary differentiation, and the increase in *Hnf6* and *Hnf1b* expression might be secondary to *Cebpa* misregulation. This model is supported by the temporal profile of loss of *Cebpa* expression and the known role of *Cebpa* as a suppressor of cholangiocyte differentiation.²⁸ However, it requires the presence of a transcriptional me-

diator because Tbx3 is a bona fide transcriptional repressor.²⁹ Indeed, our cell culture experiments with a dominant-negative form of Tbx3, Tbx2-VP16, argue for the presence of a Tbx3-repressed transcriptional repressor of *Hnf4a* and *Cebpa* transcription. In a second model, Tbx3 is primarily required to suppress the cholangiocyte gene program. Up-regulation of transcriptional regulators of cholangiocyte differentiation including *Onecut1* and its target *Hnf1b*^{20,22} in *Tbx3*^{-/-} embryos may result in cholangiocyte differentiation, which in turn represses *Cebpa* and *Hnf4* expression and hepatocyte differentiation. This model gains support from a number of experimental findings. First, up-regulation of *Onecut1* expression directly correlates with the expression profile of *Tbx3* and the temporal onset of defects in the *Tbx3*-deficient embryo. Second, ectopic expression of *Onecut1* in hepatoblasts and hepatocytes represses transcription of *Hnf4a* and *Cebpa* and enhances the effect of Tbx3 inhibition on cholangiocyte differentiation. Third, up-regulation of *Onecut1* is compatible with the nature of Tbx3 as a repressor of transcription and does not need further intermediary steps. Although a direct regulation of *Onecut1* by Tbx3 is circumstantially supported by the finding that the closely related gene *Onecut2* is a direct target of the T-domain protein Tbet,³⁰ we currently have no molecular evidence for such a mode of regulation. Indeed, the up-regulation of *Onecut1* in Tbx3-overexpressing cells seems to contradict this assumption. We currently cannot resolve the discrepancy between the regulation of *Onecut1* by Tbx3 *in vivo* and *in vitro*. Possibly, the cellular system is inadequate to fully reflect the endogenous regulation by Tbx3 because of lack of cofactors present in the early liver bud. Future work will analyze the possibility of combinatorial regulation of *Onecut1* by Tbx3 and other transcriptional regulators.

As a third possibility, Tbx3 may simultaneously maintain hepatocyte and suppress cholangiocyte differentiation. This may be achieved by independently maintaining the transcription of regulators of hepatocyte differentiation and repressing regulatory genes for cholangiocyte differentiation.

Proliferation and Migration Defects in the Tbx3-Deficient Liver Bud Are Secondary to Cell Fate Changes. Recent analysis of *Tbx3*-mutant hepatoblasts suggested that the cell-cycle inhibitors p21^{Cip1} and p19^{Arf} might be primary molecular targets of Tbx3 function in the liver.⁶ This implied that proliferation and migration defects of hepatoblasts precede and cause aberrant cell differentiation.⁶ Our molecular analyses of *Tbx3* loss- and gain-of-function scenarios both *in vivo* and *in vitro*, however, clearly show that loss and gain of *Tbx3* expression does not result in immediate changes of cell-cycle regulators, including p19^{Arf} and p21^{Cip1}. Hence, proliferation and migration defects and up-regulation of p19^{Arf} are

likely to be secondary and late consequences of the cell fate changes in the liver bud.

We assume that severe reduction of cellular proliferation in the hepatic epithelium at E9.5 is a consequence of the failure to maintain *Cebpa* and *Hnf4a* expression, and thus hepatocyte fate. However, the molecular mediators of this phenotype remain unknown.

In *Tbx3*^{-/-} embryos, delamination of hepatoblasts failed, the laminin-rich membrane around the liver bud remained intact, and cells of the hepatic epithelium retained strong expression of E-cadherin. This phenotype mimics the findings in *Prox1*^{-/-} animals¹⁶ and suggested an epistatic relation between the two genes in liver development. Intriguingly, *Prox1* expression was established normally in *Tbx3*^{-/-} embryos, but expression dramatically declined from E9.5 on. Hence, Tbx3 does not establish *Prox1* expression but is indirectly required for its maintenance. Because *Prox1* remains continuously expressed in hepatocytes but is lost from cholangiocytes,³¹ down-regulation of *Prox1* in the mutant is likely to reflect the hepatoblast fate switch at E9.5. The fact that *Prox1* suppresses gallbladder-specific genes may further contribute to or reinforce cholangiocyte differentiation in *Tbx3* mutants.³²

Intriguingly, *Onecut1*, whose expression is up-regulated in the *Tbx3*-deficient liver bud, has been implicated in both cell proliferation and migration in ways contrary to our findings. It was previously shown that forced expression of *Onecut1* stimulates hepatocyte proliferation and leads to increased expression of *hepatocyte growth factor-alpha*, *cyclin D1*, and *Foxm1* in mature hepatocytes.³³ Hence, increased expression of *Onecut1* in the *Tbx3*-deficient liver bud should stimulate proliferation by increased expression of these target genes. Yet, proliferation in the *Tbx3*-mutant liver bud is reduced and *hepatocyte growth factor-alpha*, *cyclin D1*, and *Foxm1* expression was unchanged. We cannot explain the discrepancy of these findings but suggest that *Onecut1* transcriptional activity may depend on cofactors as shown before for the activation of *Foxa2* transcription by a *Onecut1/Cebpa* binary complex.³⁴ Because *Cebpa* is dramatically reduced in the *Tbx3*-deficient liver bud, it is plausible that *Onecut1* transcriptional activity may shift by changed complex formation.

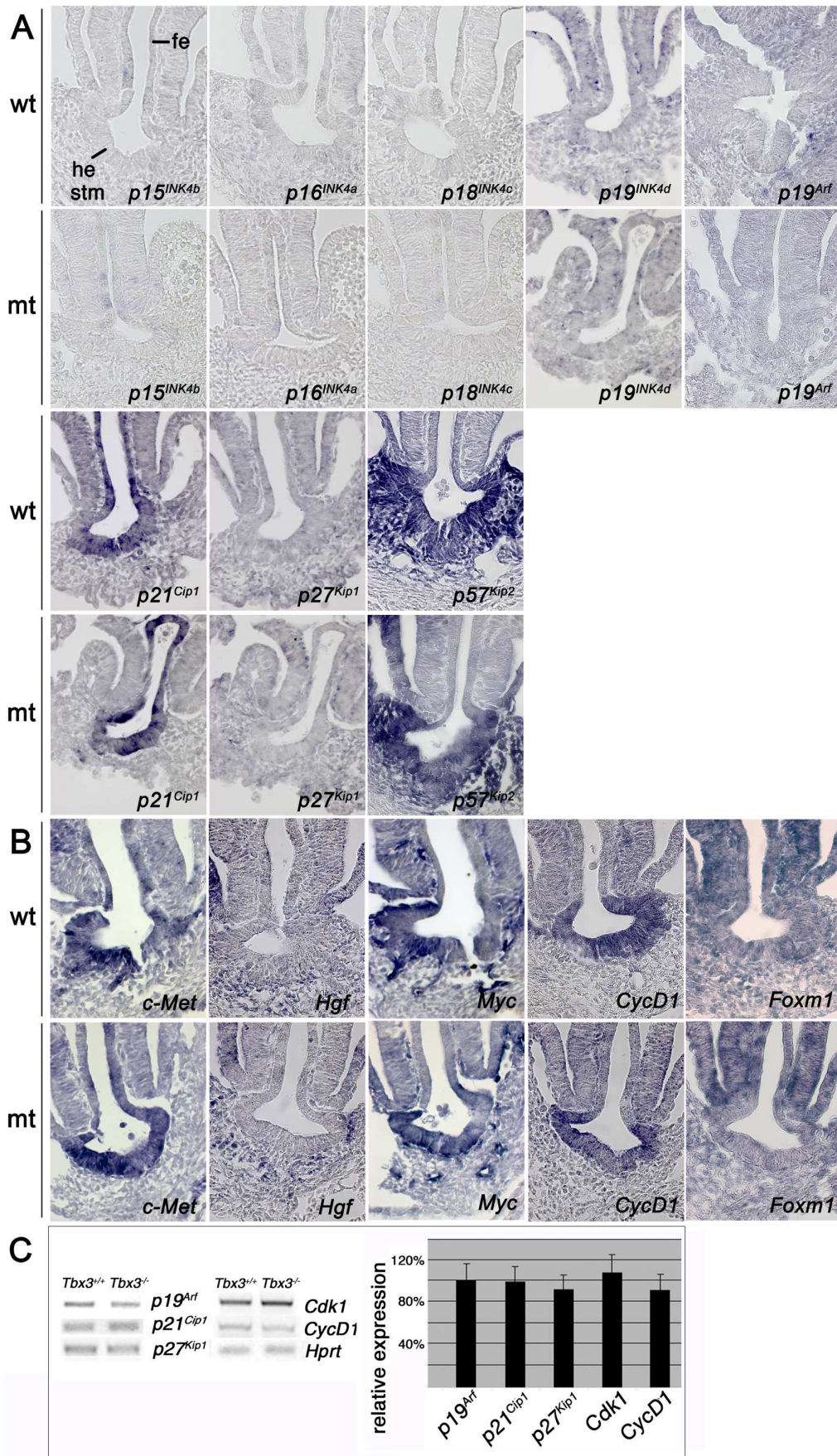
In *Oc1/Oc2* double mutants, the basal lamina surrounding the liver bud remains intact, and hepatoblasts fail to delaminate from the epithelium.²¹ Up-regulation of *Onecut1* in the *Tbx3*-deficient liver buds makes it unlikely that the two factors are causally involved in the proliferation and migration defects. We favor instead that down-regulation of *Prox1* may cause this phenotype. It is currently unclear whether *Prox1* and *Oc1/Oc2* act independently in liver bud expansion or whether they represent independent pathways.

Our *in situ* hybridization analysis has shown that high *Tbx3* expression is confined to a short time window in hepatic development and tightly correlates with the onset of morphological and molecular changes in *Tbx3*-mutant livers at E9.5. Yet, our overexpression experiments in hepatoma cells argue that low-level expression of *Tbx3* in mature hepatocytes is required to maintain the fate of these cells and prevent trans-differentiation into cholangiocytes. Conditional ablation of *Tbx3* at later time points may open avenues to further analyze its role in liver development and homeostasis.

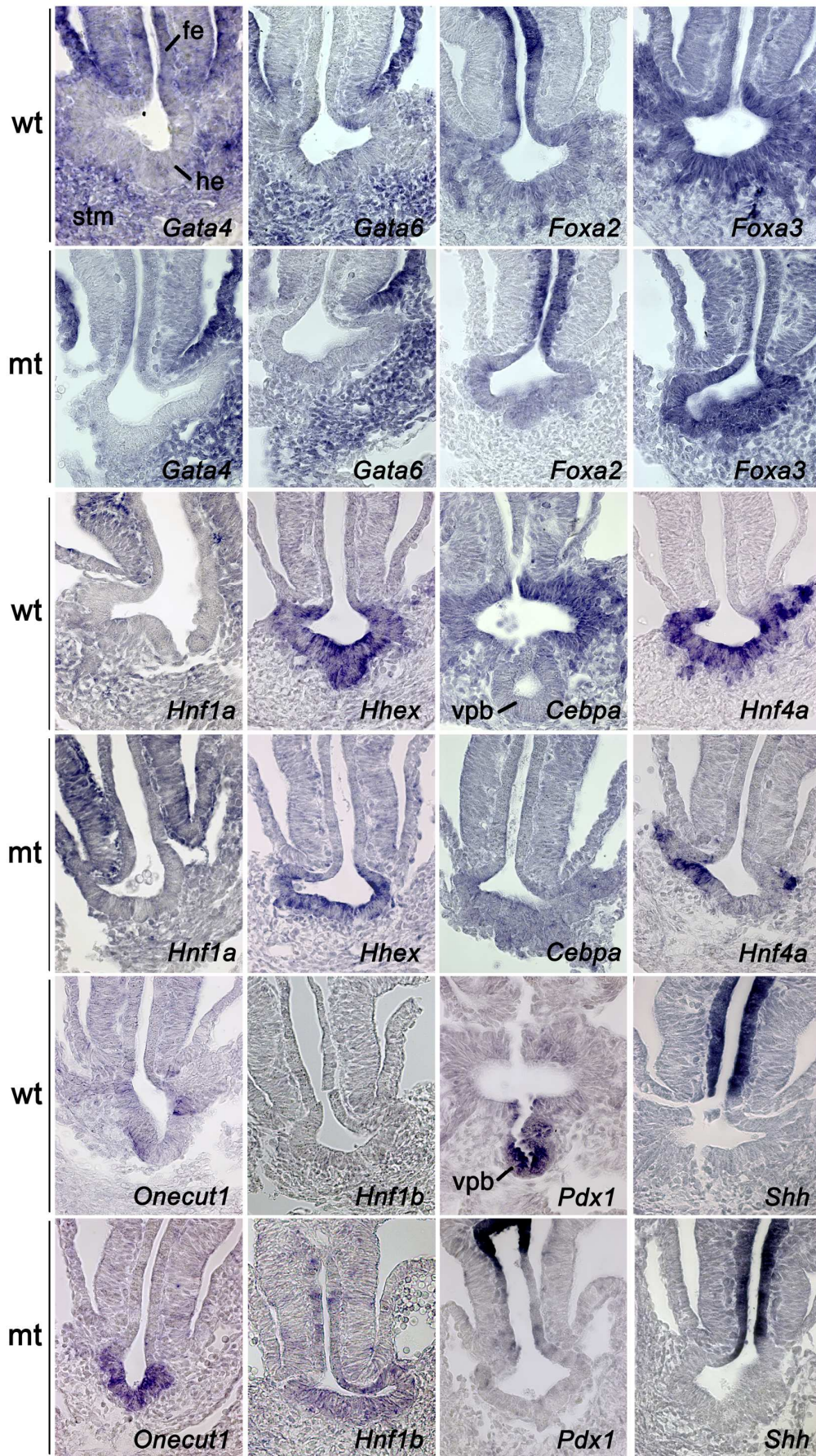
Acknowledgments: The authors thank Dr. D. Tosh for providing us with complementary DNAs for *Cebpa* and *Hnf4a*, Dr. C. J. Sherr for plasmids with various *INK4* DNAs, M.C. Weiss and U. Kossatz-Böhlert for cells, Dr. R. Kemler for antibodies, H. Farin for practical advice, and H. Farin, M.-O. Trowe, and N. Malek for discussion and critical reading of the manuscript.

References

- Spagnoli FM, Amicone L, Tripodi M, Weiss MC. Identification of a bipotential precursor cell in hepatic cell lines derived from transgenic mice expressing cyto-met in the liver. *J Cell Biol* 1998;143:1101-1112.
- Zaret KS. Regulatory phases of early liver development: paradigms of organogenesis. *Nat Rev Genet* 2002;3:499-512.
- Spear BT, Jin L, Ramasamy S, Dobierzevska A. Transcriptional control in the mammalian liver: Liver development, perinatal repression, and zonal gene regulation. *Cell Mol Life Sci* 2006;63:2922-2938.
- Bamshad M, Lin RC, Law DJ, Watkins WC, Krakowiak PA, Moore ME, et al. Mutations in human *TBX3* alter limb, apocrine and genital development in ulnar-mammary syndrome. *Nat Genet* 1997;16:311-315.
- Davenport TG, Jerome-Majewska LA, Papaioannou VE. Mammary gland, limb and yolk sac defects in mice lacking *Tbx3*, the gene mutated in human ulnar mammary syndrome. *Development* 2003;130:2263-2273.
- Suzuki A, Sekiya S, Buscher D, Izpisua Belmonte JC, Taniguchi H. *Tbx3* controls the fate of hepatic progenitor cells in liver development by suppressing p19ARF expression. *Development* 2008;135:1589-1595.
- Hoogaars WM, Engela A, Brons JF, Verkerk AO, de Lange FJ, Wong LY, et al. *Tbx3* controls the sinoatrial node gene program and imposes pacemaker function on the atria. *Genes Dev* 2007;21:1098-1112.
- Moorman AF, Houweling AC, de Boer PA, Christoffels VM. Sensitive nonradioactive detection of mRNA in tissue sections: novel application of the whole-mount *in situ* hybridization protocol. *J Histochem Cytochem* 2001;49:1-8.
- Bussen M, Petry M, Schuster-Gossler K, Leitges M, Gossler A, Kispert A. The T-box transcription factor *Tbx18* maintains the separation of anterior and posterior somite compartments. *Genes Dev* 2004;18:1209-1221.
- Strick-Marchand H, Weiss MC. Inducible differentiation and morphogenesis of bipotential liver cell lines from wildtype mouse embryos. *HEPATOLOGY* 2002;36:794-804.
- Farin HF, Bussen M, Schmidt MK, Singh MK, Schuster-Gossler K, Kispert A. Transcriptional repression by the T-box proteins *Tbx18* and *Tbx15* depends on groucho corepressors. *J Biol Chem* 2007;282:25748-25759.
- Huh CG, Factor VM, Sanchez A, Uchida K, Conner EA, Thorgeirsson SS. Hepatocyte growth factor/c-met signaling pathway is required for efficient liver regeneration and repair. *Proc Natl Acad Sci U S A* 2004;101:4477-4482.
- Bort R, Signore M, Tremblay K, Martinez Barbera JP, Zaret KS. Hex homeobox gene controls the transition of the endoderm to a pseudostratified, cell emergent epithelium for liver bud development. *Dev Biol* 2006;290:44-56.
- Watt AJ, Zhao R, Li J, Duncan SA. Development of the mammalian liver and ventral pancreas is dependent on GATA4. *BMC Dev Biol* 2007;7:37.
- Zhao R, Watt AJ, Li J, Luebke-Wheeler J, Morrissy EE, Duncan SA. GATA6 is essential for embryonic development of the liver but dispensable for early heart formation. *Mol Cell Biol* 2005;25:2622-2631.
- Sosa-Pineda B, Wigle JT, Oliver G. Hepatocyte migration during liver development requires Prox1. *Nat Genet* 2000;25:254-255.
- Flodby P, Barlow C, Kylefjord H, Ahrlund-Richter L, Xanthopoulos KG. Increased hepatic cell proliferation and lung abnormalities in mice deficient in CCAAT/enhancer binding protein alpha. *J Biol Chem* 1996;271:24753-24760.
- Tomizawa M, Garfield S, Factor V, Xanthopoulos KG. Hepatocytes deficient in CCAAT/enhancer binding protein alpha (C/EBP alpha) exhibit both hepatocyte and biliary epithelial cell character. *Biochem Biophys Res Commun* 1998;249:1-5.
- Li J, Ning G, Duncan SA. Mammalian hepatocyte differentiation requires the transcription factor HNF-4alpha. *Genes Dev* 2000;14:464-474.
- Coffinier C, Gresh L, Fiette L, Tronche F, Schutz G, Babinet C, et al. Bile system morphogenesis defects and liver dysfunction upon targeted deletion of HNF1beta. *Development* 2002;129:1829-1838.
- Margagliotti S, Clotman F, Pierreux CE, Beaudry JB, Jacquemin P, Rousseau GG, et al. The oncut transcription factors HNF-6/OC-1 and OC-2 regulate early liver expansion by controlling hepatoblast migration. *Dev Biol* 2007;311:579-589.
- Clotman F, Lannoy VJ, Reber M, Cereghini S, Cassiman D, Jacquemin P, et al. The oncut transcription factor HNF6 is required for normal development of the biliary tract. *Development* 2002;129:1819-1828.
- Hale MA, Kagami H, Shi L, Holland AM, Ekasser HP, Hammer RE, et al. The homeodomain protein PDX1 is required at mid-pancreatic development for the formation of the exocrine pancreas. *Dev Biol* 2005;286:225-237.
- Darlington GJ, Bernhard HP, Miller RA, Ruddle FH. Expression of liver phenotypes in cultured mouse hepatoma cells. *J Natl Cancer Inst* 1980;64:809-819.
- Germain L, Blouin MJ, Marceau N. Biliary epithelial and hepatocytic cell lineage relationships in embryonic rat liver as determined by the differential expression of cytokeratins, alpha-fetoprotein, albumin, and cell surface-exposed components. *Cancer Res* 1988;48:4909-4918.
- Lemaigre FP. Development of the biliary tract. *Mech Dev* 2003;120:81-87.
- Eeckhoutte J, Formstecher P, Laine B. Hepatocyte nuclear factor 4alpha enhances the hepatocyte nuclear factor 1alpha-mediated activation of transcription. *Nucleic Acids Res* 2004;32:2586-2593.
- Yamasaki H, Sada A, Iwata T, Niwa T, Tomizawa M, Xanthopoulos KG, et al. Suppression of C/EBPalpha expression in periportal hepatoblasts may stimulate biliary cell differentiation through increased *Hnf6* and *Hnf1b* expression. *Development* 2006;133:4233-4243.
- He M, Wen L, Campbell CE, Wu JY, Rao Y. Transcription repression by xenopus ET and its human ortholog *TBX3*, a gene involved in ulnar-mammary syndrome. *Proc Natl Acad Sci U S A* 1999;96:10212-10217.
- Furuno K, Ikeda K, Hamano S, Fukuyama K, Sonoda M, Hara T, et al. Oncut transcription factor OC2 is a direct target of T-bet in type-1 T-helper cells. *Genes Immun* 2008;9:302-308.
- Dudas J, Papoutsi M, Hecht M, Elmaouhoub A, Saile B, Christ B, et al. The homeobox transcription factor Prox1 is highly conserved in embryonic hepatoblasts and in adult and transformed hepatocytes, but is absent from bile duct epithelium. *Anat Embryol (Berl)* 2004;208:359-366.
- Papoutsi M, Dudas J, Becker J, Tripodi M, Opitz L, Ramadori G, et al. Gene regulation by homeobox transcription factor Prox1 in murine hepatoblasts. *Cell Tissue Res* 2007;330:209-220.
- Tan Y, Yoshida Y, Hughes DE, Costa RH. Increased expression of hepatocyte nuclear factor 6 stimulates hepatocyte proliferation during mouse liver regeneration. *Gastroenterology* 2006;130:1283-1300.
- Yoshida Y, Hughes DE, Rausa FM 3rd, Kim IM, Tan Y, Darlington GJ, et al. C/EBPalpha and HNF6 protein complex formation stimulates HNF6-dependent transcription by CBP coactivator recruitment in HepG2 cells. *HEPATOLOGY* 2006;43:276-286.



Supporting Fig. 1A



Supporting Fig. 1B

***Tbx3* is regulated by canonical Wnt signaling and represses NOTCH mediated biliary differentiation**

Timo H.-W. Lüdtkke¹, Henner F. Farin^{1,†}, Karin Schuster-Gossler¹, Marianne Petry¹, Vincent M. Christoffels², and Andreas Kispert^{1,*}

¹Institute for Molecular Biology, OE5250, Medizinische Hochschule Hannover, Carl-Neuberg-Str. 1, 30625 Hannover, Germany

²Department of Anatomy, Embryology and Physiology, Academic Medical Center, University of Amsterdam, Meibergdreef 15 L2-108, 1105 AZ Amsterdam, The Netherlands

[†]Present address: Hubrecht Institute, Uppsalalaan 8, 3584 CT Utrecht, The Netherlands

unpublished results

Running title: Regulation of *Tbx3*

Abstract

Bile duct formation in the mouse starts around embryonic day 13.5 with the formation of the ductal plate, a single layer of epithelial cells around the hepatic portal veins. Induced by *Jag1* expression in the endothelium of the veins, the surrounding hepatoblasts activate Notch-signaling and start to differentiate into cholangiocytes (biliary epithelial cells). *Tbx3* at this time point is already downregulated. Recently we have shown that *Tbx3* favors hepatocyte fate in the early liver bud. However, whether downregulation of *Tbx3* is a prerequisite to bile duct formation and how expression of *Tbx3* is regulated, in particular if it is repressed by Notch signals in this context, was unclear.

Here we show by loss- and gain-of-function experiments that ectopic expression of the with *Tbx3* biochemically identical and functional redundant *TBX2* potently inhibits cholangiocyte differentiation in the late phase of liver development and that Notch signaling from the portal veins does not repress *Tbx3* expression. Rather we identified canonical Wnt signaling as the initiator of *Tbx3*.

Conclusion: Canonical Wnt signaling via the expression of *Tbx3*, and Notch signaling opposingly regulate cholangiocyte differentiation and bile duct development in parallel pathways.

Introduction

Bile or gall produced in hepatocytes is necessary to emulsify fats and thereby is an essential adjuvant in the process of digestion of lipids in the small intestine. Liquid gall is carried from the liver to the intestine by the intrahepatic bile ducts (IHBD) and congenital malformations of the biliary system is a major cause of morbidity and mortality. In humans, mutations in the Notch ligand JAG1 or in the NOTCH2 receptor cause an autosomal-dominant disorder, the Alagille syndrome (AGS) that manifests in IHBD paucity and is associated with craniofacial defects and hypoplasia of the pulmonary artery (1-3).

Bile duct development in the mouse starts around E13.5 by the formation of a single biliary epithelial cell layer called the portal plate. Its formation is induced by Notch signaling activated by the ligand Jag1 in the endothelium of the portal veins, that commits adjacent hepatoblasts expressing several Notch receptors to the biliary fate(2, 7-9). Several studies have implicated Notch in the regulation of hepatoblast differentiation(4-6), indicating that Notch signaling might have an opposing function during liver development by favoring a biliary epithelial cell (BEC) fate decision. Intriguingly, timed differentiation of cholangiocytes around embryonic day (E) 13.5 and formation of the IHBD is attended by downregulation of *Tbx3* in the mouse(9).

Interestingly, after hepatic specification, *Tbx3* controls migration of hepatoblasts from the foregut endoderm into the underlying mesenchyme and extensive growth by suppressing cholangiocyte fate(9). Canonical Wnt/Ctnnb1 signaling is an important regulator of hepatic specification of the foregut, and hepatic morphogenesis(11) and has been described to be sufficient to induce *Tbx3* in liver cancer(12). Nevertheless, if *Ctnnb1* dependent downregulation of *Tbx3* is prerequisite for IHBD development and how *Tbx3* is interconnected with the Notch pathway has not been addressed yet.

Here, we expand the analysis of IHBD development by a temporal and spatial requirement of *Tbx3* and demonstrate a requirement of hepatic downregulation of *Tbx3* for the onset of Notch induced cholangiocyte differentiation. We suggest functions of *Ctnnb1* dependent expression of *Tbx3* inhibiting IHBD development and Notch induced initiation of BEC differentiation in two parallel pathways.

Materials and Methods

Mice and Genotyping

Mice carrying a null allele of *Tbx3* (*Tbx3*^{tm1.1^(cre)V^{mc}}, synonym: *Tbx3*^{ox}), mice with two loxP sites located in introns 1 and 6 of *Cttnb1* (*Cttnb1*^{tm2^{Kem}/J}, synonym: *Cttnb*^h)(13), mice carrying a loxP-flanked DNA segment that prevents expression of a *lacZ* gene (*Gt(ROSA)26Sor*^{tm1^{Sor}})(14), mice containing a sequence encoding an intracellular portion of the mouse *Notch1* gene blocked by a loxP-flanked STOP fragment *Gt(ROSA)26Sor*^{tm1^(Notch1)Dam}(15), conditional *TBX2* overexpressing mice (*Hprt*^{TBX2}) and mice carrying a null allele of *Foxg1* (*Foxg1*^{tm1^(cre)S^{kem}})(16) were maintained on an outbred NMRI (National Marine Research Institute) background. For timed pregnancies, vaginal plugs were checked in the morning after mating; noon was taken as embryonic day (E) 0.5. Embryos were harvested in phosphate-buffered saline, fixed in 4% paraformaldehyde overnight, and stored in 100% methanol at -20°C before further use. Genomic DNA prepared from yolk sacs or tail biopsy specimens was used for genotyping by polymerase chain reaction (PCR). All mice received humane care, and their use was approved by the Institutional Animal Care Committee of Hannover Medical School.

Histological Analysis and Immunofluorescence

Embryos were embedded in paraffin wax and sectioned to 5 µm. For histological analyses, sections were stained with hematoxylin-eosin. For the detection of antigens, the following primary antibodies were used: mouse monoclonal antibody against GFP (1:200, Roche), Onecut1 (1:200, Abcam) and Cytokeratin18 (1:200, Acris Antibodies).

In Situ Hybridization Analysis

In situ hybridization analysis on 10 µm transverse sections of embryos was performed following a standard procedure with digoxigenin-labeled antisense riboprobes.

Semiquantitative Reverse Transcription PCR

Total RNA was extracted from dissected livers of given stages with RNAPure reagent (Peqlab). RNA (500 ng) was reverse transcribed with RevertAid M-MuLV Reverse Transcriptase (Fermentas). For semiquantitative PCR, the number of cycles was adjusted to the mid-logarithmic phase. Quantification was performed with Quantity One software (Bio-Rad). Assays were performed at least twice in duplicate, and statistical analysis was done as described previously. Primers and PCR conditions are available on request.

Documentation

Sections were photographed using a Leica DM5000 microscope with a Leica DFC300FX digital camera. Whole mount specimens were photographed on a Leica M420 microscope with a Fujix digital camera HC-300Z. Images were processed in Adobe Photoshop CS3.

Results

***Ctnnb1* activates *Tbx3* in vivo**

Analyses from cancer cells suggested canonical Wnt signaling to induce *Tbx3* via *Ctnnb1*(12). A possible similar developmental function *in vivo* however, had not been shown so far. Here, by a conditional *Ctnnb1* loss-of-function experiment, we investigated a potential dependence of *Tbx3* on canonical Wnt-signaling during liver development. Therefore we used a floxed *Ctnnb1* knock-out allele recombined by *Foxg1^{cre}* that was reported to drive recombination in the foregut endoderm(17). To confirm efficient recombination by *Foxg1^{cre}* also in the liver bud expression of *LacZ* in a *R26R^{LacZ}* reporter mouse was analyzed in sections of 23s and 26s liver buds (Fig. 1). Expression of *LacZ* in the liver bud (23s) and emigrating hepatoblasts (26s) approved the suitability of this allele for further experiments (Fig. 1).

Expression of *Tbx3* in E10.5 wildtype and *Foxg1^{cre/+}; Ctnnb1^{fl/fl}* mice was tested by *in situ* hybridization. Indeed, *Tbx3* expression is severely downregulated in the liver bud and the forming liver lobe. Surprisingly *Tbx3* expression is also lost in the mesenchyme surrounding the foregut epithelium (Fig. 1) arguing for an inductive *Ctnnb1* dependent signal for this expression domain of *Tbx3* coming from the foregut endoderm. However, *Onecut1* expression stays off, suggesting that some *Tbx3* protein is still remanent (Fig. 1). Accordingly the hepatoblast marker *alpha fetoprotein (Afp)* is only slightly reduced (Fig. 1) indicating a normal hepatic specification prior to this time point. The Notch target genes *Hairy and enhancer of split 1 (Hes1)* and *Hes5* are not ectopically activated in *Ctnnb1* depleted liver buds (Fig. 1), arguing against a repression of Notch signaling by canonical Wnt signaling.

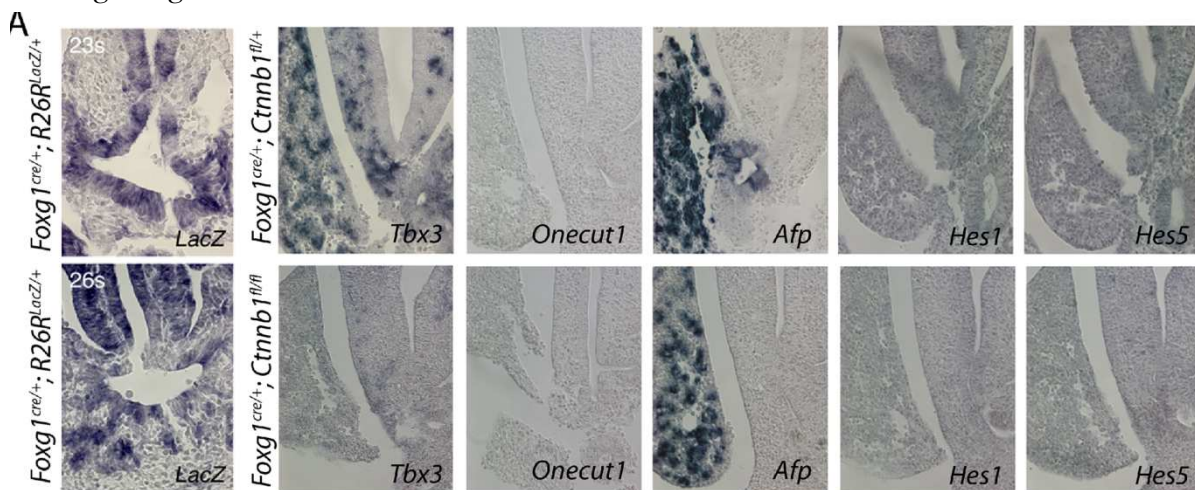


Fig. 1. *Ctnnb1* activates *Tbx3* in vivo. *In situ* hybridization analysis of E10.5 liver sections in *Ctnnb1* depleted E10.5 mice. Tested genes and genotypes as indicated in the figure. Expression of *Tbx3* is lost in *Foxg1^{cre/+}; Ctnnb1^{fl/fl}* mice, nevertheless *Onecut1* is not activated in the conditional *Ctnnb1* mutant. *Afp* expression is slightly reduced. Notch target genes *Hes1* and *Hes5* are not ectopically activated.

Notch signaling is not active in the early liver bud stage.

Other groups recently reported Notch signaling to be essential for the differentiation of cholangiocytes (bile duct cells)(2, 18), but they had neglected a possible function of *Tbx3* in regulating timed differentiation of biliary cells. Intriguingly, downregulation of *Tbx3* at E13.5 prior to bile duct formation is consistent with a direct repressive function of *Tbx3* for the Notch pathway. To test the assumption that *Tbx3* represses Notch signaling in the early liver bud to allow efficient propagation of hepatoblasts we analyzed Notch signaling in the *Tbx3* mutant case. Therefore we performed *in situ* hybridization experiments on E9.5 liver buds. We found neither an ectopic activation in Notch ligands and receptors nor in Notch target gene expression (*Hes1* and *Hes5*)(19) (Fig. 2). These findings do not exclude a repressive function of *Tbx3* on Notch signaling but show that Notch signaling is not activated in the early liver bud stage.

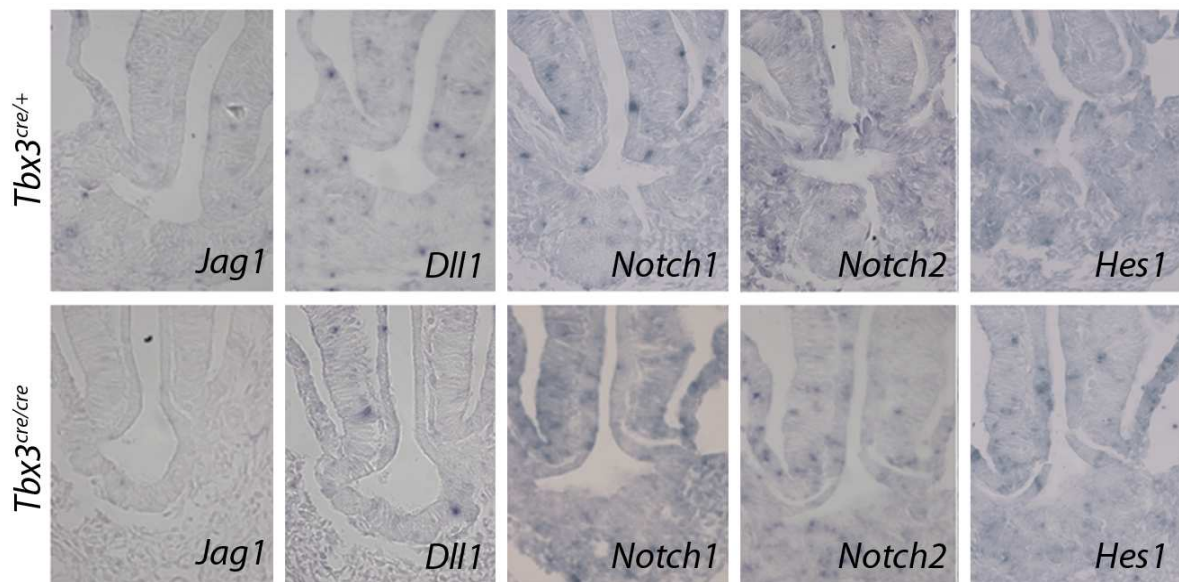


Fig. 2 Notch signaling is not active in the early liver bud stage. *In situ* hybridizations for Notch signaling components in E9.5 wildtype and *Tbx3* deficient mice. Tested genes are as indicated in the figure. Neither Notch ligands, receptors or target genes are ectopically activated in the loss-of-function mutant.

Ectopic activation of Notch signaling initiates biliary programs

To further investigate if activation of Notch signaling at E13.5 of development is the key regulatory event for deactivation of *Tbx3* instead, we prematurely activated Notch signaling in the early liver bud by *Foxg1^{ov}* in combination with a *Rosa^{NICD}* allele that allows the overexpression of the *Notch1* intracellular domain. Activation of Notch signaling was evaluated by the expression of Notch target genes *Hes1* and *Hes5* in E9.5 *Foxg1^{ov/+}; Rosa^{NICD/+}* mice (Fig. 3A). Expression analysis by *in situ* hybridization experiments at E10.5 showed unchanged expression of *Tbx3* (Fig. 3B). Presence of the fetal hepatoblast marker *Afp* demonstrates that the hepatic program is started,

suggesting that Notch signaling is not impedimental for hepatic initiation (Fig. 3B). Ongoing expression of *Hes1* in the foregut endoderm, the remaining liver bud and the liver lobes shows that Notch signaling remains activated at E10.5 in the misexpression mutant (Fig. 3B). Lineage specific transcription factor expression shows a change of cellular fate decision (Fig. 3C). Hepatocyte specific transcription factors are lost (*Cebpa*) or downregulated (*Hnf1a*), while the biliary associated transcription factor *Onecut1* is ectopically activated in conditionally Notch activated mice (Fig. 3C).

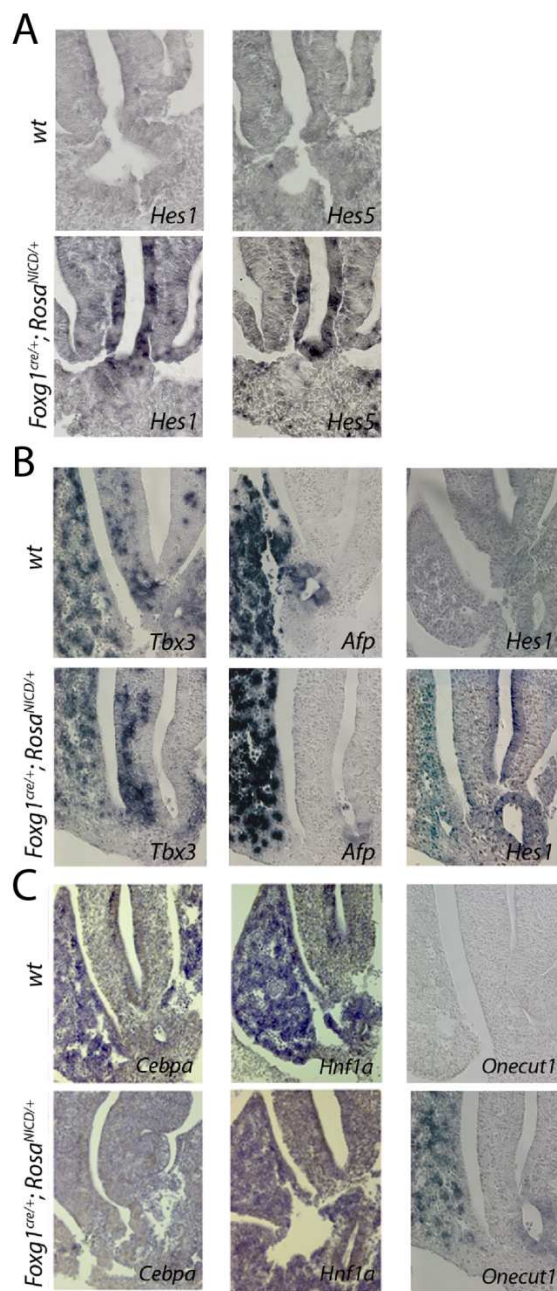


Fig. 3. Ectopic activation of Notch signaling initiates biliary programs. *In situ* hybridization experiments in E9.5 (A) and E10.5 mice (B, C). Genes and genomes are as indicated in the figure. Activation of the Notch target genes *Hes1* and *Hes5* displays the activation of Notch signaling in E9.5 *Foxg1^{cre/+}; Rosa^{NICD/+}* mice (A). Expression of *Tbx3* and the fetal hepatoblast marker *Afp* demonstrates the initiation of the hepatic program in conditionally Notch activated mice (B). Expression of *Hes1* in the foregut endoderm, the remaining liver bud and the liver lobes can be detected in the misexpression mutant (B). Hepatocyte specific transcription factors are lost (*Cebpa*) or downregulated (*Hnf1a*), while *Onecut1* is ectopically activated in conditionally Notch activated mice (C).

Moderate liver and gall bladder paucity in *Alb^{cre/+};Hprt^{TBX2/+}* mice.

Our former studies showed that *Tbx3* is downregulated in the liver at E12.5. To address the question, if *Tbx3* function after that stage impedes normal hepatobiliary development or if it is just dispensible in late liver organogenesis, we set up a gain-of-function approach. Unfortunately we were missing the tools to overexpress *Tbx3*. However, since *Tbx2* is a closely related transcriptional repressor that was described to be functional redundant(20-22), we decided to use an overexpression construct for *TBX2* in the developing liver. For this gain-of-function experiment, we used a conditional *Alb^{cre}/loxP*-based *Hprt^{Tbx2}* misexpression that allows recombination around E13.5(23). Integration of a bicistronic transgene-cassette containing the *TBX2* ORF followed by *IRE5-GFP* in the ubiquitously expressed X-chromosomal *Hypoxanthine guanine phosphoribosyl transferase* (*Hprt*) locus allows to trace transgene-expressing cells *in vivo* by GFP-fluorescence. This system represents a useful tool to study cellular phenotypes both under mosaic conditions in mosaic females (due to random X-chromosome inactivation) but also under uniform expression in hemizygous males. Prolonged expression of *TBX2* manifested in a slight size reduction of post natal day (P) 28 *Alb^{cre/+};Hprt^{TBX2/+}* mice (Fig. 4A). Morphological analysis of the inner organs showed a modest size reduction of the liver and gall bladder. *Albumin* is not expressed in spleen and kidneys, coherently, these control organs are of normal size (Fig. 4B). Consistent with our previous finding that *Tbx3* favors hepatocyte fate at the expense of cholangiocyte differentiation(10), antibody staining for the bile duct marker Ck18 shows the loss of cholangiocytes around the hepatic veins (Fig. 4C). Presence of GFP around the endothelium is compatible with a direct repression of differentiation by *TBX2* (Fig. 4C). Intriguingly, most of the adult liver tissue does not express *GFP*, arguing for a replacement of mutant cells by their wildtype counterparts in the heterozygous case. Male adult littermates could not be obtained. Seemingly constant overexpression of *TBX2* also in other expression domains of *Foxg1* is not compatible with liver after birth.

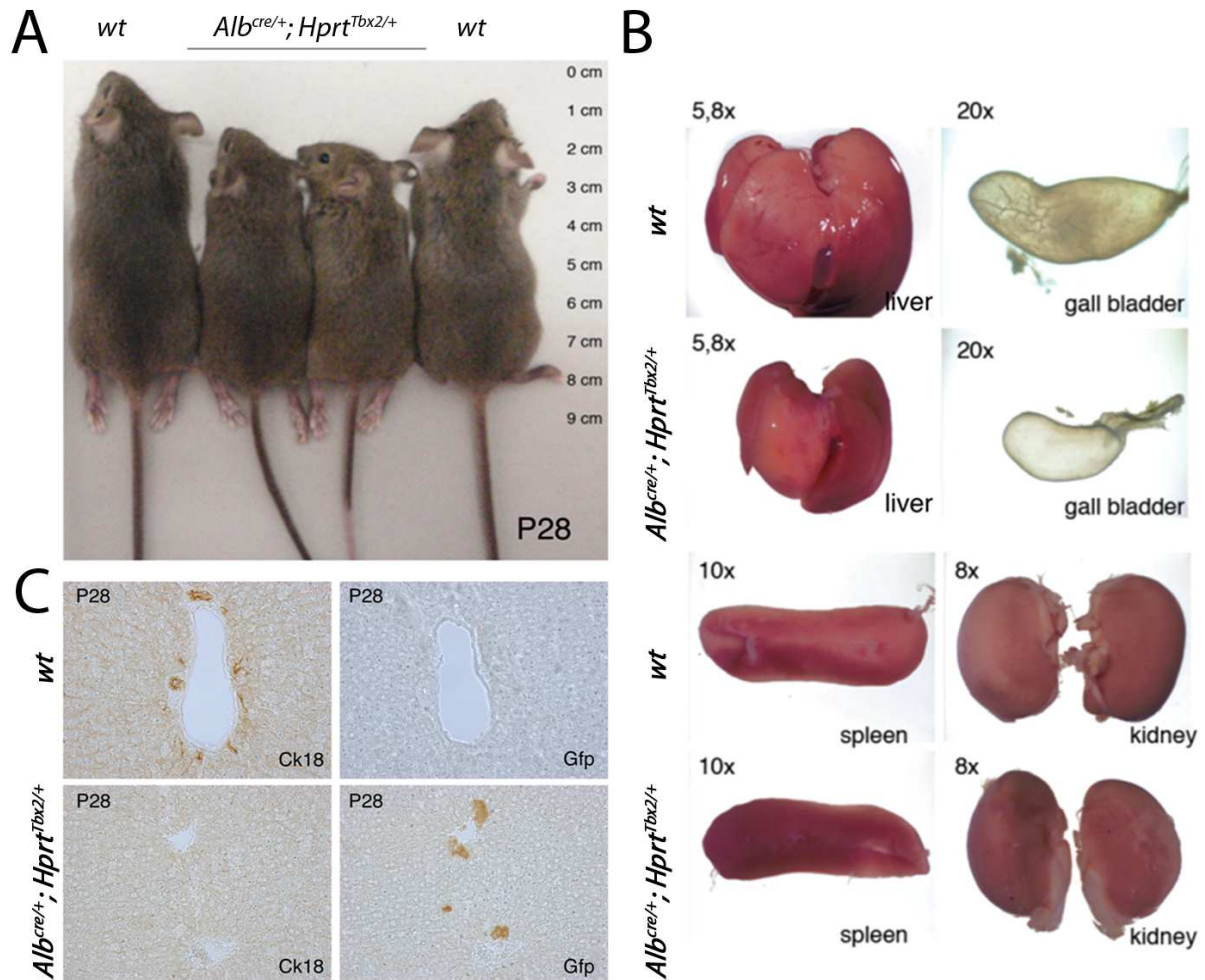


Fig. 3 Moderate liver and gall bladder paucity in *Alb^{cre/+}; Hprt^{TBX2/+}* mice. Morphology of 4 weeks old mice (A) and of inner organs (B). Liver specific conditional overexpression of *TBX2* results in reduced adult body size (A). Liver and gall bladder show modest size reduction, while spleen and kidneys are comparable with wildtype organs. Ck18 specific immunostainings reveal a loss of the bile duct cell marker in the overexpression mutant (C). Antibody staining for GFP marks expression of *TBX2* around the hepatic veins (C).

Loss of bile duct formation and cholangiocyte differentiation but unchanged Notch component expression in the *TBX2* overexpressing liver.

To determine if downregulation of *Tbx3* after E12.5 in the developing liver is a prerequisite to bile duct formation the previous analysis was supplemented with temporal misexpression experiments *in vivo*. Indeed immunostainings for the biliary differentiation marker Ck18(24) and the key regulatory transcription factor Onecut1(25) were lost from the intrahepatic veins at E16.5 in *Alb^{cre/+}; Hprt^{TBX2/y}* mice (Fig. 5A), thus showing disturbed formation of the ductal plate, a layer of cuboidal biliary precursors(26). To further check if cellular differentiation is altered in the whole liver, qRT-PCR experiments of E16.5 livers were performed. Not surprisingly *Ck7*, another cholangiocyte differentiation marker (24), is downregulated in heterozygous *TBX2* misexpressing

mice and even stronger decreased in the homozygous male case (Fig. 5B). Unexpectedly, the hepatocyte marker *Alb* is increased in a similar dose dependent manner suggesting a stimulating effect on hepatocyte differentiation for *TBX2* (Fig. 5B). To check for the presence of Notch signaling around the vascular endothelium *in situ* hybridization experiments were performed. As expected the Notch ligand in the endothelium *Jag1* and the receptor *Notch1* in the surrounding tissue were expressed in the wildtype (Fig. 5C). However, expression of both genes was unchanged in the misexpression mutant (Fig. 5C).

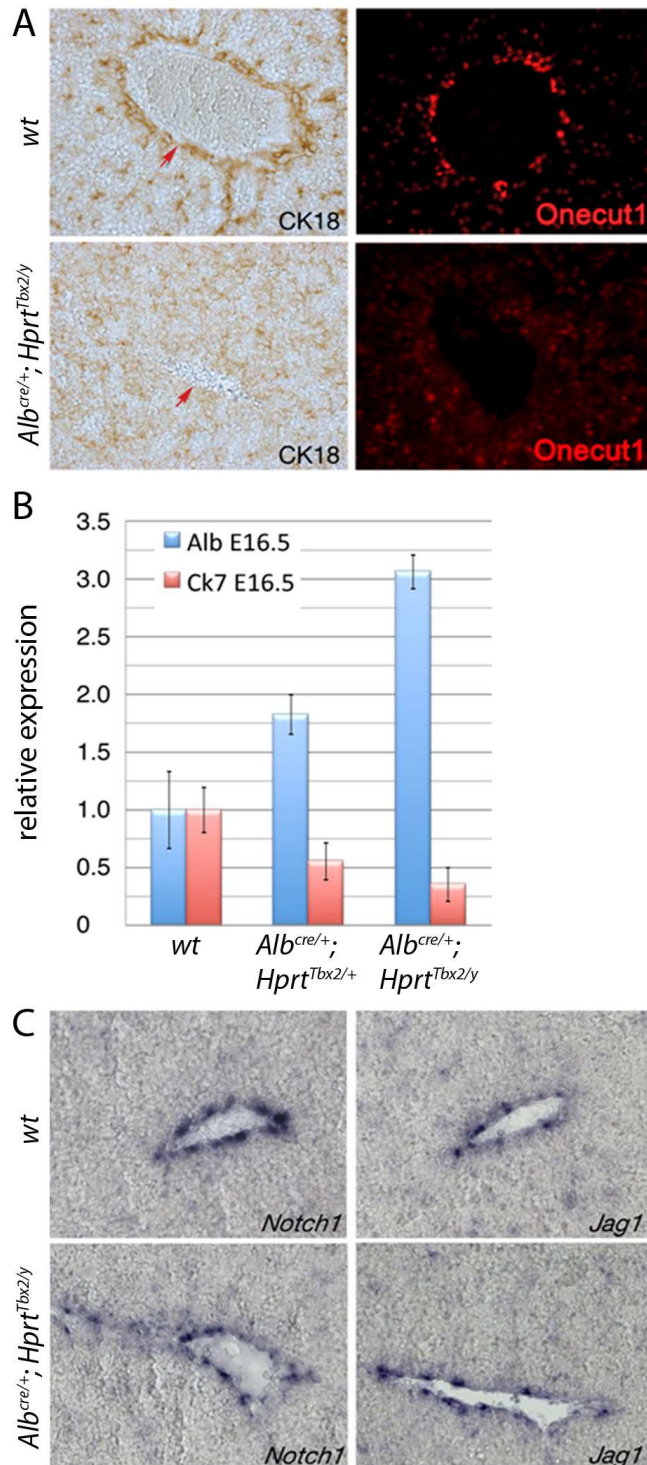


Fig 5. Loss of bile duct formation and cholangiocyte differentiation but unchanged Notch component expression in the *TBX2* overexpressing liver. Antibody stainings for biliary differentiation (A), qRT-PCR for hepatocyte (*Alb*) and cholangiocyte (*Ck7*) differentiation markers (B) and *in situ* hybridizations for Notch components (C) in E16.5 *Alb^{cre/+}; Hprt^{TBX2/y}* mice. Immuno-stainings for the cholangiocytes marker Ck18 and the biliary transcription factor Onecut1 show complete loss of ductal plate formation in male *TBX2* misexpression mutants (A). RT-PCR analysis revealed reduced expression of the cholangiocyte differentiation marker *Ck7* and an increase of the hepatocyte marker *Alb* dependent on the number of mutant alleles (B). Endothelial expression of *Jag1* in the portal veins and expression of *Notch1* in the surrounding cell layer is not disturbed (C).

***TBX2* rescues bile duct hypertrophy in NICD misexpressing mice**

The onset of bile duct formation and cholangiocyte differentiation is temporally strict regulated(26, 27). Yet the hierarchy of *Tbx3* and Notch signaling remains unclear. In order to address this question a combined overexpression experiment with simultaneous expression of *Tbx3* and *NICD* was set up. For that purpose we analyzed organ morphology of E18.5 *Alb^{cre/+}; Rosa^{NICD/+}; Hprt^{TBX2/+}* mice and compared them with wildtype and *NICD* overexpressing littermates (Fig. 6). As was reported before the *NICD* overexpression mutant exhibits ectopic bile ducts that manifest in visible cavities distributed all over the liver parenchyma(18, 28) (Fig. 6). However, temporal and spatial over activation of Notch signaling together with concurrent expression of *TBX2* leads to a minor size reduction compared with the wildtype without other visible morphological changes. The albumin negative spleen as an internal negative control organ is unchanged in all three genotypes.

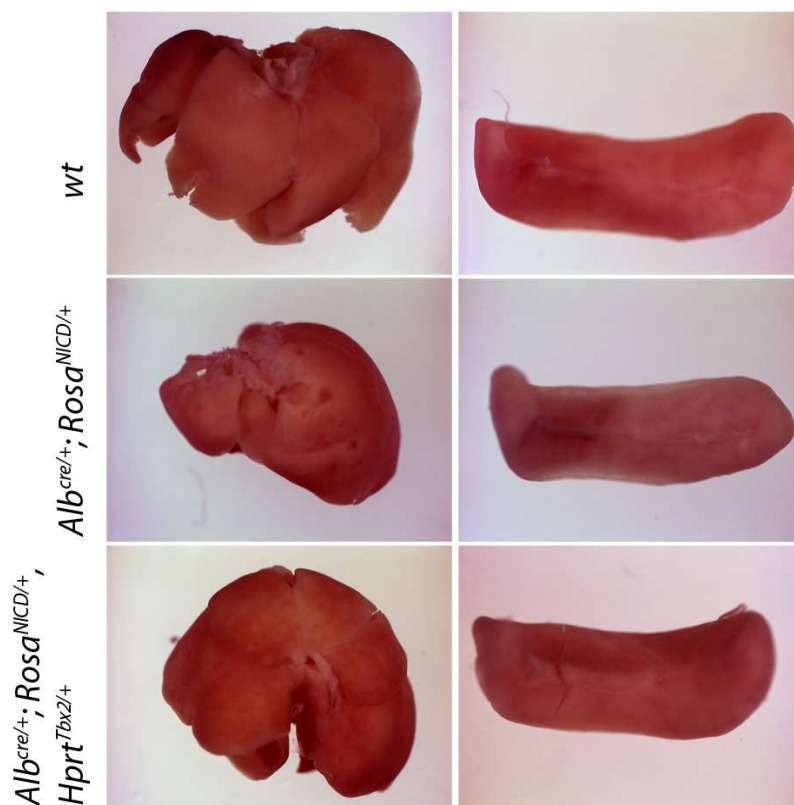


Fig. 6 *TBX2* rescues bile duct hypertrophy in *NICD* misexpressing mice. Morphology of liver and spleen of E18.5 wild-type and mutant mice. Genotypes are as indicated in the figure. Mice with conditional Notch over activity in the liver exhibit hypertrophic bile ducts that manifest in a multitude of small cavities in the liver parenchyma. Combined *NICD* and *TBX2* expression results in an externally normal phenotype with a minor size reduction. The morphology of the negative control organ spleen is unchanged in all three genotypes.

Discussion

Recently a number of works has been published that extensively analyzed the development of bile ducts(2, 9, 29). Their unanimous finding was that cholangiocyte differentiation is dependent on Notch signaling that emanates from the portal veins in the liver. The portal endothelium expresses the Notch ligand *Jag1* which signals to the surrounding Notch receptor expressing hepatoblasts. In a very elegant work Antoniou et al.(29) found that Notch activates the expression of the transcription factor *Onecut1*. *Onecut1* in turn activates *Sox9* expression which furthermore represses the hepatocyte transcription factor *Cebpa*. However, none of these works concentrated on the regulatory function or regulation of *Tbx3* in this context.

***Tbx3* and Notch signaling regulate biliary development in two independent pathways.**

An important question was, how temporal development of bile ducts was achieved. Intriguingly *Tbx3* is downregulated just at the onset of cholangiocyte differentiation(10). Here we wanted to find out if activation of biliary differentiation and downregulation of *Tbx3* is mere coincidence or functionally linked. Our results indicate that downregulation of *Tbx3* is indeed necessary as *Tbx3* efficiently blocks cholangiocyte fate. However, although in *NICD* misexpressing mice *Hes1*, a target gene of Notch is ectopically activated, *Tbx3* expression is present. Thus activated Notch signaling neither downregulates expression of *Tbx3* nor can *Tbx3* inhibit signaling by *NICD* (Fig. 3B). Still it cannot be ruled out that *Tbx3* shares at least some target genes with Notch signaling that may then be directly repressed. Nevertheless activated Notch signaling is sufficient to induce *Onecut1* expression (Fig. 3C). *NICD* misexpression at E10.5 also results in the downregulation of *Cebpa* and *Hnf1a* (Fig. 3C). Seemingly the reported cascade from activation of the *Onecut1* transcription factor to the point of downregulation of *Cebpa*(29) is established. That *Onecut1* target genes are likewise targeted by *Tbx3* appears therefore unlikely.

***Tbx3* is a downstream target of Wnt/*Ctnnb1* during embryonic development.**

In liver cancer *Tbx3* was described as a target of canonical Wnt signaling some time ago(12). Although misexpression of *Ctnnb1* was sufficient to induce expression of *Tbx3* *in vitro* and *in vivo* and ChIP experiments demonstrated direct binding of *Ctnnb1* to the *Tbx3* promoter, a functional relevance for developmental processes in the embryo had not been shown so far. However, our results clearly show that *Tbx3* expression in the early developing liver is lost after depletion of *Ctnnb1* (Fig. 1). Interestingly *Tbx3* expression is not only lost in the *Foxg1* domain but also in the mesenchyme surrounding the foregut endoderm. Possibly there is an additional inductive signal-

for *Tbx3* coming from the foregut endoderm. However, despite the finding that the fetal hepatoblast marker *Afp* is slightly reduced, loss of *Tbx3* expression does not result in upregulation of cholangiocyte specific markers as one could suggest from the analysis of the *Tbx3* loss-of-function mutant(10). Most likely *Tbx3* protein is stable for some time and remains present even though gene expression is not detectable anymore.

Taken from the results above a necessity of both *Tbx3* and Notch signaling for the regulation of timed bile duct formation is without doubt. However whether repression of cholangiocyte differentiation by *Tbx3* or activation of the biliary program by Notch signaling is more important remains unclear. Since *Hes1* is activated in E10.5 NICD overexpressing mice although *Tbx3* still is expressed (Fig. 3B), both an inhibition of Notch signaling in general by *Tbx3* and repression of *Tbx3* by activated Notch signaling are unlikely. However, Notch induced bile duct hypertrophy can be at least partially rescued by concurrent *TBX2* expression (Fig.6). If this rescue is only partial or reflects maybe even the *TBX2* overexpression phenotype, needs to be elucidated in further experiments. Analyses on the histological and molecular level will reveal additional information of possible interactions between Notch signaling and *Tbx3*.

So far our results all argue for independent parallel modes of action on the regulation of cholangiocyte differentiation and bile duct formation for *Tbx3* and Notch signaling. We therefore propose a model where *Tbx3* is clearly downstream of canonical Wnt signaling and is induced by *Ctnnb1* (Fig.7). *Tbx3* then subsequently prohibits cholangiocyte differentiation directly or even if it is unlikely by inhibition of *Onecut1* activity. In a parallel path Notch signaling activates *Onecut1* which in turn induces biliary differentiation. Reciprocal inhibition of Notch signaling and *Tbx3* is unlikely while it is still in question for *Tbx3* and *Onecut1*.

In summary canonical Wnt/*Ctnnb1* signaling via the expression of *Tbx3* and Notch signaling by activation of *Onecut1* expression jointly regulate cholangiocyte differentiation and bile duct development in parallel pathways.

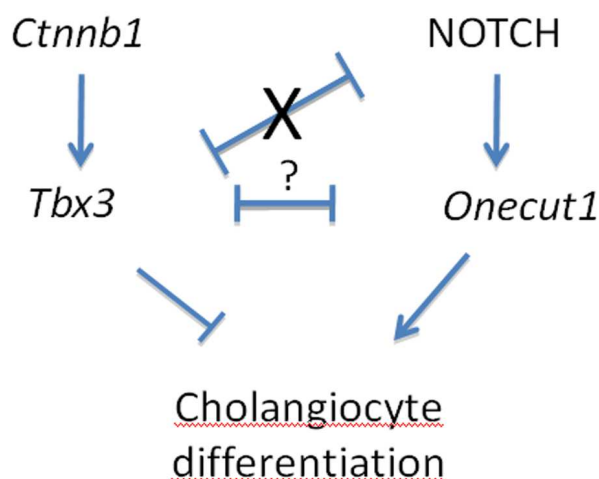


Fig. 7. A network of signaling pathways regulates differentiation of bile duct cells. Scheme for hepatocellular differentiation. *Ctnnb1* activates *Tbx3* which subsequently represses biliary differentiation. In parallel Notch signaling activates the transcription factor *Onecut1* promoting cholangiocyte differentiation. While reciprocal repression of *Onecut1* and *Tbx3* remains unclear, this mode of interaction can be excluded for *Tbx3* and Notch signaling.

This function may even be important in liver regeneration. Köhler et al.(30) found strong upregulation of Notch ligands and receptors in rat livers after 2/3 hepatectomy. Reactivation of *Tbx3* might inhibit differentiation of cholangiocytes despite active Notch signaling and stimulate of both cholangiocyte and hepatocyte proliferation thereby achieving fast recovery of the liver mass. Downregulation of *Tbx3* then subsequently would allow cholangiocyte differentiation and restoration of bile ducts. Based on these findings further work on supposable functions for *Tbx3* in the reestablishment of liver mass and functional bile ducts during liver regeneration and repair might be worthwhile.

Acknowledgements

The authors thank D. Tosh for providing us with complementary DNAs for *Cebpa* and *Hnf1a*, and U. Kossatz-Böhlert for antibodies and discussions.

References

1. Alagille D, Estrada A, Hadchouel M, Gautier M, Odievre M, Dommergues JP. Syndromic paucity of interlobular bile ducts (alagille syndrome or arteriohepatic dysplasia): Review of 80 cases. *J Pediatr* 1987; **110**(2): 195-200.
2. Hofmann JJ, Zovein AC, Koh H, Radtke F, Weinmaster G, Iruela-Arispe ML. Jagged1 in the portal vein mesenchyme regulates intrahepatic bile duct development: Insights into alagille syndrome. *Development* 2010; **137**(23): 4061-4072.
3. Sousa AB, Medeira A, Kamath BM, Spinner NB, Cordeiro I. Familial stenosis of the pulmonary artery branches with a JAG1 mutation. *Rev Port Cardiol* 2006; **25**(4): 447-452.
4. Tanimizu N, Miyajima A. Notch signaling controls hepatoblast differentiation by altering the expression of liver-enriched transcription factors. *J Cell Sci* 2004; **117**(Pt 15): 3165-3174.
5. Yuan ZR, Kobayashi N, Kohsaka T. Human jagged 1 mutants cause liver defect in alagille syndrome by overexpression of hepatocyte growth factor. *J Mol Biol* 2006; **356**(3): 559-568.
6. Zong Y, Panikkar A, Xu J, Antoniou A, Raynaud P, Lemaigre F, Stanger BZ. Notch signaling controls liver development by regulating biliary differentiation. *Development* 2009; **136**(10): 1727-1739.
7. Yamasaki H, Sada A, Iwata T, Niwa T, Tomizawa M, Xanthopoulos KG, Koike T, et al. Suppression of C/EBP α expression in periportal hepatoblasts may stimulate biliary cell differentiation through increased Hnf6 and Hnf1b expression. *Development* 2006; **133**(21): 4233-4243.
8. Shiojiri N, Nagai Y. Preferential differentiation of the bile ducts along the portal vein in the development of mouse liver. *Anat Embryol (Berl)* 1992; **185**(1): 17-24.
9. Lozier J, McCright B, Gridley T. Notch signaling regulates bile duct morphogenesis in mice. *PLoS One* 2008; **3**(3): e1851.
10. Ludtke TH, Christoffels VM, Petry M, Kispert A. *Tbx3* promotes liver bud expansion during mouse development by suppression of cholangiocyte differentiation. *Hepatology* 2009; **49**(3): 969-978.
11. Lade AG, Monga SP. Beta-catenin signaling in hepatic development and progenitors: Which way does the WNT blow? *Dev Dyn* 2011; **240**(3): 486-500.
12. Renard C-, Labalette C, Armengol C, Cougot D, Wei Y, Cairo S, Pineau P, et al. *Tbx3* is a downstream target of the wnt/ β -catenin pathway and a critical mediator of β -catenin survival functions in liver cancer. *Cancer Research* 2007; **67**(3): 901-910.
13. Brault V, Moore R, Kutsch S, Ishibashi M, Rowitch DH, McMahon AP, Sommer L, et al. Inactivation of the beta-catenin gene by Wnt1-cre-mediated deletion results in dramatic brain malformation and failure of craniofacial development. *Development* 2001; **128**(8): 1253-1264.
14. Soriano P. Generalized lacZ expression with the ROSA26 cre reporter strain. *Nat Genet* 1999; **21**(1): 70-71.

15. Murtaugh LC, Stanger BZ, Kwan KM, Melton DA. Notch signaling controls multiple steps of pancreatic differentiation. *Proc Natl Acad Sci U S A* 2003; **100**(25): 14920-14925.
16. Hebert JM, McConnell SK. Targeting of cre to the *Foxg1* (BF-1) locus mediates loxP recombination in the telencephalon and other developing head structures. *Dev Biol* 2000; **222**(2): 296-306.
17. Li Y, Gordon J, Manley NR, Litingtung Y, Chiang C. *Bmp4* is required for tracheal formation: A novel mouse model for tracheal agenesis. *Dev Biol* 2008; **322**(1): 145-155.
18. Zong Y, Panikkar A, Xu J, Antoniou A, Raynaud P, Lemaigre F, Stanger BZ. Notch signaling controls liver development by regulating biliary differentiation. *Development* 2009; **136**(10): 1727-1739.
19. Katoh M, Katoh M. Integrative genomic analyses on HES/HEY family: Notch-independent HES1, HES3 transcription in undifferentiated ES cells, and notch-dependent HES1, HES5, HEY1, HEY2, HEYL transcription in fetal tissues, adult tissues, or cancer. *Int J Oncol* 2007; **31**(2): 461-466.
20. Horton AC, Mahadevan NR, Minguillon C, Osoegawa K, Rokhsar DS, Ruvinsky I, de Jong PJ, et al. Conservation of linkage and evolution of developmental function within the *Tbx2/3/4/5* subfamily of T-box genes: Implications for the origin of vertebrate limbs. *Dev Genes Evol* 2008; **218**(11-12): 613-628.
21. Jerome-Majewska LA, Jenkins GP, Ernstoff E, Zindy F, Sherr CJ, Papaioannou VE. *Tbx3*, the ulnar-mammary syndrome gene, and *Tbx2* interact in mammary gland development through a p19Arf/p53-independent pathway. *Dev Dyn* 2005; **234**(4): 922-933.
22. Ribeiro I, Kawakami Y, Buscher D, Raya A, Rodriguez-Leon J, Morita M, Rodriguez Esteban C, et al. *Tbx2* and *Tbx3* regulate the dynamics of cell proliferation during heart remodeling. *PLoS One* 2007; **2**(4): e398.
23. Postic C, Magnuson MA. DNA excision in liver by an albumin-cre transgene occurs progressively with age. *Genesis* 2000; **26**(2): 149-150.
24. Blakolmer K, Jaskiewicz K, Dunsford HA, Robson SC. Hematopoietic stem cell markers are expressed by ductal plate and bile duct cells in developing human liver. *Hepatology* 1995; **21**(6): 1510-1516.
25. Clotman F, Lannoy VJ, Reber M, Cereghini S, Cassiman D, Jacquemin P, Roskams T, et al. The one-cut transcription factor HNF6 is required for normal development of the biliary tract. *Development* 2002; **129**(8): 1819-1828.
26. Lemaigre FP. Development of the biliary tract. *Mech Dev* 2003; **120**(1): 81-87.
27. Raynaud P, Carpentier R, Antoniou A, Lemaigre FP. Biliary differentiation and bile duct morphogenesis in development and disease. *Int J Biochem Cell Biol* 2011; **43**(2): 245-256.
28. Tchorz JS, Kinter J, Muller M, Tornillo L, Heim MH, Bettler B. Notch2 signaling promotes biliary epithelial cell fate specification and tubulogenesis during bile duct development in mice. *Hepatology* 2009; **50**(3): 871-879.

29. Antoniou A, Raynaud P, Cordi S, Zong Y, Tronche F, Stanger BZ, Jacquemin P, et al. Intrahepatic bile ducts develop according to a new mode of tubulogenesis regulated by the transcription factor SOX9. *Gastroenterology* 2009; **136**(7): 2325-2333.
30. Kohler C, Bell AW, Bowen WC, Monga SP, Fleig W, Michalopoulos GK. Expression of notch-1 and its ligand jagged-1 in rat liver during liver regeneration. *Hepatology* 2004; **39**(4): 1056-1065.

***Tbx2* maintains the mesenchymal signaling center of the developing lung**

Timo Lüdtke¹, Henner F. Farin^{1,†}, Karin Schuster-Gossler¹, Marianne Petry¹, Vincent M. Christoffels², and Andreas Kispert^{1,*}

¹Institute for Molecular Biology, OE5250, Medizinische Hochschule Hannover, Carl-Neuberg-Str. 1, 30625 Hannover, Germany

²Department of Anatomy, Embryology and Physiology, Academic Medical Center, University of Amsterdam, Meibergdreef 15 L2-108, 1105 AZ Amsterdam, The Netherlands

[†]Present address: Hubrecht Institute, Uppsalalaan 8, 3584 CT Utrecht, The Netherlands

*Author for correspondence (kispert.andreas@mh-hannover.de)

Running title: *Tbx2* in lung mesenchyme

Total length: 6427 words, 8 figures

Keywords: lung development; epithelial-mesenchymal signaling; T-box; *Tbx2*; mouse; Wnt; *Ctnnb1*; *Cdkn1a*; *Cdkn1b*; p21; p27; CyclinD1

Abstract

Development of the mammalian lung is a tightly orchestrated process that depends on well concerted reciprocal epithelial-mesenchymal tissue interactions.

Here we report that the T-box transcription factor *Tbx2* is expressed in the mesenchyme of the forming lungs throughout whole embryonic development in the mouse. Mice homozygous mutant for *Tbx2* exhibit a hypoplastic lung phenotype with reduced branching morphology arguing that *Tbx2* is an important contributor in the orchestra of regulators that administer the formation of the respiratory tree. We suggest *Tbx2* as a proliferative factor for the maintenance of a mesenchymal signaling center by direct repression of *Cdkn1a* and *Cdkn1b* and furthermore promoter of canonical Wnt signaling in the mesenchyme which provokes epithelial growth and branching.

Introduction

The lung is the key respiratory organ of mammals in supplying oxygen to the body and releasing carbon dioxide from the blood stream. These functions are supported by a complex architecture that is characterized by the appearance of highly specialized cell types and a vast surface expansion that together assure effective gas exchange. Epithelial cell types of the lung respiratory tree have been well characterized. Columnar epithelial Clara cells in the distal airways as well as goblet cells in the bronchi and small bronchioles together with neighbored ciliated cells achieve the clearing of the lung. Clara and goblet cells produce mucus for pathogen defense and trap dust and other particles while ciliated cells sweep out the mucus(1, 2). Basal cells hold important functions for lung regeneration by their ability to differentiate into other respiratory epithelial cell types(3). Tight association of respiratory pneumocytes with the surrounding endothelium ensures efficient oxygen supply. Surfactant produced by the cuboidal type II pneumocytes (also called alveolar epithelial cells II (AEC2)) in the alveoli facilitates diffusion of air and prevents collapsing of the alveoli at the end of exhalation(4). Flat and thin walled respiratory type I pneumocytes (AEC1) in close proximity to and in cooperation with the capillary endothelium finally accomplish the exchange of oxygen and carbon dioxide(5). In addition less characterized mesenchymal fibroblasts and smooth muscle cells contribute to the cellular complexity of the lung. Airway smooth muscle cells (ASM) assure the contractility of the bronchi and regulate dispersal of air into the alveoli while fibroblasts facilitate ventilation by deposition of matrix proteins(6, 7).

Timed differentiation of these cell types and the complex architecture of the respiratory tree are the result of a complex developmental program. In the mouse, lung development starts at embryonic day (E) 9.5, when a diverticulum from the ventral foregut endoderm invades the surrounding visceral mesoderm(8, 9). This initial phase of lung development, the pseudoglandular stage (E9.5-E16.5)(10), is characterized by ongoing dichotomous branching of the forming bronchial tree(11). In the canalicular stage (E16.5-E17.5), the terminal buds become smaller and differentiation of respiratory type I pneumocytes begins(10). In the saccular phase (E17.5 - postnatal day (P)5), all generations of respiratory branches have been formed and small sacs, the precursor of the alveoli, are formed(10). In the final alveolar stage, which lasts roughly until P30, lung development is completed by elaboration of the alveoli(10). Although branching morphogenesis does not continue postnatally, the lung increases in size for a significant time after birth by intercalating growth(5, 12).

Branching morphogenesis and timed cell differentiation are controlled by reciprocal mesenchymal-epithelial cell and tissue interactions that are mediated by a large number of signaling pathways in between the two tissue compartments. Localized expression of Fibroblast growth factor

(*Fgf10*) in the distal mesoderm acting through Fgf receptor 2 (*Fgfr2*) in the endoderm stimulates epithelial proliferation and outgrowth of the endodermal buds(13-15). Sonic hedgehog (*Sbb*) expression in the distal epithelial tips(16, 17) locally represses *Fgf10*(18-20) and promotes wingless-related MMTV integration site (*Wnt*)2 and Bone morphogenetic protein (*Bmp*)4 expression in the mesenchyme(20). Additional *Bmp4* expression in the endodermal buds similarly antagonizes Fgf mediated outgrowth of lung epithelium by confined repression of proliferation(21). Together with *Sbb* this mechanism efficiently inhibits growth of the distal tips and permits epithelial growth just at the flanks leading to epithelial branching. In addition, canonical (beta-catenin (*Ctnnb1*)-dependent) Wnt signaling in lung mesenchyme via *Wnt2* and *Wnt5a* regulates mesenchymal *Fgfr2*(22, 23). Epithelial *Wnt7b* promotes the expression of *Bmp4* and *Fgfr2* in the epithelium(24, 25) and is essential for smooth muscle differentiation in the underlying mesenchyme(25, 26). Although we have learned a lot about the function of these signaling moieties in inducing changes both of tissue morphology and cellular fate, it has remained less clear how the epithelial and mesenchymal signaling centers are maintained and finally extinguished.

T-box (*Tbx*) genes encode a family of transcription factors that have been implicated in the control of patterning and differentiation during the development of numerous vertebrate organs. Expression studies identified several members of this family in the developing lung: *Tbx1* in the pulmonary epithelium and *Tbx2*, *Tbx3*, *Tbx4* and *Tbx5* in the surrounding tracheal and lung mesenchyme(27). Inhibition experiments with antisense oligonucleotides in cultures implicated the closely related pair of transcriptional activators, *Tbx4* and *Tbx5*, in the initiation of new epithelial branches by the locally restricted activation of *Fgf10* signaling in the mesenchyme(28). The same experimental approach did not reveal a role of the two closely related transcriptional repressors *Tbx2* and *Tbx3* in branching morphogenesis. However, *Tbx2* and *Tbx3* are still attractive candidates to regulate mesenchymal proliferation and differentiation. This is rooted in the finding that *Tbx2* can directly repress the genes encoding cyclin-dependent kinase inhibitor (*Cdkn*) 2a (*p19ARF*) and 1a (*p21*) *in vitro*(29-31), and on the report of a function of *Tbx3* in the control of cell differentiation by *Cdkn2a* repression in cell culture(32).

Here, we show by loss- and gain-of-function experiments in the mouse supported by *ex vivo* organ culture that *Tbx2* plays a crucial role in maintaining the proliferative state of the mesenchymal signaling center that regulates branching of the bronchial tree. We provide evidence that *Tbx2* regulates lung growth and branching morphogenesis by maintenance of canonical Wnt signaling and prevents mesenchymal differentiation by promoting cell cycle progression by an additive direct repression of *Cdkn1a* and *Cdkn1b* (*p27*).

Material and Methods

Generation of the *Hprt*^{TBX2} allele

A 'knock-in' strategy into the X-chromosomal *hypoxanthine guanine phosphoribosyl transferase* (*Hprt*) gene locus was designed to replace mayor parts of the *Hprt* exon 1 (including the ATG) by a cassette suited for cre-mediated (mis-) expression described previously by Luche et al.(33) Homologous recombination results in a functional *Hprt* null allele, allowing direct selection of successfully targeted ES cells by 6-Thioguanine. The targeting vectors contained a 2.2 kbp 5'-homology region, followed by the ubiquitously expressed CMV early enhancer/chicken b-actin (CAG) promoter, the conditional expression cassette (33), and a 5.1 kbp 3'-homology region. The open reading frame (ORF) of human *TBX2* (cDNA NM_005994.3)(34) was first subcloned in the vector *pSL1180* (GE-healthcare), 5' of an *IRES-EGFP* sequence, and then shuttled as 5'-*NbeI*-ORF-*IRES-EGFP-MluI*-3' fragment into the *MluI* and *NbeI*-sites of the targeting vector. This results in a reverse orientation of the ORF, relative to the CAG promoter, avoiding 'leaky' expression. After cre-mediated 'flipping'- and excision events between pairs of *loxP* and *loxM* sequences, the ORF locates in sense direction, directly downstream of the CAG promoter. The targeting vector was verified by sequencing before linearization and electroporation in *Hprt*-positive SV129 ES cells (maintained beforehand in HAT medium). A two-step selection protocol was employed, starting 24 h after electroporation with the addition of 100 mg/ml G418, followed by the addition of 1.67 mg/ml 6-Thioguanine (Sigma) after additional 5 days. Surviving colonies were expanded and genotyped by PCR (conditions are available upon request). To test the functionality of the expression cassette in candidate ES clones, the GFP-epifluorescence was analyzed 6 days after electroporation with a cre-expression plasmid (*pCAG::turbo-cre*, kind gift from Achim Gossler). Verified ES clones were microinjected into CD1 mouse blastocysts. Chimeric males were obtained and mated to NMRI females, to produce heterozygous F1 females.

Mice and Genotyping

Mice carrying a null allele of *Cdkn1a* (*Cdkn1a*^{atm1Tyl}, synonym *Cdkn1a*^{ko})(35), a null allele of *Cdkn1b* (*Cdkn1b*^{tm1Mjf}, synonym: *Cdkn1b*^{ko})(36), a null allele of *Tbx2* (*Tbx2*^{tm1.1(cre)Vmc}, synonym: *Tbx2*^{ex})(37) or a conditional *Tbx2* allele (*Tbx2*^{tm2.1Vmc}, synonym: *Tbx2*^{lox})(38), mice with two *loxP* sites flanking exon 3 of the *Ctnnb1* locus (*Ctnnb1*^{tm1Mmt}, synonym: *Ctnnb1*^{(Ex3)fl})(39), were maintained on an outbred NMRI (National Marine Research Institute) background. For timed pregnancies, vaginal plugs were checked in the morning after mating; noon was taken as embryonic day (E) 0.5. Embryos were harvested in phosphate-buffered saline, fixed in 4% paraformaldehyde overnight, and

stored in 100% methanol at -20°C before further use. Genomic DNA prepared from yolk sacs or tail biopsy specimens was used for genotyping by polymerase chain reaction (PCR). All mice received humane care. Their use was approved by the Institutional Animal Care Committee of Hannover Medical School.

Histological Analysis and Immunofluorescence

Embryos were embedded in paraffin wax and sectioned to 5 μm . For histological analyses, sections were stained with hematoxylin and eosin. For the detection of antigens, antigen retrieval was performed using citrate-based antigen unmasking solution (H-3300, Vector Laboratories Inc). Sections were pressure cooked for 5 min and signal amplification was performed with the Tyramide Signal Amplification (TSA) system (NEL702001KT, Perkin Elmer LAS). The following primary antibodies were used: rabbit anti-mouse E-cadherin (gift from Rolf Kemler)(40), rabbit polyclonal antibody against GFP (1:200, sc-8334, Santa Cruz), mouse monoclonal antibody against GFP (1:200, 11814460001, Roche), monoclonal antibody against alpha-Smooth muscle actin (*Acta2*), Cy3 Conjugate (1:200, C 6198, Sigma), monoclonal antibody against alpha-Smooth muscle actin (*Acta2*), FITC Conjugate (1:200, F3777, Sigma), rabbit polyclonal against SM22alpha (TagIn) (1:200, ab14106, Abcam), rat monoclonal antibody against endomucin (*Emcn*) (1:2, a kind gift of D. Vestweber, MPI Münster; Germany)(41), Rabbit polyclonal against *Tbx2* (1:100, ab33298, Abcam), *Cdkn1a* (1:200, sc-397, SantaCruz), *Cdkn1b* (1:200, 554069, BD Biosciences), uteroglobin (*Scgb1a1*) (1:200, ab40873, Abcam), Cytokeratin 14 (*Ck14*) (1:200, ab7800, Abcam), *Tubb4* (1:100, ab11315, Abcam), prosurfactant protein C antibody (*Sftpc*) (1:200, ab40879, Abcam), aquaporin 5 antibody (1:100, ab92320, Abcam), Hamster monoclonal to podoplanin (*Pdpln*)(1:50, ab11936, Abcam).

***In Situ* Hybridization Analysis**

In situ hybridization analysis on 10 μm transverse sections of embryos was performed following a standard procedure with digoxigenin-labeled antisense riboprobes(42).

Proliferation and Apoptosis Assays

Cell proliferation in tissues of E9.0 and E9.5 embryos was investigated by detection of incorporated bromodeoxyuridine (BrdU) similar to published protocols. A total of nine sections from three individual embryos per genotype and time point were used for quantification. Statistical analysis was performed using the two-tailed Student's t-test. Data were expressed as mean \pm standard deviation. Differences were considered significant when the P-value was below 0.05.

For detection of apoptotic cells in 5 µm paraffin sections of E9.5 embryos, the terminal deoxynucleotidyl transferase-mediated nick-end labeling (TUNEL) assay was performed as recommended by the manufacturer (Serologicals Corp.) of the ApopTag kit used.

Semi-quantitative reverse transcription PCR

Total RNA was extracted from dissected lungs with RNAPure reagent (PepLab). RNA (500 ng) was reverse transcribed with RevertAid M-MuLV reverse transcriptase (Fermentas). For semi-quantitative PCR, the number of cycles was adjusted to the mid-logarithmic phase. Quantification was performed with Quantity One software (Bio-Rad). Assays were performed at least twice in duplicate, and statistical analysis was done as described previously(43). Primers and PCR conditions are available on request.

Chromatin Immunoprecipitation Assays

Chromatin immunoprecipitations were performed essentially as described previously(44). Dissected E15.5 lung were treated with 4% paraformaldehyde overnight. The DNA-containing supernatants were incubated overnight with *Tbx2* antibodies and collected on protein G beads. Cross-linked products were reversed by cooking for 15 min, treated with ProteinaseK and RNase H at 56 °C for 30 min and the immunoprecipitated DNA was purified. Primers for PCR amplification were 5'-CCGAGAGGTGTGAGCCGC-3' (Cdkn1a-f1) and 5'-GTCATCCACCTGCCGCGG-3' (Cdkn1a-r1); 5'-GGCTTAGATTCCCAGAGGG-3' (Cdkn1a-f2) and 5'-TTCTGGGGACACCCACTGG-3' (Cdkn1a-r2) for the p21 promoter and 5'-CAAGTTCAGTAACTAAGTAGG-3' (Cdkn1b-f1) and 5'-GCACATATGTGGACAACTCG-3' (Cdkn1b-r1) for the 5'-T-site in the p27 promoter. For the intron located T-site 5'-ATATACCTTCTACAGACATAGC-3' (Cdkn1b-f2) and 5'-GCTTTTGACTAGAGTCTTATGG-3' (Cdkn1b-r2) oligos were used. Oligos for the negative control region were 5'-CTCTGAACTCGAACAGGCC-3' (ncr-f1) and 5'-ACTCTGAATTGGATTCCTAGC-3' (ncr-r1).

Organ culture

For analysis of branching morphogenesis E11.5 lung rudiments were dissected and kept on Transwell® permeable 0.4-mm PET 12-well plates (Corning) supplied with DMEM supplemented with 10% fetal calf serum, 2mM Glutamax, 100 units/ml Penicillin, 100 µg/ml Streptomycin (Gibco). Lungs were cultivated at 37°C and 5% CO₂ for 4 to 6 days and number of branching endpoints was counted.

Documentation

Sections were photographed using a Leica DM5000 microscope with a Leica DFC300FX digital camera. Whole mount specimens were photographed on a Leica M420 microscope with a Fujix digital camera HC-300Z. Images were processed in Adobe Photoshop CS3. Confocal images were obtained with a Zeiss LSM 510 Meta and processed with ImageJ(45).

Results

T-box genes are expressed during embryonic lung development

Earlier studies reported expression of *Tbx2*, *Tbx3*, *Tbx4* and *Tbx5* in the pulmonary mesenchyme at selected stages(27). However, a detailed and comparative analysis of expression of these T-box family members during embryonic development of the lung has not yet been performed. *In situ* hybridization analysis revealed that *Tbx2* and *Tbx3* are coexpressed at high levels throughout the lung mesenchyme from E10.5 to E14.5 (Fig. 1). Expression of *Tbx3* declined sharply after this stage whereas *Tbx2* was maintained at E18.5 (Fig. 1). *Tbx2* expression was maintained postnatally at P5 in ~30% of mesenchymal cells but was lost at P10 (Fig. S1A). Coexpression of *Tbx4* and *Tbx5* was found between E10.5 to E16.5 in the lung mesenchyme (Fig. 1). Together, these findings argue for redundant and possibly antagonistic roles of the transcriptional activators *Tbx4* and *Tbx5*, and the transcriptional repressors *Tbx2* and *Tbx3*, respectively, in early lung development but leave the possibility for a unique function of *Tbx2* in the late phase of the pseudoglandular stage, and subsequent stages of pulmonary development.

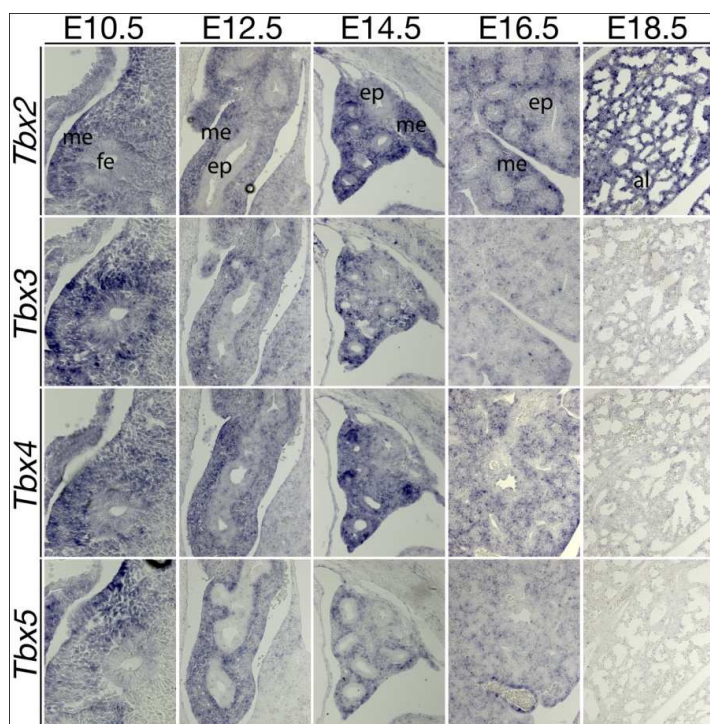


Fig. 1. The four T-box genes *Tbx2*, *Tbx3*, *Tbx4* and *Tbx5* are expressed in the mesenchyme of the developing murine lung. Analysis of *Tbx* gene expression during lung development by RNA *in situ* hybridization on serial transverse sections of wildtype embryos. Developmental stages and probes are as indicated in the figure. fg, foregut endoderm; ep, epithelium; me, mesenchyme, al, alveoli.

Tbx2-deficient mice exhibit hypoplastic lungs

Since *Tbx2* and *Tbx3* have not yet been functionally implicated in lung development, we wanted to study the phenotypic consequences of loss of either gene for the formation of this organ. Mice homozygous for a null allele of *Tbx3* died at E14.5 with lungs that were morphologically and histologically indistinguishable from the wildtype (data not shown). Conditional *Tbx3*-mutant mice were not available to us preventing the analysis at later stages. Since mice with more than two mutant alleles of *Tbx2* and *Tbx3* die around E9.5 due to cardiac defects, analysis of the functional redundancy of the two genes in early lung development was not possible either. In contrast, mice homozygous for a null allele of *Tbx2* (*Tbx2^{fl/fl}*) that was maintained on an NMRI outbred background survived embryogenesis and died shortly after birth due to a cleft palate(43). Morphological examination at E18.5 revealed hypoplastic lungs (Fig. 2A). Relative lung weight was reduced to approx. 50% of wildtype level arguing against a general growth retardation problem (Fig. 2B). Lobulation of the lung was normal but all four right lobes (cranial, medial, caudal, accessory) and most prominently the left lobe appeared smaller (Fig. 2C). Histological analysis of E18.5 frontal sections confirmed a decreased lung size and revealed reduced segmentation and thickened mesenchyme in proximal and distal lung compartments in the mutant (Fig 2D). Collectively, these data suggest a unique requirement for *Tbx2* in late lung development.

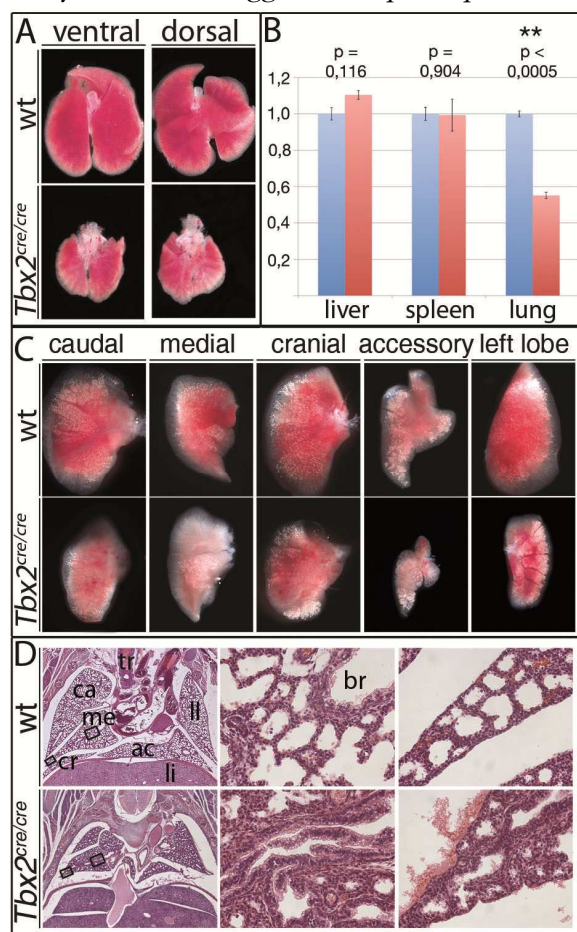


Fig. 2. *Tbx2*-deficient lungs are hypoplastic and show a thickened mesenchyme at E18.5. (A) Morphology of whole wildtype and *Tbx2*-mutant lungs in ventral and dorsal views. **(B)** Statistical analysis of relative lung per body weight; liver and spleen were analyzed as control organs. Reduction of the lung weight to 54.4%±1.7% of the wildtype value (100%) was statistically highly significant (**) whereas liver (110%±2.4%) and spleen weight (98%±8.8%) were without significant change in *Tbx2*-deficient embryos. **(C)** Morphology of all four right lobes and the left lung lobe. **(D)** Histological analysis by eosin and hematoxylin staining of frontal sections of the lung. Black rectangles indicate anterior and posterior regions that are presented in higher magnification. li, liver; tr, trachea; ll, left lung lobe; cl, caudal lobe; ml, medial lobe; cr, cranial lobe; ac, accessory lobe; br, bronchi.

Onset of pulmonary defects in the late pseudoglandular stage in *Tbx2*-deficient lungs

To determine the onset of pulmonary defects in *Tbx2*-deficient embryos, we carried out a detailed histological analysis of earlier developmental stages (Fig. 3). At E14.5 no obvious difference in morphology and histology of the lungs was observed between wildtype and *Tbx2*-deficient embryos. In contrast, lung size was decreased and branching morphogenesis appeared reduced at E16.5 (Fig. 3A). Morphological changes at these stages were not accompanied by altered apoptosis (Fig. 3B). At E14.5, the epithelial and mesenchymal tissue compartments of the lung were highly proliferative irrespective of the genotype (Fig. 3C, D). However, at E16.5 proliferation in the lung mesenchyme showed a highly significant reduction from 29.2% in the wildtype to 18.7% in the mutant tissue while the lung epithelium or the diaphragm were unaffected (Fig. 3C, D). To more carefully address alterations in branching morphogenesis in *Tbx2*-deficient lungs, we explanted E11.5 lung rudiments and analyzed their (2-dimensional) outgrowth after six days of culture (Fig. 3E). Whole mount *in situ* hybridizations for the epithelial tip marker *Id2* showed an almost 3-fold reduction of branching endpoints in the *Tbx2*-mutant lung culture suggesting that epithelial branching morphogenesis is indeed severely hampered by loss of mesenchymal *Tbx2* (Fig. 3E). Immunofluorescent analysis of the fibroblast marker S100a4 and the extracellular matrix protein fibronectin on frontal sections of the left lung lobe revealed a massive reduction of expression of the first, and increased expression of the latter at E14.5 and E16.5 in the *Tbx2*-mutant lung mesenchyme indicating premature differentiation of fibrocytes before onset of histological changes (Fig. 3F). Together, these data suggest that *Tbx2* controls proliferation and differentiation in the mesenchyme of the developing lung at the pseudoglandular stage. Branching defects may indicate an independent function of *Tbx2* in controlling mesenchymal signals promoting this program but may alternatively be secondary to changes in the proliferation and differentiation status of the pulmonary mesenchyme.

Loss of *Tbx2* preferentially affects the mesenchymal tissue compartment

We next investigated whether reduced lung size is associated with defects of cytodifferentiation in the two tissue compartments of this organ at E18.5. Immunohistochemistry of markers for Clara cells (*Scgb1a1*)(46), ciliated cells (*Tubb4*)(47), AECII cells (*Sftpc*)(48), endothelial cells (*Emcn*)(41), AEC-1 cells (*Aqp5*)(48, 49) and basal cells (*Ck14*)(50) did not detect changes in the *Tbx2*-deficient lung, whereas a second marker for AEC-1 cells (*Pdpr*)(51) was downregulated in the mutant. Absence of *Tbx2* was irrelevant for mesenchymal smooth muscle differentiation at this stage, as shown by immunofluorescent detection of *Acta2*(52) in the mutant tissue (Fig. S1B). In contrast, the differentiation status of the mesenchymal fibrous tissue was dramatically affected.

Expression of the fibroblast marker S100a4(53) was completely lost at E18.5 whereas the fibrocyte marker Fibronectin(54) was massively increased in *Tbx2*-deficient lungs (Fig. 3F). Hence, removal of *Tbx2* from the pulmonary mesenchyme marginally affects cytodifferentiation of the epithelial compartments and of SMCs, but prevents the terminal differentiation of fibroblasts.

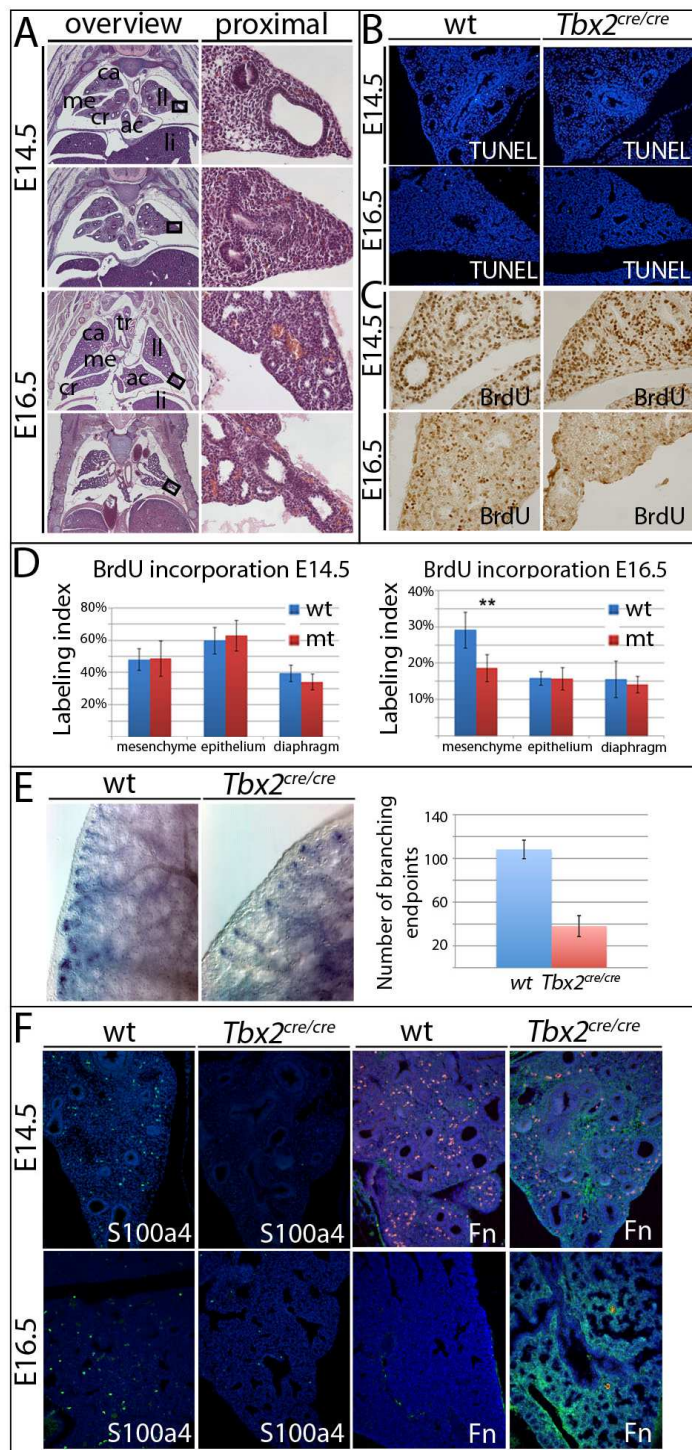


Fig. 3. Onset of proliferation and differentiation defects of *Tbx2*-deficient lung mesenchyme. (A) Histological analysis by eosin and hematoxylin staining of frontal sections of the lung in overviews and in higher magnifications of regions marked by black rectangles at E14.5 and E16.5. **(B)** Detection of apoptotic cells by TUNEL staining and **(C)** analysis of cell proliferation by immunohistochemistry for BrdU at E14.5 and E16.5. **(D)** Statistical analysis of BrdU incorporation of wild-type and mutant lung mesenchyme and epithelium and the diaphragm as a control at E14.5 and E16.5. Genotypes are as indicated. **(E)** Whole mount *in situ* hybridization analysis for expression of the distal epithelial tip marker *Id2* in 6-day old lung cultures. Statistical analysis of the *Id2* analysis shows a significant reduction ($p < 0.005$, $n = 4$) of the branch endpoints from 108 ± 9 in the wildtype to 38 ± 10 in mutant cultures. **(F)** Immunofluorescent stainings for the fibroblast marker S100a4 and the extracellular matrix protein fibronectin (Fn) of E14.5 and E16.5 wildtype and mutant mice. S100a4 was downregulated in both stages in *Tbx2*^{cre/cre} mice while Fn is complementary upregulated.

Maintenance of *Tbx2* expression retains the highly proliferative state of the lung mesenchyme

To get further insights into the cellular function of *Tbx2* in the developing lung, we determined the effect of prolonged *Tbx2* expression on proliferation and differentiation in this organ. For this gain-of-function experiment, we used a conditional *Tbx2^{re}/loxP*-based *TBX2* misexpression approach. Integration of a bicistronic transgene-cassette containing the human *TBX2* ORF followed by *IRES-GFP* in the ubiquitously expressed X-chromosomal *hypoxanthine guanine phosphoribosyl transferase* (*Hprt*) locus allows to trace transgene-expressing cells *in vivo* by GFP-fluorescence. This system represents a useful tool to study cellular phenotypes both under mosaic conditions in heterozygous females (due to random X-chromosome inactivation) but also under uniform expression in hemizygous males.

Male *Tbx2^{re/+};Hprt^{TBX2/y}* mice were not recovered after birth suggesting that uniform overexpression of *TBX2* in its own expression domains is deleterious for postnatal life. In contrast, female *TBX2*-overexpressing mice survived at least for 2 months. At P40, *Tbx2^{re/+};Hprt^{TBX2/+}* mice appeared smaller while the size of the lung was not obviously changed (Fig. 4A). The relative lung mass, however, was significantly increased at this stage (1.27 ± 0.03 , $p=0.009$), and even more at P56 (1.45 ± 0.08 times, $p<0.005$) (Data not shown). Histological analysis showed a single cell layer surrounding the wildtype alveoli. In *TBX2*-overexpressing lungs, alveoli were surrounded by a thick mesenchyme of several cell layers and clusters of cells were frequently observed (Fig. 4B). TUNEL staining showed that apoptosis was not affected by overexpression of *TBX2* (Fig. 4C). In contrast, BrdU incorporation assay revealed a hyperproliferative state of *TBX2* overexpressing adult lung (Fig. 4C). Statistical analysis revealed highly proliferative mesenchym in the *Tbx2* overexpression mouse ($33.8\% \pm 5.2$), while in wildtype adult mice proliferation is at a low level ($3.9\% \pm 2.4$) (Fig. 4D). Immunofluorescent stainings showed that S100a4 is detectable in a few cells in the wildtype lung and S100a4 positive cells are strongly increased in the overexpression mutant. Fn is strongly present in the wildtype and severely downregulated in *Hprt^{TBX2/+}* mice. Sm22a is not changed while *Tbx2* detection in approximately half of the cells in the overexpression mutant shows functionality of the conditional allele. Together, these data show that maintenance of *Tbx2* expression in the lung mesenchyme leads to overproliferation of pulmonary fibroblasts and reduced mesenchymal cell differentiation.

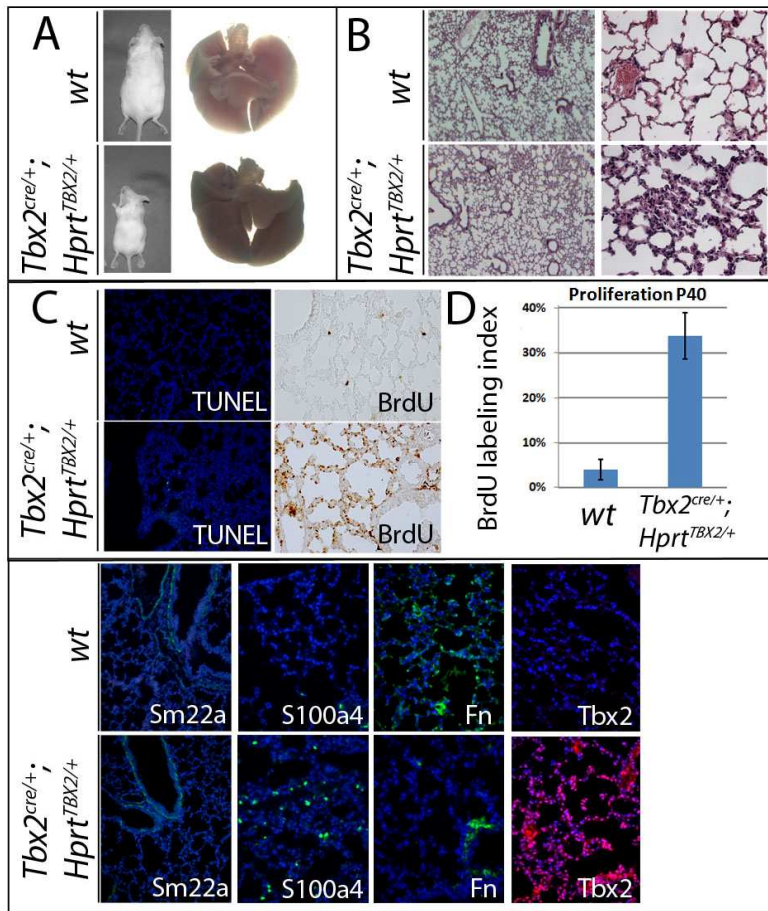


Fig. 4. Maintenance of *Tbx2* expression retains the proliferative state of the lung mesenchyme. (A) Morphology of P40 mice and lungs. (B) Histological analysis by eosin and hematoxylin staining of frontal sections of the lung and in higher magnifications of regions marked by black rectangles. (C) TUNEL staining and BrdU incorporation assay of frontal sections of the lung. (D) Statistical analysis of wildtype and *Tbx2*^{cre/+}; *Hprt*^{TBX2/+} mice shows highly increased BrdU incorporation in the *TBX2*-overexpressing lung. Labeling index of wt is 3.9%±2.4; labeling index of *Tbx2*-gain-of-function lungs is 33.8%±5.1. (E) Immunofluorescent stainings for S100a4, fibronectin (Fn), Sm22a and *Tbx2* on P40 wildtype and constitutively *TBX2* expressing mice.

Derepression of cell cycle inhibitors and reduction of canonical Wnt signaling accompany proliferation defects in the *Tbx2*-mutant lung

To determine the underlying molecular changes that cause premature differentiation and reduced proliferation of the lung mesenchyme, and reduced epithelial branching morphogenesis in the *Tbx2* loss-of-function we analyzed the expression of a panel of genes/signaling pathways that have been implicated in epithelial-mesenchymal tissue interactions during lung development as well as those directly controlling the cell cycle. For the latter we focused on expression of cell cycle regulators that have previously been implicated as targets of *Tbx2*/*Tbx3* function *in vitro*. To accurately identify expression changes we used quantitative RT-PCR of whole lung extracts at different developmental stages. We started our analysis with lungs from E16.5 when differentiation, proliferation and branching defects were fully apparent (Fig. 5). At this stage, we observed a significant downregulation of components of the Bmp-pathway such as *Bmp4* and *Bmpr2*, which are expressed in the epithelium of the bronchi as well as the Bmp target gene *Msx1* (Fig. 5A). Expression of *Bmp2* and *Bmpr1a*, in contrast, were not significantly altered. The sonic hedgehog pathway was also affected indicated by a significant reduction of the signaling molecule *Shh*. The Sonic hedgehog target gene and receptor *Ptc1* was found slightly but not significantly reduced.

However, mesenchymal Wnt-signaling was strongly reduced as indicated by reduced expression of the Wnt ligands *Wnt2* and *Wnt5a*, and the canonical Wnt target gene *Axin2* (Fig. 5A). Unexpectedly, no changes in Fgf pathway components were found. Mesenchymal *Fgf10* expression was at wildtype levels as well as the epithelially expressed receptor *Fgfr2* and the known Fgf target gene *Pea3*. Expression of *Tbx3* was not altered in the mutant, arguing against a compensatory mechanism for the loss of *Tbx2* (Fig. 5A). Among the tested cell cycle activators, *Cdk1* and intriguingly another canonical Wnt target gene *Ccnd1* showed significant reduction while *Ccnd2* and *Ccnd3* were unchanged. The cell cycle inhibitors *Cdkn1a* (*p21*), *Cdkn1c* (*p57*), *Cdkn2a* (*p19ARF*) and *Cdkn2d* (*p19ink4d*) were not altered. Most notably, *Cdkn1b* (*p27*) was upregulated more than 7-fold in the mutant (Fig. 5A). At E14.5, when no obvious histological phenotype was detectable, most of the tested genes were unaltered (Fig. 5A). However, *Wnt5a* and *Axin2* were strongly down-regulated whereas *Cdkn1a* and *Cdkn1b* were 4-fold upregulated, indicating a direct interaction of *Tbx2* with Wnt/Ctnnb1 signaling and a direct repression of cell cycle repressors. At E13.5, *Cdkn1a* was already upregulated while *Ccnd1*, *Axin2* and the tested Wnt ligands were unchanged. No changes in gene expression were found at E12.5 (Fig. S1C).

However, at E18.5 most genes tested by qRT-PCR were of wildtype expression levels (Fig. 5B), indicating the deactivation of most signaling pathways, which correleates with completed morphogenetic processes like branching of the respiratory epithelium at this stage. Slight reduction of *Bmpr2* in the *Tbx2* mutant and a minor upregulation in the gain-of-function mutant could be detected. Conversely *Cdkn1a* and especially *Cdkn1b* are extremely upregulated (2.6 ± 0.8 fold, $p=0.01$ and 24.3 ± 2.3 fold $p<0,005$ respectively) in the *Tbx2*^{ov/ov} situation and downregulated in the constitutively *TBX2* expressing mouse. Relative expression levels were 0.2 ± 0.8 , $p=0.01$ for *Cdkn1a* and 0.3 ± 0.1 , $p<0.005$ for *Cdkn1b*.

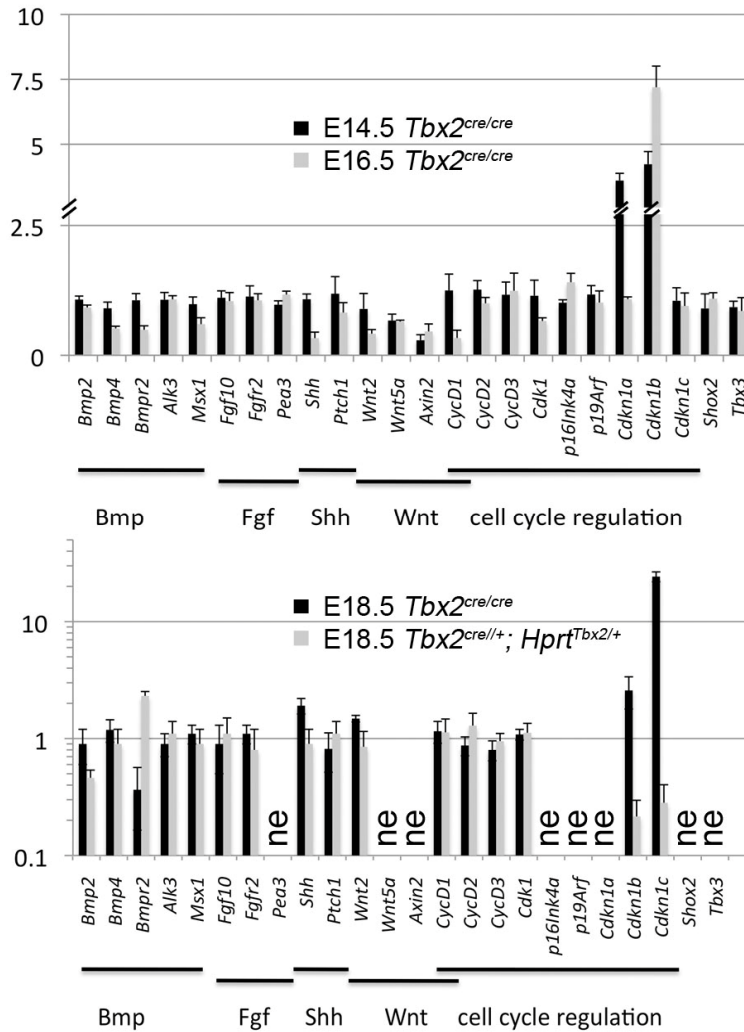


Fig. 5. Derepression of cell cycle inhibitors and reduction of canonical Wnt signaling accompany proliferation defects in the *Tbx2*-deficient lung. (A) qRT-PCR analysis of marker gene expression on mRNA from E14.5 and E16.5 wildtype and *Tbx2*^{cre/cre} lungs showing relative expression levels. Wildtype expression is set to 1. **(B)** qRT-PCR on E18.5 wildtype, *Tbx2*-mutant and *TBX2*-overexpressing lungs. Wildtype expression is set to 1. Genes and affiliations to signaling pathways or functional equivalence are as indicated in the figure.

Tbx2* directly represses *Cdkn1a* and *Cdkn1b

A direct binding of *TBX2* to the *CDKN1A* promoter in cell culture experiments had been described recently(30) whereas *Cdkn1b* has not been described as a direct target of *Tbx2* repressive activity before. To validate regulation of the cell cycle inhibitors *Cdkn1a* and *Cdkn1b* by *Tbx2* in the mouse *in vivo*, we performed *in situ hybridization* experiments. Indeed, upregulation of both cell cycle inhibitors could be shown in the lung mesenchyme in E14.5 mice (Fig. 6A). Consistent with the results of the RT-PCR at E16.5 *Cdkn1a* was not upregulated while *Cdkn1b* expression was highly increased (Fig. 6A). Expression levels in E18.5 and adult mice were below sensitivity of *in situ hybridization*, therefore immunofluorescent stainings were performed on P40 wildtype and *TBX2*-overexpressing mice (Fig. 6A). *TBX2*-overexpression mutants showed a strong reduction of *Cdkn1a* and *Cdkn1b* protein, strengthening the assumption of a direct repression of both cell cycle inhibitors by *TBX2*.

In silico analysis of the mouse *Cdkn1a* and *Cdkn1b* genes revealed one consensus binding site for T-box proteins (TBE, also T-site) (AGGTGTGA) in the *Cdkn1a* promoter and two possible TBEs in the *Cdkn1b* locus. A first site was detected 2.5 kbp upstream of the 5' UTR (AGGTGTGTG). A second putative site with the complementary sequence CACACCT was present in an intron sequence (Fig. 6B). ChIP experiments with E15.5 lung tissue revealed binding of *Tbx2* to the known TBE in the *Cdkn1a* locus *in vivo* and binding to the 5' located TBE but not to the intron located TBE in the *Cdkn1b* gene (Fig. 6C). Together these experiments suggest that *Tbx2* maintains proliferation of the lung mesenchyme by direct repression of the cell cycle inhibitors *Cdkn1a* and *Cdkn1b*.

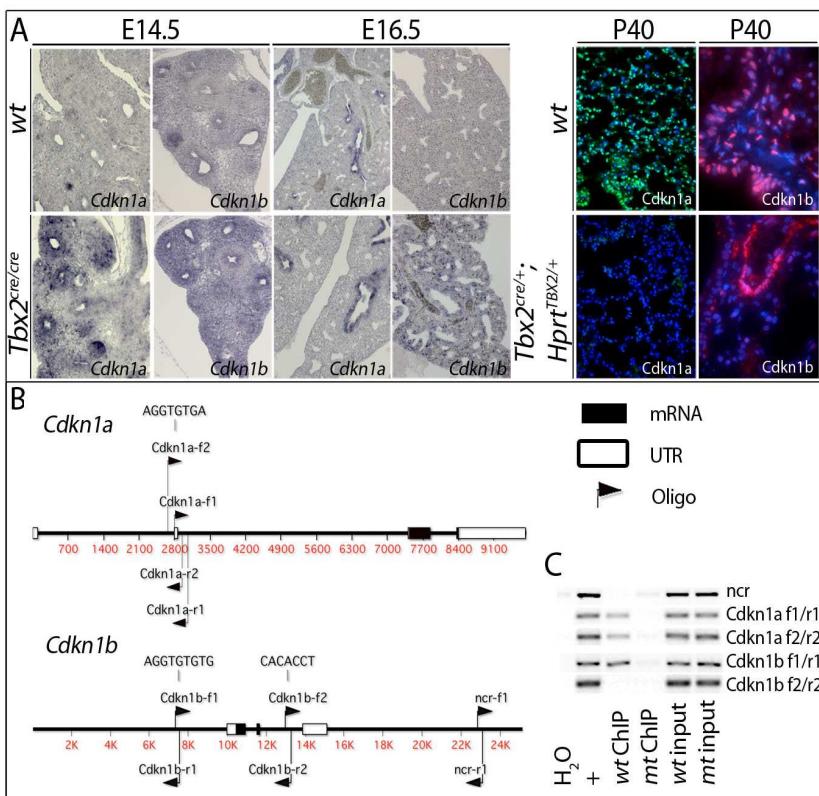


Fig. 6. *Tbx2* directly represses *Cdkn1a* and *Cdkn1b* promoters. (A) *In situ* hybridization analysis of E14.5 and E16.5 wildtype and *Tbx2*^{cre/cre} lungs and immunofluorescent stainings for *Cdkn1a* and *Cdkn1b* of P40 wildtype and constitutively *TBX2* expressing mice. Genes and stages are as indicated in the figure. (B) Schematic diagram of *Cdkn1a* and *Cdkn1b* gene loci showing positions of T binding elements and oligos. (C) Chromatin immunoprecipitation assay on E15.5 wildtype and *Tbx2*^{cre/cre} lungs. Tail DNA was used as positive control for the PCR reaction. Input control DNA was collected before application of the *Tbx2* antibody.

Genetic ablation of *Cdkn1a* and *Cdkn1b* does not rescue lung growth in the *Tbx2* mutant

To further unravel the contribution of increased expression of *Cdkn1a* and *Cdkn1b* for the growth deficit of the *Tbx2*-deficient lung, we wished to ablate the two genes in the mutant background. Double mutants of *Tbx2* with *Cdkn1a* and *Cdkn1b*, respectively, exhibited lungs that were morphologically indistinguishable from the *Tbx2*-single mutant organ (Fig. 7A). Furthermore, the relative weight of the lungs of *Tbx2*^{cre/cre};*Cdkn1a*^{-/-} and *Tbx2*^{cre/cre};*Cdkn1b*^{-/-} embryos, respectively, did not significantly alter compared to the *Tbx2*^{cre/cre} organ (Fig. 7B).

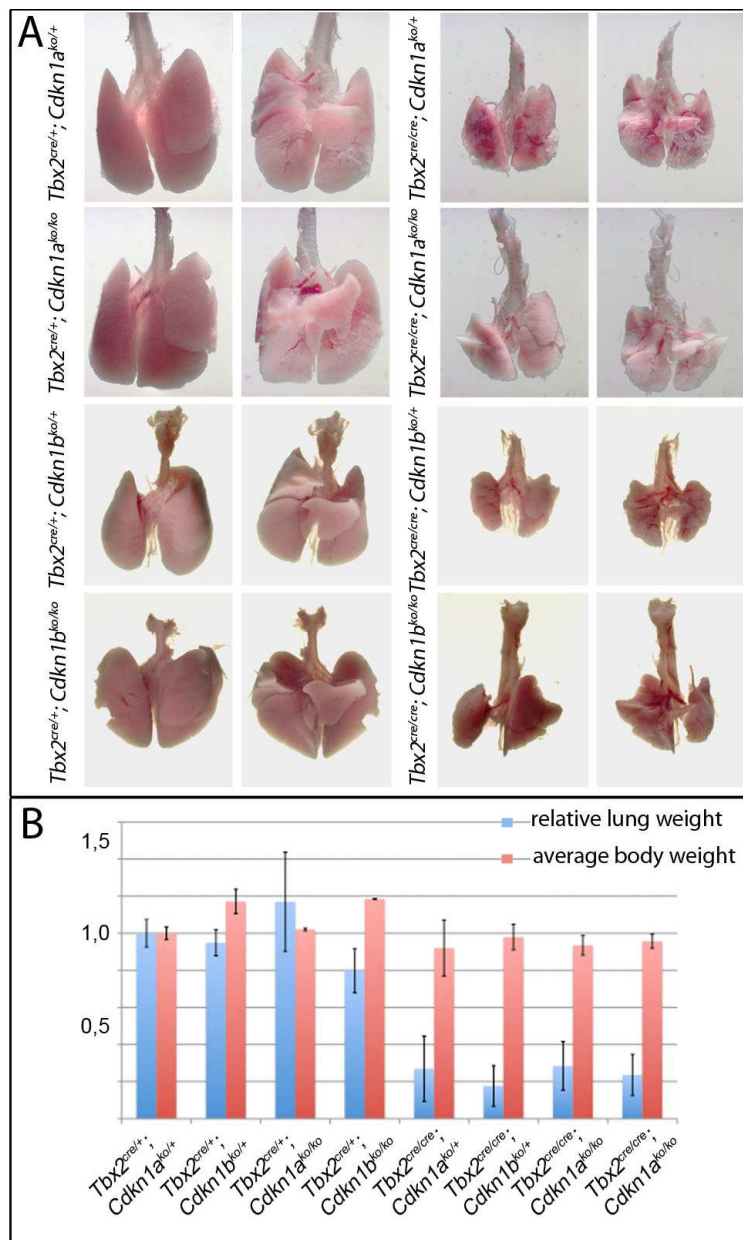


Fig. 7 Genetic ablation of *Cdkn1a* and *Cdkn1b* does not rescue lung growth in the *Tbx2*-deficient embryos. (A) Morphology of E18.5 lungs. Genotypes are indicated in the figure. The size of the lungs on a *Tbx2*-deficient background is severely reduced independent from genetic ablation of one or both alleles of *Cdkn1a* or *Cdkn1b*. (B) Statistical analysis of body weight and relative lung weight of E18.5 mice of the indicated genotypes. Mice homozygous for *Tbx2*^{cre} and heterozygous for *Cdkn1a* or *Cdkn1b* show dramatically decreased relative weights comparable to *Tbx2*^{cre/cre} mice. Double homozygous mice show no increase in relative lung weight in comparison to *Tbx2*-deficient mice.

Chemical and genetic restoration of canonical Wnt signaling restores growth and lung branching in *Tbx2*-mutant mice

Since *Wnt2*, *Wnt5a* as well as the Wnt target gene *Axin2* were significantly decreased already at E14.5 (Fig. 5A), we hypothesized a primary requirement for *Tbx2* to support canonical Wnt signaling in the lung mesenchyme. *In situ* hybridization experiments confirmed the expression changes detected in RT-PCR (Fig. 7A). *Wnt2* and *Axin2* were strongly downregulated in *Tbx2*-

mutant mice at E14.5 and E16.5. However, in *TBX2*-overexpressing adult mice, Wnt signaling was not ectopically activated (Fig. 8).

To further elucidate if a change of canonical Wnt signaling pathway is pivotal to the observed phenotype of *Tbx2*-deficient lungs, we performed pharmaceutical rescue experiments in organ culture. LiCl, a known inhibitor of GSK3b and for this reason a stabilizer for Ctnnb1(55) was added to the cultures in order to restore canonical Wnt signaling in the mutant lungs. A concentration of 20 mM LiCl was recently described to repress branching in lung and lacrimal gland organ cultures(56). Since *Wnt7b* is strongly expressed in the lung epithelium, high LiCl concentrations most likely also strongly affect the epithelium. To overcome these negative effects and to determine the best working concentration of LiCl in this rescue experiment, a dilution series of 2 mM, 10 mM, 20 mM and 40 mM LiCl was tested on wildtype lungs. *Axin2* and *CyclinD1* expression levels were checked by qRT-PCR to verify the upregulation of canonical Ctnnb1 signaling and branching endpoints were counted after 24h, 48h and 72h of culture (Fig. S2A). Concentrations of up to 10 mM of LiCl had no obvious effect on epithelial branching, while less branching endpoints were detected at both time points with 20 mM and 40 mM LiCl (Fig. S2A). Expression of *Axin2* was only slightly affected at a low concentration of LiCl, but its expression increased with higher LiCl levels. In contrast, *Ccnd1* was notably (3.6-fold) upregulated already by addition of 2 mM LiCl, but expression decreased with increasing LiCl concentrations (Fig. S2B). Since we were interested in the restoration of lung growth and branching, we decided to use 2 mM LiCl in the following organ culture experiments because of the strongest upregulation of the cell cycle activating *Ccnd1*. After 6 days of culture the *Tbx2*-mutant lung showed significantly decreased branching with less than half of branching endpoints compared to wildtype cultures (Fig. 3E). 2 mM LiCl did not enhance branching in wildtype cultures but restored branching in the *Tbx2*-mutant to almost wildtype level (Fig. 8B). Quantitative RT-PCR verified restoration of *Wnt/Ctnnb1* signaling (Fig. 8D). LiCl had only minor effects on wildtype cultures leading to a 1.8 fold increase of *Ccnd1*. Discrepancy to the previous 3.6 fold upregulation might be explained by variations in the experimental settings. Relatively low doses of LiCl probably led to a high pipetting error. However, all cultures in one experiment were treated with the same batch of medium and therefore received the same concentrations of the Gsk3b inhibitor. *Ccnd1* and *Axin2* were reduced to 60% and 40% in *Tbx2*-mutant cultures while addition of LiCl led to a strong upregulation of both genes similar to the levels observed in wildtype cultures supplemented with LiCl (Fig. 8C). The Wnt ligands *Wnt2* and *Wnt5a*, however, were not altered by addition of LiCl. Similar to findings in E16.5 mutant lungs *Cdnk1a* was also unchanged in *Tbx2*-mutant cultures. In

contrast, *Cdnk1b* was highly upregulated in *Tbx2*-mutant cultures and stayed at high levels even with addition of LiCl (Fig. 8C).

Genetic restoration of canonical Wnt signaling was achieved by *Tbx2^{rev/+}*-mediated expression of a stabilized form of Ctnnb1, that lacks the phosphorylation site and cannot be degraded by the proteasome, from a floxed allele (*Ctnnb1^{fl3}*). *Tbx2^{rev/+};Ctnnb1^{fl3/+}* lungs show enhanced growth and branching compared with wildtype littermates. In *Tbx2^{rev/fl};Ctnnb1^{fl3/+}* lung cultures, growth and branching were restored. The numbers of branches after dissection were 9.3 ± 0.6 for the wildtype, 10.0 ± 1.0 for *Tbx2^{rev/+}; Ctnnb1^{(Ex3)fl/+}* mice, 9.5 ± 0.7 for *Tbx2^{rev/fl}; Ctnnb1^{(Ex3)fl/+}* and 9.3 ± 0.6 for *Tbx2^{rev/fl}* mice and were without any significant difference. The total increase of branches was 14.3 ± 1.5 for the wildtype, 21.7 ± 1.5 for *Tbx2^{rev/+};Ctnnb1^{(Ex3)fl/+}* mice, 11.0 ± 1.4 for *Tbx2^{rev/fl};Ctnnb1^{(Ex3)fl/+}* and 6.0 ± 1.0 for *Tbx2^{rev/fl}* mice. Increase of branches in *Tbx2^{rev/+};Ctnnb1^{(Ex3)fl/+}* mice compared with the wildtype was highly significant ($p < 0.005$). Comparison of wildtype and *Tbx2^{rev/fl};Ctnnb1^{(Ex3)fl/+}* mice showed a slight but not significant reduction of branching events ($p = 0.09$). The increase of branches in *Tbx2^{rev/fl};Ctnnb1^{(Ex3)fl/+}* compared to *Tbx2^{rev/fl}* mice was highly significant ($p > 0.005$). Taken together, these results show that canonical Wnt signaling acts downstream of *Tbx2* in the lung mesenchyme to enhance mesenchymal proliferation and epithelial branching.

However, *in situ* hybridization experiments of P40 wildtype and *TBX2*-overexpressing mice for *Wnt2*, *Axin2* showed no activation of the canonical Wnt pathway by *TBX2* (Fig. S2C).

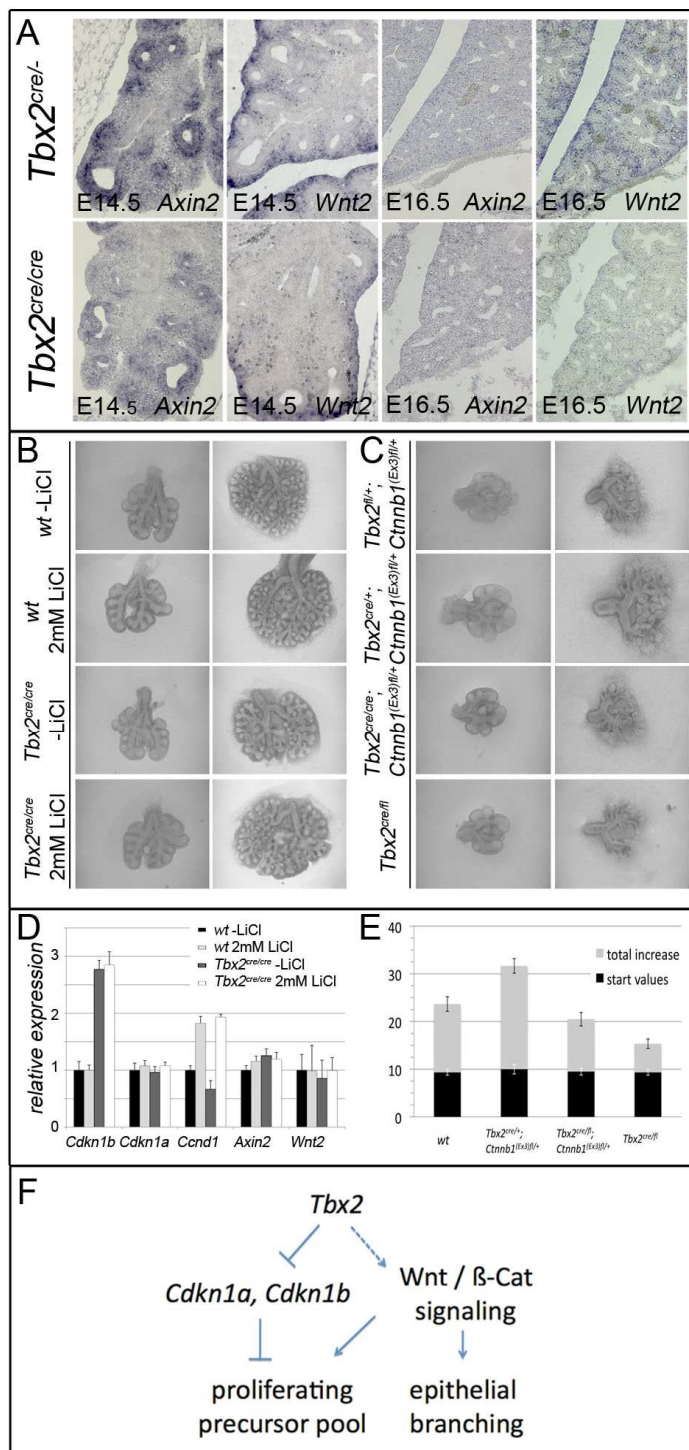


Fig. 8 Epithelial branching in *Tbx2*-deficient mice can be restored by stabilization of mesenchymal *Ctnnb1*. (A) *In situ* hybridization analysis for expression of for *Axin2* and *Wnt2* in E14.5 and E16.5 wildtype and *Tbx2*-mutant lungs. (B) Organ culture of E11.5 genetically modified lungs at day 0 (left) and day 4 (right) of culture. Genotypes are as indicated in the figure. (C) Organ culture of E12.5 wt and *Tbx2*-deficient lungs with and without treatment of 2 mM LiCl at day 0 (left) and day 4 (right) of culture. (D) qRT-PCR on mRNA of wildtype and LiCl treated lungs cultured for 4 days. (E) Statistical quantification of branching endpoint of genetically modified lungs cultured for 4 days. (F) Schematic diagram of a model proposing the function of *Tbx2* in the lung mesenchyme.

Discussion

Lung development is regulated by reciprocal signaling between the mesenchymal and epithelial tissue compartments. Here, we have identified *Tbx2* as a crucial mesenchymal factor that maintains the mesenchymal signaling center for epithelial branching morphogenesis. We suggest that *Tbx2* promotes mesenchymal proliferation directly via repression of cell cycle inhibitors and indirectly by promoting canonical Wnt signaling, the latter of which also accounts for maintenance of epithelial growth and branching.

***Tbx2* directly represses cell cycle regulators in the lung mesenchyme**

In a former report Cebra-Thomas et al.(28) demonstrated in an antisense oligonucleotide approach with cultured lung rudiments a requirement for mesenchymal *Tbx4* and *Tbx5* in the regulation of branching morphogenesis. *Tbx4/Tbx5* function is mediated by direct transcriptional activation of *Fgf10* (28, 57, 58), that encodes a potent growth factor in the lung but also in other developmental contexts(13, 15, 21, 59-61).

Given the molecular nature of *Tbx2* and *Tbx3* as transcriptional repressors it was hypothesized that *Tbx2* and *Tbx3* compete with *Tbx4/Tbx5* for binding to conserved TBEs in the promotor of *Fgf10*, similar to the antagonistic control of *Nppa* expression in the heart by *Tbx5* and *Tbx2/Tbx3*(62).

Our analysis of *Tbx2*-deficient lungs did not detect changes, i.e. up-regulation of *Fgf10* expression in the mutant pulmonary mesenchyme strongly arguing against a direct competitive regulation of *Fgf10* by *Tbx4* and *Tbx5* on one hand, and *Tbx2* and *Tbx3* on the other hand. However, our analysis indicated that *Tbx2* directly represses the expression of the genes encoding the cyclin-dependent kinase inhibitors *Cdkn1a* and *Cdkn1b* by binding to conserved TBEs in the genomic region.

Cdkn1a and *Cdkn1b* belong to the Cip/Kip family of cyclin dependent kinase inhibitors and negatively regulate cell cycle by their interaction with the Cyclin E/Cdk2 kinase complex(35, 63-65). This complex hyperphosphorylates the retinoblastoma protein, which is a prerequisite for G₁/S phase transition as it releases E2F transcription factors to induce transcription of S-phase genes necessary for replication start(66, 67). Intriguingly *Cdkn1a* mediated cell cycle arrest was associated in cell culture and *in vitro* experiments with neural differentiation(68). Hence, deregulation of *Cdkn1a* and *1b* in our loss- and gain-of-*Tbx2* genetic models may well account for the observed opposing changes of mesenchymal proliferation and differentiation.

However, individual deletion of *Cdkn1a* and *Cdkn1b* function in the *Tbx2*-deficient lung mesenchyme did not restore proliferation and overall lung growth. At this point, we cannot exclude that *Cdkn1a* and *Cdkn1b* can compensate for each other in this rescue experiments, and that the simultaneous removal of both activities is required to restore proliferation and inhibit premature differentiation. Alternatively, repression of *Cdkn1a* and *Cdkn1b* may represent only one of several pathways regulated in parallel by *Tbx2* to ensure cell cycle progression.

***Tbx2* is required to maintain Wnt signaling in the lung mesenchyme**

Our RT-PCR analysis indicated a noteworthy reduction of the Bmp signaling pathway and canonical Wnt signaling at E16.5. Both pathways have been described to regulate differentiation and cell cycle progression in numerous contexts. *Bmp4* inhibits proliferation and facilitates differentiation by downregulation of cyclin D and *Cdk2*(69), while Wnt signaling promotes cell cycle progression by the activation of *Ccnd1*(70). Notably, we detected decreased expression of Wnt components as early as E14.5, whereas *Bmp4* was unchanged at that stage. Furthermore, *Bmp4* and *Bmpr2* are epithelially expressed and can therefore not be a direct target of mesenchymal *Tbx2*. Together, this argues for a secondary nature of *Bmp4* reduction in the mutant lung.

In contrast, a couple of evidences have accumulated that canonical Wnt signaling is directly regulated by *Tbx2*. Zebrafish experiments suggested that *tbx2b* mediates canonical WNT signaling(71). A dominant negative version of the receptor *fz7* phenocopied cell migration defects observed by depletion of *tbx2* and overexpression of *fz7* led to downregulation of *tbx2*. Importantly, a requirement of canonical Wnt signaling for branching morphogenesis of the pulmonary tree has been reported(23). In mice with conditional deletion of mesenchymal *Ctnnb1* less epithelial branches formed and the lung was severely hypoplastic.

Our rescue experiments both by genetic and chemical stabilization of *Ctnnb1* clearly showed that *Tbx2* is necessary to maintain mesenchymal Wnt signaling and that Wnt signaling acts downstream of *Tbx2* to provide the signals from the mesenchyme to regulate epithelial branching. Furthermore, direct activation of *Ccnd1* by canonical Wnt signaling provides an independent pathway to promote cell cycle progression.

However, constitutive expression of *Tbx2* in the lungs of adult mice was not sufficient to reactivate WNT/CTNNB1 signaling, arguing that *Tbx2* represses an inhibitor of canonical Wnt signaling in the lung mesenchyme.

Preliminary experiments with known inhibitors in *Tbx2*-deficient lungs did not identify a candidate for such an activity.

Tbx2 acts late in lung development

Our expression analysis revealed that *Tbx2* is expressed in the pulmonary mesenchyme starting from E9.5 to postnatal stages. Hence, *Tbx2* expression occurs in the pseudoglandular stage where growth occurs by massive branching morphogenesis(11), but also in the canalicular and saccular phase in which terminal buds are established and differentiation of pneumocytes occur(10). Given the finding that signaling systems that are required to mediate branching morphogenesis are shut down after E16.5, *Tbx2* is likely to directly repress *Cdkn1* and *Cdkn1b* throughout the pseudoglandular into the saccular stage, whereas *Tbx2* promotes canonical Wnt signaling only until the end of the pseudoglandular stage. However, our gain-of-function experiments strongly imply that *Tbx2* does not induce Wnt signaling in the lung mesenchyme but represses an inhibitor of this pathway. With the down-regulation of the activator around E16.5, *Tbx2* regulation of this pathway becomes irrelevant. Molecular and cellular changes in the lung mesenchyme of *Tbx2*-deficient lungs only occur after E14.5, in the late phase of the pseudoglandular stage. This coincides with the down-regulation of *Tbx3* expression in the lung mesenchyme around this time. Biochemical equivalence as transcriptional repressors suggest that *Tbx2* and *Tbx3* act redundantly until E14.5 to promote growth and branching of the lungs.

Maintenance of the mesenchymal signaling center by Tbx2

Our data suggest that *Tbx2* probably in combination with *Tbx3* in the early phase of the pseudoglandular stage maintains the mesenchymal signaling by two pathways. First, *Tbx2* represses *Cdkn1a* and *Cdkn1b* thereby facilitating mesenchymal proliferation and inhibiting differentiation. Second, *Tbx2* promotes Wnt/*Ctnnb1* signaling that independently keeps mesenchymal cells in a proliferating state by activating expression of *Cnd1*. Canonical Wnt signaling also ensures continuation of epithelial branching morphogenesis (Fig. 7)

Acknowledgements

The authors thank D. Tosh for providing us with complementary DNAs for *Cebpa* and *Hnf1a*, and U. Kossatz-Böhlert and Michaela Mai for antibodies and discussions.

References

1. Davis CW, Dickey BF. Regulated airway goblet cell mucin secretion. *Annu Rev Physiol* 2008; **70**: 487-512.
2. Tompkins DH, Besnard V, Lange AW, Wert SE, Keiser AR, Smith AN, Lang R, et al. Sox2 is required for maintenance and differentiation of bronchiolar clara, ciliated, and goblet cells. *PLoS One* 2009; **4**(12): e8248.
3. Cole BB, Smith RW, Jenkins KM, Graham BB, Reynolds PR, Reynolds SD. Tracheal basal cells: A facultative progenitor cell pool. *Am J Pathol* 2010; **177**(1): 362-376.
4. Whitsett JA, Wert SE, Weaver TE. Alveolar surfactant homeostasis and the pathogenesis of pulmonary disease. *Annu Rev Med* 2010; **61**: 105-119.
5. Morrissey EE, Hogan BL. Preparing for the first breath: Genetic and cellular mechanisms in lung development. *Dev Cell* 2010; **18**(1): 8-23.
6. Amrani Y, Panettieri RA. Airway smooth muscle: Contraction and beyond. *Int J Biochem Cell Biol* 2003; **35**(3): 272-276.
7. Dunsmore SE, Rannels DE. Extracellular matrix biology in the lung. *Am J Physiol* 1996; **270**(1 Pt 1): L3-27.
8. Wells JM, Melton DA. Vertebrate endoderm development. *Annu Rev Cell Dev Biol* 1999; **15**: 393-410.
9. Cardoso WV, Lu J. Regulation of early lung morphogenesis: Questions, facts and controversies. *Development* 2006; **133**(9): 1611-1624.
10. Warburton D, Schwarz M, Tefft D, Flores-Delgado G, Anderson KD, Cardoso WV. The molecular basis of lung morphogenesis. *Mech Dev* 2000; **92**(1): 55-81.
11. Metzger RJ, Klein OD, Martin GR, Krasnow MA. The branching programme of mouse lung development. *Nature* 2008; **453**(7196): 745-750.
12. Kauffman SL. Cell proliferation in the mammalian lung. *Int Rev Exp Pathol* 1980; **22**: 131-191.
13. Bellusci S, Grindley J, Emoto H, Itoh N, Hogan BL. Fibroblast growth factor 10 (FGF10) and branching morphogenesis in the embryonic mouse lung. *Development* 1997; **124**(23): 4867-4878.
14. Min H, Danilenko DM, Scully SA, Bolon B, Ring BD, Tarpley JE, DeRose M, et al. Fgf-10 is required for both limb and lung development and exhibits striking functional similarity to drosophila branchless. *Genes Dev* 1998; **12**(20): 3156-3161.
15. Sekine K, Ohuchi H, Fujiwara M, Yamasaki M, Yoshizawa T, Sato T, Yagishita N, et al. Fgf10 is essential for limb and lung formation. *Nat Genet* 1999; **21**(1): 138-141.
16. Bitgood MJ, McMahon AP. Hedgehog and bmp genes are coexpressed at many diverse sites of cell-cell interaction in the mouse embryo. *Dev Biol* 1995; **172**(1): 126-138.

17. Bellusci S, Furuta Y, Rush MG, Henderson R, Winnier G, Hogan BL. Involvement of sonic hedgehog (shh) in mouse embryonic lung growth and morphogenesis. *Development* 1997; **124**(1): 53-63.
18. Lebeche D, Malpel S, Cardoso WV. Fibroblast growth factor interactions in the developing lung. *Mech Dev* 1999; **86**(1-2): 125-136.
19. White AC, Xu J, Yin Y, Smith C, Schmid G, Ornitz DM. FGF9 and SHH signaling coordinate lung growth and development through regulation of distinct mesenchymal domains. *Development* 2006; **133**(8): 1507-1517.
20. Pepicelli CV, Lewis PM, McMahon AP. Sonic hedgehog regulates branching morphogenesis in the mammalian lung. *Curr Biol* 1998; **8**(19): 1083-1086.
21. Weaver M, Dunn NR, Hogan BL. Bmp4 and Fgf10 play opposing roles during lung bud morphogenesis. *Development* 2000; **127**(12): 2695-2704.
22. Li C, Hu L, Xiao J, Chen H, Li JT, Bellusci S, Delanghe S, et al. Wnt5a regulates shh and Fgf10 signaling during lung development. *Dev Biol* 2005; **287**(1): 86-97.
23. Yin Y, White AC, Huh SH, Hilton MJ, Kanazawa H, Long F, Ornitz DM. An FGF-WNT gene regulatory network controls lung mesenchyme development. *Dev Biol* 2008; **319**(2): 426-436.
24. Rajagopal J, Carroll TJ, Guseh JS, Bores SA, Blank LJ, Anderson WJ, Yu J, et al. Wnt7b stimulates embryonic lung growth by coordinately increasing the replication of epithelium and mesenchyme. *Development* 2008; **135**(9): 1625-1634.
25. Shu W, Guttentag S, Wang Z, Andl T, Ballard P, Lu MM, Piccolo S, et al. Wnt/beta-catenin signaling acts upstream of N-myc, BMP4, and FGF signaling to regulate proximal-distal patterning in the lung. *Dev Biol* 2005; **283**(1): 226-239.
26. Cohen ED, Ihida-Stansbury K, Lu MM, Panettieri RA, Jones PL, Morrisey EE. Wnt signaling regulates smooth muscle precursor development in the mouse lung via a tenascin C/PDGFR pathway. *J Clin Invest* 2009; **119**(9): 2538-2549.
27. Chapman DL, Garvey N, Hancock S, Alexiou M, Agulnik SI, Gibson-Brown JJ, Cebra-Thomas J, et al. Expression of the T-box family genes, *Tbx1-Tbx5*, during early mouse development. *Dev Dyn* 1996; **206**(4): 379-390.
28. Cebra-Thomas JA, Bromer J, Gardner R, Lam GK, Sheipe H, Gilbert SF. T-box gene products are required for mesenchymal induction of epithelial branching in the embryonic mouse lung. *Dev Dyn* 2003; **226**(1): 82-90.
29. Jacobs JJ, Keblusek P, Robanus-Maandag E, Kristel P, Lingbeek M, Nederlof PM, van Welsem T, et al. Senescence bypass screen identifies TBX2, which represses *Cdkn2a* (p19(ARF)) and is amplified in a subset of human breast cancers. *Nat Genet* 2000; **26**(3): 291-299.
30. Prince S, Carreira S, Vance KW, Abrahams A, Goding CR. *Tbx2* directly represses the expression of the p21(WAF1) cyclin-dependent kinase inhibitor. *Cancer Res* 2004; **64**(5): 1669-1674.

31. Vance KW, Carreira S, Brosch G, Goding CR. *Tbx2* is overexpressed and plays an important role in maintaining proliferation and suppression of senescence in melanomas. *Cancer Res* 2005; **65**(6): 2260-2268.
32. Suzuki A, Sekiya S, Buscher D, Izpisua Belmonte JC, Taniguchi H. *Tbx3* controls the fate of hepatic progenitor cells in liver development by suppressing p19ARF expression. *Development* 2008; **135**(9): 1589-1595.
33. Luche H, Weber O, Nageswara Rao T, Blum C, Fehling HJ. Faithful activation of an extra-bright red fluorescent protein in "knock-in" cre-reporter mice ideally suited for lineage tracing studies. *Eur J Immunol* 2007; **37**(1): 43-53.
34. Lingbeek ME, Jacobs JJ, van Lohuizen M. The T-box repressors TBX2 and TBX3 specifically regulate the tumor suppressor gene p14ARF via a variant T-site in the initiator. *J Biol Chem* 2002; **277**(29): 26120-26127.
35. Brugarolas J, Chandrasekaran C, Gordon JI, Beach D, Jacks T, Hannon GJ. Radiation-induced cell cycle arrest compromised by p21 deficiency. *Nature* 1995; **377**(6549): 552-557.
36. Fero ML, Rivkin M, Tasch M, Porter P, Carow CE, Firpo E, Polyak K, et al. A syndrome of multiorgan hyperplasia with features of gigantism, tumorigenesis, and female sterility in p27(Kip1)-deficient mice. *Cell* 1996; **85**(5): 733-744.
37. Aanhaanen WT, Brons JF, Dominguez JN, Rana MS, Norden J, Airik R, Wakker V, et al. The *Tbx2*+ primary myocardium of the atrioventricular canal forms the atrioventricular node and the base of the left ventricle. *Circ Res* 2009; **104**(11): 1267-1274.
38. Wakker V, Brons JF, Aanhaanen WT, van Roon MA, Moorman AF, Christoffels VM. Generation of mice with a conditional null allele for *Tbx2*. *Genesis* 2010; **48**(3): 195-199.
39. Harada N, Tamai Y, Ishikawa T, Sauer B, Takaku K, Oshima M, Taketo MM. Intestinal polyposis in mice with a dominant stable mutation of the beta-catenin gene. *EMBO J* 1999; **18**(21): 5931-5942.
40. Young P, Boussadia O, Halfter H, Grose R, Berger P, Leone DP, Robenek H, et al. E-cadherin controls adherens junctions in the epidermis and the renewal of hair follicles. *EMBO J* 2003; **22**(21): 5723-5733.
41. Brachtendorf G, Kuhn A, Samulowitz U, Knorr R, Gustafsson E, Potocnik AJ, Fassler R, et al. Early expression of endomucin on endothelium of the mouse embryo and on putative hematopoietic clusters in the dorsal aorta. *Dev Dyn* 2001; **222**(3): 410-419.
42. Moorman AF, Houweling AC, de Boer PA, Christoffels VM. Sensitive nonradioactive detection of mRNA in tissue sections: Novel application of the whole-mount in situ hybridization protocol. *J Histochem Cytochem* 2001; **49**(1): 1-8.
43. Zirzow S, Ludtke TH, Brons JF, Petry M, Christoffels VM, Kispert A. Expression and requirement of T-box transcription factors *Tbx2* and *Tbx3* during secondary palate development in the mouse. *Dev Biol* 2009; **336**(2): 145-155.

44. Braunstein M, Rose AB, Holmes SG, Allis CD, Broach JR. Transcriptional silencing in yeast is associated with reduced nucleosome acetylation. *Genes Dev* 1993; **7**(4): 592-604.
45. Rasband WS. ImageJ. U S National Institutes of Health, Bethesda, Maryland, USA 1997-2011; .
46. Rawlins EL, Okubo T, Xue Y, Brass DM, Auten RL, Hasegawa H, Wang F, et al. The role of Scgb1a1+ clara cells in the long-term maintenance and repair of lung airway, but not alveolar, epithelium. *Cell Stem Cell* 2009; **4**(6): 525-534.
47. Tabuchi Y, Doi T, Takasaki I, Takahashi R, Ueda M, Suzuki Y, Obinata M. Establishment and functional characterization of a tracheal epithelial cell line RTEC11 from transgenic rats harboring temperature-sensitive simian virus 40 large T-antigen. *Cell Biol Int* 2008; **32**(11): 1344-1352.
48. Degiulio JV, Kaufman CD, Dean DA. The SP-C promoter facilitates alveolar type II epithelial cell-specific plasmid nuclear import and gene expression. *Gene Ther* 2010; **17**(4): 541-549.
49. Kreda SM, Gynn MC, Fenstermacher DA, Boucher RC, Gabriel SE. Expression and localization of epithelial aquaporins in the adult human lung. *Am J Respir Cell Mol Biol* 2001; **24**(3): 224-234.
50. Rock JR, Onaitis MW, Rawlins EL, Lu Y, Clark CP, Xue Y, Randell SH, et al. Basal cells as stem cells of the mouse trachea and human airway epithelium. *Proc Natl Acad Sci U S A* 2009; **106**(31): 12771-12775.
51. Xu K, Nieuwenhuis E, Cohen BL, Wang W, Canty AJ, Danska JS, Coultas L, et al. Lunatic fringe-mediated notch signaling is required for lung alveogenesis. *Am J Physiol Lung Cell Mol Physiol* 2010; **298**(1): L45-56.
52. Grieskamp T, Rudat C, Ludtke TH, Norden J, Kispert A. Notch signaling regulates smooth muscle differentiation of epicardium-derived cells. *Circ Res* 2011; **108**(7): 813-823.
53. Lawson WE, Polosukhin VV, Zoia O, Stathopoulos GT, Han W, Plieth D, Loyd JE, et al. Characterization of fibroblast-specific protein 1 in pulmonary fibrosis. *Am J Respir Crit Care Med* 2005; **171**(8): 899-907.
54. Gomperts BN, Strieter RM. Fibrocytes in lung disease. *J Leukoc Biol* 2007; **82**(3): 449-456.
55. Klein PS, Melton DA. A molecular mechanism for the effect of lithium on development. *Proc Natl Acad Sci U S A* 1996; **93**(16): 8455-8459.
56. Dean CH, Miller LA, Smith AN, Dufort D, Lang RA, Niswander LA. Canonical wnt signaling negatively regulates branching morphogenesis of the lung and lacrimal gland. *Dev Biol* 2005; **286**(1): 270-286.
57. Agarwal P, Wylie JN, Galceran J, Arkhitko O, Li C, Deng C, Grosschedl R, et al. *Tbx5* is essential for forelimb bud initiation following patterning of the limb field in the mouse embryo. *Development* 2003; **130**(3): 623-633.
58. Minguillon C, Del Buono J, Logan MP. *Tbx5* and *Tbx4* are not sufficient to determine limb-specific morphologies but have common roles in initiating limb outgrowth. *Dev Cell* 2005; **8**(1): 75-84.

59. Marguerie A, Bajolle F, Zaffran S, Brown NA, Dickson C, Buckingham ME, Kelly RG. Congenital heart defects in *Fgfr2-IIIb* and *Fgf10* mutant mice. *Cardiovasc Res* 2006; **71**(1): 50-60.
60. Watanabe Y, Miyagawa-Tomita S, Vincent SD, Kelly RG, Moon AM, Buckingham ME. Role of mesodermal FGF8 and FGF10 overlaps in the development of the arterial pole of the heart and pharyngeal arch arteries. *Circ Res* 2010; **106**(3): 495-503.
61. Bates CM. Role of fibroblast growth factor receptor signaling in kidney development. *Pediatr Nephrol* 2011; .
62. Habets PE, Moorman AF, Clout DE, van Roon MA, Lingbeek M, van Lohuizen M, Campione M, et al. Cooperative action of *Tbx2* and *Nkx2.5* inhibits ANF expression in the atrioventricular canal: Implications for cardiac chamber formation. *Genes Dev* 2002; **16**(10): 1234-1246.
63. Harper JW, Adami GR, Wei N, Keyomarsi K, Elledge SJ. The p21 cdk-interacting protein Cip1 is a potent inhibitor of G1 cyclin-dependent kinases. *Cell* 1993; **75**(4): 805-816.
64. Cariou S, Donovan JC, Flanagan WM, Milic A, Bhattacharya N, Slingerland JM. Down-regulation of p21^{WAF1/CIP1} or p27^{Kip1} abrogates antiestrogen-mediated cell cycle arrest in human breast cancer cells. *Proc Natl Acad Sci U S A* 2000; **97**(16): 9042-9046.
65. Coverley D, Laman H, Laskey RA. Distinct roles for cyclins E and A during DNA replication complex assembly and activation. *Nat Cell Biol* 2002; **4**(7): 523-528.
66. Akiyama T, Ohuchi T, Sumida S, Matsumoto K, Toyoshima K. Phosphorylation of the retinoblastoma protein by cdk2. *Proc Natl Acad Sci U S A* 1992; **89**(17): 7900-7904.
67. Muller H, Moroni MC, Vigo E, Petersen BO, Bartek J, Helin K. Induction of S-phase entry by E2F transcription factors depends on their nuclear localization. *Mol Cell Biol* 1997; **17**(9): 5508-5520.
68. Tanaka H, Yamashita T, Asada M, Mizutani S, Yoshikawa H, Tohyama M. Cytoplasmic p21^{Cip1/WAF1} regulates neurite remodeling by inhibiting rho-kinase activity. *J Cell Biol* 2002; **158**(2): 321-329.
69. Jeffery TK, Upton PD, Trembath RC, Morrell NW. BMP4 inhibits proliferation and promotes myocyte differentiation of lung fibroblasts via Smad1 and JNK pathways. *Am J Physiol Lung Cell Mol Physiol* 2005; **288**(2): L370-8.
70. Shtutman M, Zhurinsky J, Simcha I, Albanese C, D'Amico M, Pestell R, Ben-Ze'ev A. The cyclin D1 gene is a target of the beta-catenin/LEF-1 pathway. *Proc Natl Acad Sci U S A* 1999; **96**(10): 5522-5527.
71. Fong SH, Emelyanov A, Teh C, Korzh V. Wnt signalling mediated by *Tbx2b* regulates cell migration during formation of the neural plate. *Development* 2005; **132**(16): 3587-3596.

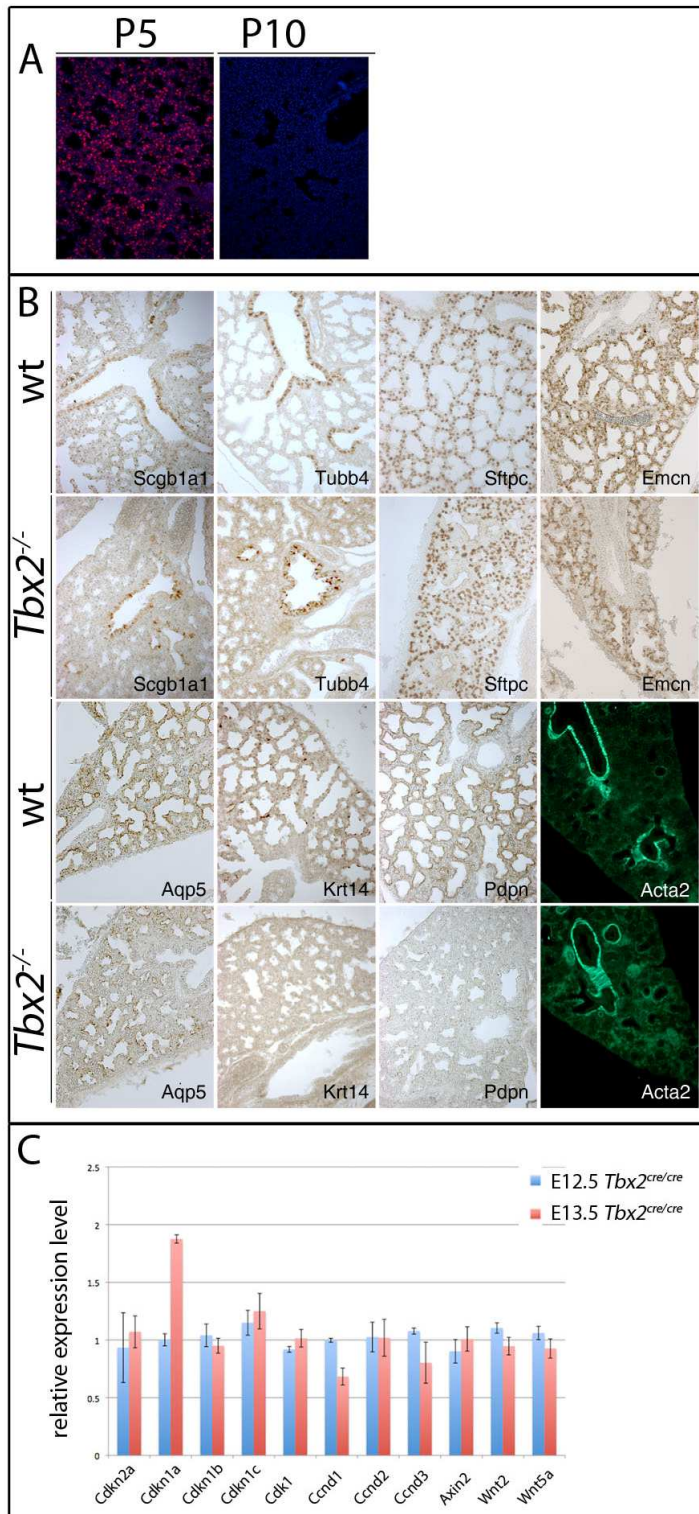


Figure S1 (A) Immunofluorescent staining for TBX2 on P5 and P10 wildtype lung sections. (B) Antibody staining on E18.5 wildtype and *Tbx2*^{cre/cre} mice. Antigens as indicated in the figure. (C) qRT-PCR of E12.5 and E13.5 dissected wildtype and *Tbx2* mutant lungs. Wildtype is set to 1. Notably at E13.5 *Cdkn1a* is considerably upregulated 2fold and *Cdkn1a* is slightly but not significantly reduced. At E12.5 no changes in the expression of the tested genes could be detected. Genes are as indicated in the figure.

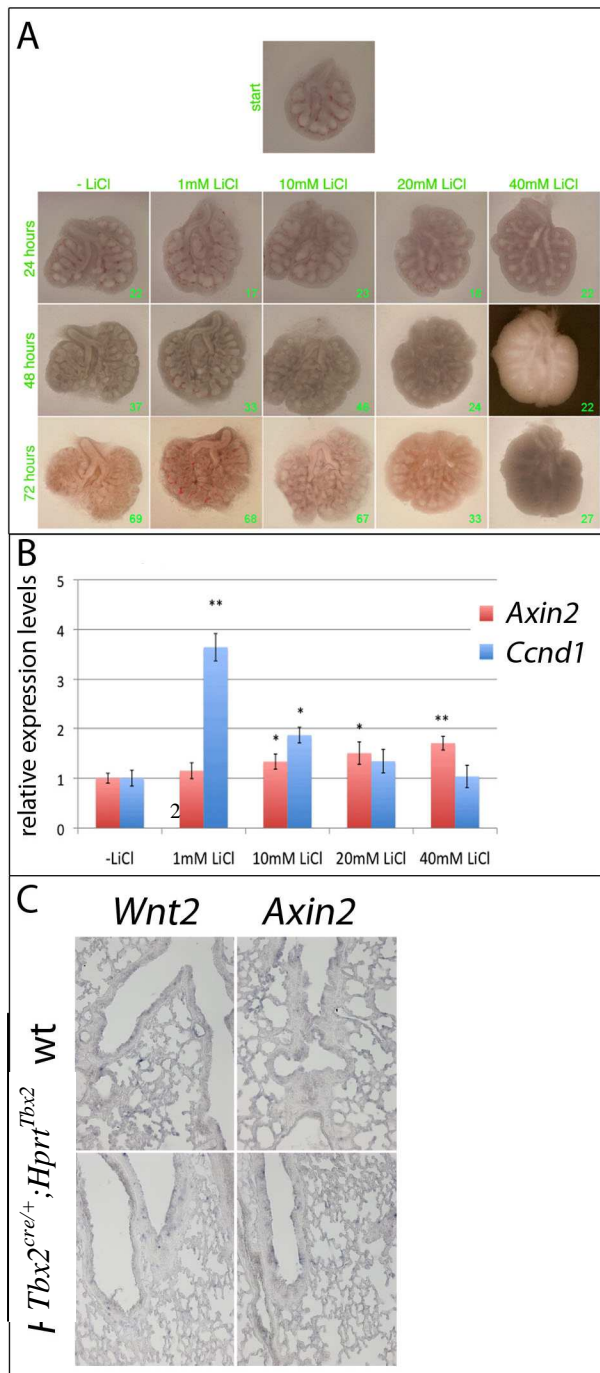


Figure S2 (A) Organ culture of at E12.5 dissected wildtype lungs treated with increasing concentrations of LiCl. Branching endpoints were counted for three days once a day. No changes were detectable up to 10 mM LiCl. Branching was reduced with 20 mM LiCl and almost stopped when cultures were supplemented with 40 mM LiCl. **(B)** qRT-PCR of 72h LiCl treated lung cultures. *Ccnd1* was upregulated with 2 mM LiCl about 3.5 fold. Expression levels of *Ccnd1* declined with higher concentrations of LiCl. *Axin2* expression was only moderately affected and increased with higher LiCl levels. **(C)** In situ hybridization experiments for *Wnt2* and *Axin2* on P40 wildtype and *Tbx2^{cre/+}; Hprt^{Tbx2/+}* mice. Both genes are not expressed at this stage in neither genotype.

Concluding remarks

Analysis of T-box genes in the last decade revealed this group of transcription factors as extremely important for embryonic development in establishing tissue boundaries(71), regulating cellular proliferation and differentiation(52), facilitating cell adhesion or cell migration(72), timing EMT processes(73) and many others.

In the present study we identified *Tbx2* and *Tbx3* as crucial transcription factors in the tightly orchestrated network regulating endoderm organogenesis. In part 1 and 2, our analysis focused on the function of *Tbx3* in the early and late developmental mechanisms underlying the growth and differentiation processes of liver formation. *Tbx3* was identified to be a potent suppressor of cholangiocyte fate decision that could even override biliary induction by Notch signaling from its natural source, the portal veins, or from constitutively activated Notch pathway (part 2 of this study). Although a lot of effort has been dedicated to the understanding of biliary development and we have learned a lot about bile duct formation recently (48, 74, 75) we still lack insights on the principals of cholangiocyte differentiation. From the presented study one can speculate that *Tbx3* represses especially up to now unknown Notch target genes, which mediate cholangiocyte differentiation while it leaves other Notch target genes unhindered. Further work will have to cope with that question maybe by performing ChIP-Seq experiments that represent potent tools to identify transcriptional targets.

Nevertheless, *Tbx3* promotes highly proliferative hepatic precursor cells, the hepatoblasts, by the inhibition of differentiation(52, 76). This function may be of special medical interest since the liver is known to possess tremendous regeneration capacities. Even after loss of two thirds of the cell mass by disease or injury the liver restores function and size within weeks. However, the mechanisms underlying this ability are not well understood. Given the here presented developmental functions of *Tbx3* a further examination of genes normally expressed in embryonic liver formation during regeneration processes might be worthwhile. I suppose that *Tbx3* dedifferentiates hepatocytes and cholangiocytes in equal manner to facilitate rapid growth and vanishes just in time to allow restoration of the bile ducts. How *Tbx3* is regulated during this process is of remarkable significance since knowledge about it will be of some relevance for treatment of diverse cancers. Glaser and Alpini in 2010(77) stated that “many questions about the regulatory mechanisms of *Tbx3* during liver development and regeneration, as well as their potential involvement in liver cancer remain to be addressed in future studies”. I agree in this respect that, as Lu et al.(65) concluded in their review 2010, that it might be smart targeting the repressor domain of *Tbx3* (and similarly *Tbx2*) by anticancer drugs. I would even add that knowing how to regulate

Tbx3, how to enable and shut down its expression, would be of great benefit not only for treating cancer but also to accelerate recreation after surgery.

Having this in mind part 3 of this work might also be considered important for cancer treatment. Though started by the simple observation that lung size is decreased in *Tbx2* loss-of-function mice, we gained insight in the molecular mechanisms processed by *Tbx2*. Repression of *Cdkn1a* in cancer by *Tbx2* was long known. However, the newly demonstrated likewise repression of *Cdkn1b*, the confirmation of a direct repression of *Cdkn1a in vivo* and the ability of *Tbx2* to facilitate, albeit not to induce canonical Wnt-signaling is likely to boost cancer progression and therefore to lead to a bad outcome. Moreover this mechanism offers the possibility of *Ctnnb1* dependent activation of *Tbx3*, which might even increase aggressiveness and invasiveness of the cancer tissue (since we described *Tbx3* to be relevant for cell migration from the liver diverticulum (part 1 of this study)).

Based on the results shown above we will certainly go on with the examination of the fundamental processes underlying all these diverse functions of T-box transcription factors. We will enforce the detection of target genes to better understand basic principles of development to expand existing models and to design new ones of course.

References

1. Lewis SL, Tam PP. Definitive endoderm of the mouse embryo: Formation, cell fates, and morphogenetic function. *Dev Dyn* 2006; **235**(9): 2315-2329.
2. Dufort D, Schwartz L, Harpal K, Rossant J. The transcription factor HNF3beta is required in visceral endoderm for normal primitive streak morphogenesis. *Development* 1998; **125**(16): 3015-3025.
3. Zorn AM, Wells JM. Molecular basis of vertebrate endoderm development. *Int Rev Cytol* 2007; **259**: 49-111.
4. Zaret KS. Regulatory phases of early liver development: Paradigms of organogenesis. *Nature Reviews Genetics* 2002; **3**(7): 499-512.
5. Zorn AM. Liver development. In: *StemBook*. Cambridge (MA): Aaron M. Zorn; 2008.
6. Burke Z, Oliver G. Prox1 is an early specific marker for the developing liver and pancreas in the mammalian foregut endoderm. *Mechanisms of Development* 2002; **118**(1-2): 147-155.
7. Matsumoto K, Yoshitomi H, Rossant J, Zaret KS. Liver organogenesis promoted by endothelial cells prior to vascular function. *Science* 2001; **294**(5542): 559-563.
8. Zaret KS. Hepatocyte differentiation: From the endoderm and beyond. *Current Opinion in Genetics and Development* 2001; **11**(5): 568-574.
9. Grapin-Botton A, Melton DA. Endoderm development: From patterning to organogenesis. *Trends Genet* 2000; **16**(3): 124-130.
10. Zaret KS. Liver specification and early morphogenesis. *Mechanisms of Development* 2000; **92**(1): 83-88.
11. Moore-Scott BA, Opoka R, Lin SC, Kordich JJ, Wells JM. Identification of molecular markers that are expressed in discrete anterior-posterior domains of the endoderm from the gastrula stage to mid-gestation. *Dev Dyn* 2007; **236**(7): 1997-2003.
12. Gualdi R, Bossard P, Zheng M, Hamada Y, Coleman JR, Zaret KS. Hepatic specification of the gut endoderm in vitro: Cell signaling and transcriptional control. *Genes and Development* 1996; **10**(13): 1670-1682.
13. Horb ME, Slack JM. Endoderm specification and differentiation in xenopus embryos. *Dev Biol* 2001; **236**(2): 330-343.
14. Wells JM, Melton DA. Vertebrate endoderm development. *Annu Rev Cell Dev Biol* 1999; **15**: 393-410.
15. Horb ME. Patterning the endoderm: The importance of neighbours. *Bioessays* 2000; **22**(7): 599-602.
16. Wells JM, Melton DA. Early mouse endoderm is patterned by soluble factors from adjacent germ layers. *Development* 2000; **127**(8): 1563-1572.

17. Dessimoz J, Opoka R, Kordich JJ, Grapin-Botton A, Wells JM. FGF signaling is necessary for establishing gut tube domains along the anterior-posterior axis in vivo. *Mech Dev* 2006; **123**(1): 42-55.
18. McLin VA, Rankin SA, Zorn AM. Repression of Wnt/beta-catenin signaling in the anterior endoderm is essential for liver and pancreas development. *Development* 2007; **134**(12): 2207-2217.
19. Deutsch G, Jung J, Zheng M, Lórá J, Zaret KS. A bipotential precursor population for pancreas and liver within the embryonic endoderm. *Development* 2001; **128**(6): 871-881.
20. Serls AE, Doherty S, Parvatiyar P, Wells JM, Deutsch GH. Different thresholds of fibroblast growth factors pattern the ventral foregut into liver and lung. *Development* 2005; **132**(1): 35-47.
21. Fukuda-Taira S. Hepatic induction in the avian embryo: Specificity of reactive endoderm and inductive mesoderm. *J Embryol Exp Morphol* 1981; **63**: 111-125.
22. Jung J, Zheng M, Goldfarb M, Zaret KS. Initiation of mammalian liver development from endoderm by fibroblast growth factors. *Science* 1999; **284**(5422): 1998-2003.
23. Rossi JM, Dunn NR, Hogan BL, Zaret KS. Distinct mesodermal signals, including BMPs from the septum transversum mesenchyme, are required in combination for hepatogenesis from the endoderm. *Genes Dev* 2001; **15**(15): 1998-2009.
24. Kispert A, Herrmann BG. The brachyury gene encodes a novel DNA binding protein. *EMBO J* 1993; **12**(8): 3211-3220.
25. Carlson H, Ota S, Campbell CE, Hurlin PJ. A dominant repression domain in Tbx3 mediates transcriptional repression and cell immortalization: Relevance to mutations in Tbx3 that cause ulnar-mammary syndrome. *Hum Mol Genet* 2001; **10**(21): 2403-2413.
26. Carreira S, Dexter TJ, Yavuzer U, Easty DJ, Goding CR. Brachyury-related transcription factor Tbx2 and repression of the melanocyte-specific TRP-1 promoter. *Mol Cell Biol* 1998; **18**(9): 5099-5108.
27. He M, Wen L, Campbell CE, Wu JY, Rao Y. Transcription repression by xenopus ET and its human ortholog TBX3, a gene involved in ulnar-mammary syndrome. *Proc Natl Acad Sci U S A* 1999; **96**(18): 10212-10217.
28. Ouimette JF, Jolin ML, L'honore A, Gifuni A, Drouin J. Divergent transcriptional activities determine limb identity. *Nat Commun* 2010; **1**: 35.
29. Agulnik SI, Garvey N, Hancock S, Ruvinsky I, Chapman DL, Agulnik I, Bollag R, et al. Evolution of mouse T-box genes by tandem duplication and cluster dispersion. *Genetics* 1996; **144**(1): 249-254.
30. Chapman DL, Garvey N, Hancock S, Alexiou M, Agulnik SI, Gibson-Brown JJ, Cebra-Thomas J, et al. Expression of the T-box family genes, Tbx1-Tbx5, during early mouse development. *Dev Dyn* 1996; **206**(4): 379-390.
31. Gibson-Brown JJ, Agulnik S, Silver LM, Papaioannou VE. Expression of T-box genes Tbx2-Tbx5 during chick organogenesis. *Mech Dev* 1998; **74**(1-2): 165-169.

32. Lingbeek ME, Jacobs JJ, van Lohuizen M. The T-box repressors TBX2 and TBX3 specifically regulate the tumor suppressor gene p14ARF via a variant T-site in the initiator. *J Biol Chem* 2002; **277**(29): 26120-26127.
33. Morrisey EE, Hogan BL. Preparing for the first breath: Genetic and cellular mechanisms in lung development. *Dev Cell* 2010; **18**(1): 8-23.
34. Harrelson Z, Kelly RG, Goldin SN, Gibson-Brown JJ, Bollag RJ, Silver LM, Papaioannou VE. Tbx2 is essential for patterning the atrioventricular canal and for morphogenesis of the outflow tract during heart development. *Development* 2004; **131**(20): 5041-5052.
35. Naiche LA, Harrelson Z, Kelly RG, Papaioannou VE. T-box genes in vertebrate development. *Annu Rev Genet* 2005; **39**: 219-239.
36. Tremblay KD, Zaret KS. Distinct populations of endoderm cells converge to generate the embryonic liver bud and ventral foregut tissues. *Dev Biol* 2005; **280**(1): 87-99.
37. Zaret KS. Genetic programming of liver and pancreas progenitors: Lessons for stem-cell differentiation. *Nat Rev Genet* 2008; **9**(5): 329-340.
38. Holz LE, Warren A, Le Couteur DG, Bowen DG, Bertolino P. CD8+ T cell tolerance following antigen recognition on hepatocytes. *J Autoimmun* 2010; **34**(1): 15-22.
39. Strick-Marchand H, Weiss MC. Inducible differentiation and morphogenesis of bipotential liver cell lines from wild-type mouse embryos. *Hepatology* 2002; **36**(4 Pt 1): 794-804.
40. Asahina K, Tsai SY, Li P, Ishii M, Maxson RE, Jr, Sucov HM, Tsukamoto H. Mesenchymal origin of hepatic stellate cells, submesothelial cells, and perivascular mesenchymal cells during mouse liver development. *Hepatology* 2009; **49**(3): 998-1011.
41. Calmont A, Wandzioch E, Tremblay KD, Minowada G, Kaestner KH, Martin GR, Zaret KS. An FGF response pathway that mediates hepatic gene induction in embryonic endoderm cells. *Developmental Cell* 2006; **11**(3): 339-348.
42. Houssaint E. Differentiation of the mouse hepatic primordium. I. an analysis of tissue interactions in hepatocyte differentiation. *Cell Differ* 1980; **9**(5): 269-279.
43. Sosa-Pineda B, Wigle JT, Oliver G. Hepatocyte migration during liver development requires Prox1. *Nat Genet* 2000; **25**(3): 254-255.
44. Douarin NM. An experimental analysis of liver development. *Med Biol* 1975; **53**(6): 427-455.
45. Yamasaki H, Sada A, Iwata T, Niwa T, Tomizawa M, Xanthopoulos KG, Koike T, et al. Suppression of C/EBP α expression in periportal hepatoblasts may stimulate biliary cell differentiation through increased Hnf6 and Hnf1b expression. *Development* 2006; **133**(21): 4233-4243.
46. Eeckhoutte J, Formstecher P, Laine B. Hepatocyte nuclear factor 4 α enhances the hepatocyte nuclear factor 1 α -mediated activation of transcription. *Nucleic Acids Res* 2004; **32**(8): 2586-2593.

47. Odom DT, Zizlsperger N, Gordon DB, Bell GW, Rinaldi NJ, Murray HL, Volkert TL, et al. Control of pancreas and liver gene expression by HNF transcription factors. *Science* 2004; **303**(5662): 1378-1381.
48. Hofmann JJ, Zovein AC, Koh H, Radtke F, Weinmaster G, Iruela-Arispe ML. Jagged1 in the portal vein mesenchyme regulates intrahepatic bile duct development: Insights into alagille syndrome. *Development* 2010; **137**(23): 4061-4072.
49. Shiojiri N, Nagai Y. Preferential differentiation of the bile ducts along the portal vein in the development of mouse liver. *Anat Embryol (Berl)* 1992; **185**(1): 17-24.
50. Davenport TG, Jerome-Majewska LA, Papaioannou VE. Mammary gland, limb and yolk sac defects in mice lacking *Tbx3*, the gene mutated in human ulnar mammary syndrome. *Development* 2003; **130**(10): 2263-2273.
51. Eblaghie MC, Reedy M, Oliver T, Mishina Y, Hogan BL. Evidence that autocrine signaling through *Bmpr1a* regulates the proliferation, survival and morphogenetic behavior of distal lung epithelial cells. *Dev Biol* 2006; **291**(1): 67-82.
52. Suzuki A, Sekiya S, Buscher D, Izpisua Belmonte JC, Taniguchi H. *Tbx3* controls the fate of hepatic progenitor cells in liver development by suppressing p19ARF expression. *Development* 2008; **135**(9): 1589-1595.
53. unknown. Hinweise für verwandtschaft, vorderextremitäten der wirbeltiere, homologie, atavismus, rudiment, analogie. 2011-04-17.
<http://www.scheffel.og.bw.schule.de/faecher/science/biologie/evolution/2befunde/befunde.htm>
54. Eckert R, ed. *Tierphysiologie*. Stuttgart: Georg Thieme Verlag, 2000:874.
55. Gad SC. Drug safety evaluation. In: ; 2002.
56. Warburton D, Schwarz M, Tefft D, Flores-Delgado G, Anderson KD, Cardoso WV. The molecular basis of lung morphogenesis. *Mech Dev* 2000; **92**(1): 55-81.
57. Metzger RJ, Klein OD, Martin GR, Krasnow MA. The branching programme of mouse lung development. *Nature* 2008; **453**(7196): 745-750.
58. Chuang PT, McMahon AP. Branching morphogenesis of the lung: New molecular insights into an old problem. *Trends Cell Biol* 2003; **13**(2): 86-91.
59. Bellusci S, Grindley J, Emoto H, Itoh N, Hogan BL. Fibroblast growth factor 10 (FGF10) and branching morphogenesis in the embryonic mouse lung. *Development* 1997; **124**(23): 4867-4878.
60. Cebra-Thomas JA, Bromer J, Gardner R, Lam GK, Sheipe H, Gilbert SF. T-box gene products are required for mesenchymal induction of epithelial branching in the embryonic mouse lung. *Dev Dyn* 2003; **226**(1): 82-90.
61. Min H, Danilenko DM, Scully SA, Bolon B, Ring BD, Tarpley JE, DeRose M, et al. Fgf-10 is required for both limb and lung development and exhibits striking functional similarity to drosophila branchless. *Genes Dev* 1998; **12**(20): 3156-3161.

62. Sekine K, Ohuchi H, Fujiwara M, Yamasaki M, Yoshizawa T, Sato T, Yagishita N, et al. Fgf10 is essential for limb and lung formation. *Nat Genet* 1999; **21**(1): 138-141.
63. Yin Y, White AC, Huh SH, Hilton MJ, Kanazawa H, Long F, Ornitz DM. An FGF-WNT gene regulatory network controls lung mesenchyme development. *Dev Biol* 2008; **319**(2): 426-436.
64. Kauffman SL. Cell proliferation in the mammalian lung. *Int Rev Exp Pathol* 1980; **22**: 131-191.
65. Lu J, Li XP, Dong Q, Kung HF, He ML. TBX2 and TBX3: The special value for anticancer drug targets. *Biochim Biophys Acta* 2010; **1806**(2): 268-274.
66. Prince S, Carreira S, Vance KW, Abrahams A, Goding CR. Tbx2 directly represses the expression of the p21(WAF1) cyclin-dependent kinase inhibitor. *Cancer Res* 2004; **64**(5): 1669-1674.
67. Renard C-, Labalette C, Armengol C, Cougot D, Wei Y, Cairo S, Pineau P, et al. Tbx3 is a downstream target of the wnt/ β -catenin pathway and a critical mediator of β -catenin survival functions in liver cancer. *Cancer Research* 2007; **67**(3): 901-910.
68. Ribeiro I, Kawakami Y, Buscher D, Raya A, Rodriguez-Leon J, Morita M, Rodriguez Esteban C, et al. Tbx2 and Tbx3 regulate the dynamics of cell proliferation during heart remodeling. *PLoS One* 2007; **2**(4): e398.
69. Jerome-Majewska LA, Jenkins GP, Ernstoff E, Zindy F, Sherr CJ, Papaioannou VE. Tbx3, the ulnar-mammary syndrome gene, and Tbx2 interact in mammary gland development through a p19Arf/p53-independent pathway. *Developmental Dynamics* 2005; **234**(4): 922-933.
70. Bamshad M, Lin RC, Law DJ, Watkins WC, Krakowiak PA, Moore ME, Franceschini P, et al. Mutations in human TBX3 alter limb, apocrine and genital development in ulnar-mammary syndrome. *Nat Genet* 1997; **16**(3): 311-315.
71. Bussen M, Petry M, Schuster-Gossler K, Leitges M, Gossler A, Kispert A. The T-box transcription factor Tbx18 maintains the separation of anterior and posterior somite compartments. *Genes Dev* 2004; **18**(10): 1209-1221.
72. Fong SH, Emelyanov A, Teh C, Korzh V. Wnt signalling mediated by Tbx2b regulates cell migration during formation of the neural plate. *Development* 2005; **132**(16): 3587-3596.
73. Fernando RI, Litzinger M, Trono P, Hamilton DH, Schlom J, Palena C. The T-box transcription factor brachyury promotes epithelial-mesenchymal transition in human tumor cells. *J Clin Invest* 2010; **120**(2): 533-544.
74. Antoniou A, Raynaud P, Cordi S, Zong Y, Tronche F, Stanger BZ, Jacquemin P, et al. Intrahepatic bile ducts develop according to a new mode of tubulogenesis regulated by the transcription factor SOX9. *Gastroenterology* 2009; **136**(7): 2325-2333.
75. Sparks EE, Perrien DS, Huppert KA, Peterson TE, Huppert SS. Defects in hepatic notch signaling result in disruption of the communicating intrahepatic bile duct network in mice. *Dis Model Mech* 2011; .

76. Ludtke TH, Christoffels VM, Petry M, Kispert A. Tbx3 promotes liver bud expansion during mouse development by suppression of cholangiocyte differentiation. *Hepatology* 2009; **49**(3): 969-978.
77. Glaser SS, Alpini G. International hepatology. *J Hepatol* 2010; **52**(3): 450-451.

Acknowledgements

I would like to thank my supervisor Prof. Dr. Andreas Kispert for many inspiring projects, enormous support and helpful discussions. Thanks for the opportunity to work in his great research group.

I would like to thank Prof. Dr. Achim Gossler for this great institution and fantastic environment.

Thanks also to all other members of the lab and the IfM for discussions and fantastic team-work. In particular I would like to thank Carsten Rudat for sharing ideas and assistance in the lab, Marianne Petry for her great job organizing the lab and Dr. Thomas Grieskamp for “off-topics”.

Thanks to Dr. Karin Schuster-Gossler and Dr. Henner Farin for generation of mice I used in my study.

Thanks to Dr. Lorenzo Ferroni for staying in contact. I had a great time in Erlangen thanks to you and I will never forget Ferraras longest road. I hope to meet you again.

Thanks to Anna Barbara Foik. I am not the only one who depended on your constant supply of cookies.

Special thanks to our coffee club Dr. Susann Placzko and Marc-Jens Kleppa. You made life easier.

Thanks to my parents who always backed me up whenever it was needed.

And finally I want to say thank you to my daughter Freyja Sophie for her laughter and happiness and my wife Claudia. This work would not have been successful without you.

List of publications

1. Ludtke TH, Christoffels VM, Petry M, Kispert A. Tbx3 promotes liver bud expansion during mouse development by suppression of cholangiocyte differentiation. *Hepatology* 2009; **49**(3): 969-978.
2. Zirzow S, Ludtke TH, Brons JF, Petry M, Christoffels VM, Kispert A. Expression and requirement of T-box transcription factors Tbx2 and Tbx3 during secondary palate development in the mouse. *Dev Biol* 2009; **336**(2): 145-155.
3. Grieskamp T, Rudat C, Ludtke TH, Norden J, Kispert A. Notch signaling regulates smooth muscle differentiation of epicardium-derived cells. *Circ Res* 2011; **108**(7): 813-823.
4. Ntefidou M, Ludtke T, Ahmad M, Hader DP. Heterologous expression of photoactivated adenylyl cyclase (PAC) genes from the flagellate euglena gracilis in insect cells. *Photochem Photobiol* 2006; **82**(6): 1601-1605.

Curriculum Vitae

Name: Timo Hans-Werner Lüdtkke
 Date of birth: 1978-04-10
 Place of birth: Kiel
 Citizenship: German
 Marital status: Married, 2 children

Contact information:

Phone: 0511 5325961
 Email: luedtke.timo@mh-hannover.de; timoluedtke@arcor.de

School education:

1985 - 1989 Heinrich-von-Stefan Schule Kiel, elementary school
 1989 - 1997 Hebbelschule Kiel, secondary school

Alternative civilian service:

1997 - 1998 Paul-Fleming-Haus, psychiatric geriatric care (Kiel)

University studies:

1998 - 2000 Undergraduate studies of Biology ("Vordiplom")
 at the University of Kiel.
 2002 - 2004 Graduate studies of Biology ("Diplom")
 at the University of Kiel.
 2003 - 2004 Diploma thesis at the Institute for Microbiology,
 University Kiel,
 under supervision of PD Dr. W. Hausner.
 Title of the diploma thesis:
 "Untersuchungen zur Funktion von archaeellen Elongationsfaktoren"
 2005 - 2007 Research assistant in the laboratory of Prof. Dr. D-P. Häder
 at the Institute for Plant Ecophysiology, University of Erlangen-
 Nuremberg.
 Research project: "Analysis of photoperception in flagellates"
 2007 - 2011 Research assistant in the laboratory of Prof. Dr. A. Kispert
 at the Institute for Molecular Biology, Hannover Medical School.
 Dissertation with the title:
 "Functional Analysis of the T-Box Genes *Tbx2* and *Tbx3*
 in Murine Liver and Lung Development"

Declaration

“I hereby declare and confirm that this thesis is entirely the result of my own work except where otherwise indicated. This thesis has not been used as part of any other examination.”

Timo Lüdtkke

Hannover, 2011-04-19

(Signature)